

ผลของไฮดรอกซีอะปาไทด์และเบตาไตรแคลเซียมฟอสเฟตต่อสมบัติของโครงเลี้ยงเซลล์
ไฟโบรอินไหมไทยและเจลาติน



นางสาวโชติกา ดารารัตน์

ศูนย์วิทยทรัพยากร

วิทยานิพนธ์นี้เป็นส่วนหนึ่งของการศึกษาตามหลักสูตรปริญญาวิทยาศาสตรมหาบัณฑิต

สาขาวิชาวิศวกรรมเคมี ภาควิชาวิศวกรรมเคมี

คณะวิศวกรรมศาสตร์ จุฬาลงกรณ์มหาวิทยาลัย

ปีการศึกษา 2553

ลิขสิทธิ์ของจุฬาลงกรณ์มหาวิทยาลัย



5 1 7 0 5 6 0 0 2 1

EFFECT OF HYDROXYAPATITE AND β -TRICALCIUM PHOSPHATE ON THE
PROPERTIES OF THAI SILK FIBROIN/GELATIN SCAFFOLD



Miss Chotika Dararutana

ศูนย์วิทยุทรัพยากร
จุฬาลงกรณ์มหาวิทยาลัย

A Thesis Submitted in Partial Fulfillment of the Requirements
for the Degree of Master of Engineering Program in Chemical Engineering
Department of Chemical Engineering

Faculty of Engineering

Chulalongkorn University

Academic Year 2010

Copyright of Chulalongkorn University

530332

Thesis Title EFFECT OF HYDROXYAPATITE AND β -TRICALCIUM PHOSPHATE
ON THE PROPERTIES OF THAI SILK FIBROIN/GELATIN
SCAFFOLD

By Miss Chotika Dararutana

Field of Study Chemical Engineering

Thesis Advisor Associate Professor Siriporn Damrongsakkul, Ph.D.

Thesis Co-Advisor Associate Professor Sittisak Honsawek, M.D., Ph.D.

Accepted by the Faculty of Engineering, Chulalongkorn University in Partial
Fulfillment of the Requirements for the Master's Degree


..... Dean of the Faculty of Engineering
(Associate Professor Boonsom Lerdkhironwong, Dr.Ing.)

THESIS COMMITTEE


..... Chairman
(Assistant Professor Anongnat Somwangthanaroj, Ph.D.)


..... Thesis Advisor
(Associate Professor Siriporn Damrongsakkul, Ph.D.)


..... Thesis Co-Advisor
(Associate Professor Sittisak Honsawek, M.D., Ph.D.)


..... Examiner
(Assistant Professor Sorada Kanokpanont, Ph.D.)


..... External Examiner
(Tanyarut Rerkpattanapipat, Ph.D.)

โชติกา ดารารัตน์ : ผลของไฮดรอกซีอะปาไทด์และเบตาไตรแคลเซียมฟอสเฟตต่อ
สมบัติของโครงเลี้ยงเซลล์ไฟโบรอินไหมไทยและเจลาติน. (EFFECT OF
HYDROXYAPATITE AND β -TRICALCIUM PHOSPHATE ON THE PROPERTIES

OF THAI SILK FIBROIN/GELATIN SCAFFOLD) อ.ที่ปรึกษาวิทยานิพนธ์หลัก:

รศ.ดร. ศิริพร ดำรงค์ศักดิ์กุล, อ.ที่ปรึกษาวิทยานิพนธ์ร่วม: รศ.ดร.นพ.สิทธิศักดิ์ ھرรรษาเวก
, 101 หน้า.

งานวิจัยนี้มีวัตถุประสงค์เพื่อศึกษาผลของของไฮดรอกซีอะปาไทด์และเบตาไตรแคลเซียมฟอสเฟต ต่อสมบัติของโครงเลี้ยงเซลล์ไฟโบรอินไหมไทยและเจลาติน โดยการเติมสารประกอบอนินทรีย์ทั้งสองในสารละลายผสมของไฟโบรอินและเจลาตินและขึ้นรูปโดยวิธีการปั่นและทำแห้งแข็งด้วยความเย็น ทั้งนี้ได้ทำการศึกษาอิทธิพลของสัดส่วนผสมโดยน้ำหนักระหว่างสารละลายไฟโบรอิน/เจลาติน และสารประกอบอนินทรีย์ทั้งสองพบว่าลักษณะพื้นฐานของโครงเลี้ยงเซลล์ในทุกสัดส่วนผสมล้วนแต่มีโครงสร้างรูพรุนสูง และมีการกระจายตัวของอนุภาคของสารประกอบอนินทรีย์ทั้งสองอย่างสม่ำเสมอ นอกจากนี้ยังพบว่าการเติมสารประกอบอนินทรีย์ทั้งไฮดรอกซีอะปาไทด์และเบตาไตรแคลเซียมฟอสเฟตส่งผลให้ความสามารถในการอุ้มน้ำและความพรุนของโครงเลี้ยงเซลล์ลดลง ทั้งนี้เนื่องจากผลของส่วนที่ไม่ชอบน้ำในสารประกอบอนินทรีย์ อย่างไรก็ตามการเติมสารประกอบอนินทรีย์ทั้งไฮดรอกซีอะปาไทด์และเบตาไตรแคลเซียมฟอสเฟตสามารถส่งเสริมความสามารถในการทนแรงกดได้ดี เมื่อเทียบกับโครงเลี้ยงเซลล์ที่ไม่มีการเติมสารประกอบอนินทรีย์ และมีแนวโน้มว่าการเติมเบตาไตรแคลเซียมฟอสเฟตสามารถส่งผลให้โครงเลี้ยงเซลล์ทนแรงกดได้ดีกว่าการเติมไฮดรอกซีอะปาไทด์ เนื่องจากรูพรุนที่มีขนาดเล็กกว่าของโครงเลี้ยงเซลล์ที่มีการเติมเบตาไตรแคลเซียมฟอสเฟต จึงทำให้สามารถกระจายแรงได้ดีกว่าส่งผลให้ทนต่อแรงกดได้มากกว่า ผลการทดสอบการสลายตัวทางชีวภาพในระดับห้องปฏิบัติการในสารละลายคอลลาจีนพบว่า โครงเลี้ยงเซลล์โปรตีนที่ไม่มีการเติมสารประกอบอนินทรีย์ถูกย่อยสลายหมดภายใน 7 วัน ส่วนโครงเลี้ยงเซลล์ที่มีการเติมสารประกอบอนินทรีย์ในทุกอัตราส่วนพบว่าน้ำหนักที่ลดลงจะคงที่เท่ากับน้ำหนักของสารประกอบอนินทรีย์ที่เป็นองค์ประกอบ จากการทดสอบความเป็นพิษของวัสดุพบว่าโครงเลี้ยงเซลล์ทั้งหมดแสดงความเป็นพิษในระดับต่ำ ผลการเลี้ยงเซลล์จากเยื่อหุ้มกระดุกมนุษย์ในระดับห้องปฏิบัติการพบว่า โครงเลี้ยงเซลล์ที่มีการเติมสารประกอบอนินทรีย์ทั้งไฮดรอกซีอะปาไทด์และเบตาไตรแคลเซียมฟอสเฟตมีประสิทธิผลในการชักนำให้เกิดการเปลี่ยนแปลงไปเป็นกระดูกได้ดี ซึ่งสูตรที่สามารถชักนำให้เซลล์เปลี่ยนแปลงไปเป็นเซลล์กระดูกได้ดึนั้นได้แก่ สูตรที่มีเบตาไตรแคลเซียมฟอสเฟต 30-70% และสูตรที่มีไฮดรอกซีอะปาไทด์ 50% และเมื่อเปรียบเทียบทั้ง 4 สูตรพบว่า สูตรที่มีการเติมเบตาไตรแคลเซียมฟอสเฟตทั้งหมดมีแนวโน้มที่จะสามารถชักนำให้เซลล์เปลี่ยนแปลงไปเป็นเซลล์กระดูกได้ดีกว่าสูตรที่เติมไฮดรอกซีอะปาไทด์ ผลการศึกษาแสดงให้เห็นว่าโครงเลี้ยงเซลล์ที่มีการเติมสารประกอบอนินทรีย์ทั้งไฮดรอกซีอะปาไทด์และเบตาไตรแคลเซียมฟอสเฟตมีสมบัติทางกายภาพ และทางชีวภาพที่เหมาะสมสำหรับประยุกต์ใช้งานวิศวกรรมเนื้อเยื่อกระดูก

ภาควิชา..... วิศวกรรมเคมี..... ลายมือชื่อนิสิต..... โชติกา ดารารัตน์.....
สาขาวิชา..... วิศวกรรมเคมี..... ลายมือชื่ออ.ที่ปรึกษาวิทยานิพนธ์หลัก.....
ปีการศึกษา..... 2553..... ลายมือชื่ออ.ที่ปรึกษาวิทยานิพนธ์ร่วม.....

5170560021 : MAJOR CHEMICAL ENGINEERING

KEYWORDS : THAI SILK FIBROIN / GELATIN / β -TRICALCIUM PHOSPHATE / HYDROXYAPATITE

CHOTIKA DARARUTANA: EFFECT OF HYDROXYAPATITE AND β -TRICALCIUM PHOSPHATE ON THE PROPERTIES OF THAI SILK FIBROIN/GELATIN SCAFFOLD. THESIS ADVISOR: ASSOC. PROF. SIRIPORN DAMRONGSAKKUL, Ph.D., THESIS CO-ADVISOR: ASSOC. PROF. SITTISAK HONSAWEK, M.D, Ph.D., 101 pp.

This research aimed to investigate the effects of hydroxyapatite (HA) and β -tricalcium phosphate (β -TCP) on the properties of Thai silk fibroin/gelatin scaffolds. The Thai silk fibroin/gelatin solution incorporated with both inorganic compounds, β -TCP and HA, were homogenized and fabricated via freeze drying technique. The effect of different weight percentages of each inorganic compound incorporated was examined. It was found that all Thai silk fibroin/gelatin based scaffolds incorporated with β -TCP and HA possessed porous structure with uniform distribution of β -TCP and HA. The Thai silk fibroin/gelatin based scaffold incorporated with both inorganic compounds, β -TCP and HA, showed lower water absorption (%) because of the hydrophobic part of inorganic compounds and lower porosity than that of pure protein scaffolds. The incorporation of β -TCP and HA could enhance compressive strength of scaffolds compared to the pure protein scaffold in dry and wet condition. In addition, the compressive modulus of Thai silk fibroin/gelatin based scaffolds incorporated with β -TCP was slightly higher than that with HA incorporation. This could be due to the smaller pore size of scaffold incorporated with β -TCP. The scaffold with smaller pore size can give more paths for distributing to applied stress, resulting in the greater compressive modulus. The results on *in vitro* biodegradability in collagenase solution revealed that the Thai silk fibroin/gelatin based scaffolds without inorganic compounds was completely degraded within 7 days. The remaining weight (%) of scaffold incorporated with both β -TCP and HA were decreased and remained at the weight percentage of incorporated inorganic compounds after 7 days. All samples clearly presented low cytotoxic effect. The results on *in vitro* cell culture using periosteum derived cells indicated that the incorporation of both inorganic compounds could enhance osteoconductive potential of the Thai silk fibroin/gelatin based scaffolds, particularly the scaffolds containing 50-70% of β -TCP and 50% HA. When compared among the four types of scaffolds, the scaffold with 30-70% of β -TCP tended to be slightly better osteoconductive than the scaffold with 50% of HA. The results on the physical and biological properties of Thai silk fibroin/gelatin based scaffolds incorporated with β -TCP and HA markedly indicated that the scaffolds had a high potential to be applied in bone tissue engineering.

Department : Chemical Engineering Student's Signature โชติกา ดารารุตนา
 Field of Study : Chemical Engineering Advisor's Signature [Signature]
 Academic Year : 2010 Co-Advisor's Signature Sittisak Honsawek

ACKNOWLEDGEMENTS

This research is completed with the assistance and support from many people. The author would like to express her deepest gratitude to Associate Professor Dr. Siriporn Damrongsakkul, her advisor, and Associate Professor Sittisak Honsawek, her co-advisor, for their continuous guidance, helpful suggestion and warm encouragement. In addition, she is also grateful to Assistant Professor Dr. Anongnat Somwangthanaroj, Assistant Professor Dr. Sorada Kanokpanont, and Dr. Tanyarut Rerkpattanapipat serving as the chairman and the members of the thesis committee, respectively, whose comments were constructively and especially helpful.

The author would like to thank Assistant Professor Thanorm Bunprasert, Dr. Juthamas Ratanavaraporn and Mr. Thakoon Thitiset for their kind attentions and suggestions in cell culture as well as experimental, and Ms. Shatshawan Tritanipakul for her helps and suggestions with experiments.

The author would like to thank the staffs of Department of Biochemistry, Faculty of Medicine, Chulalongkorn University for their helps with experiments. She would like to extend her grateful thanks to all members of Polymer Engineering Research Laboratory at the Department of Chemical Engineering, Faculty of Engineering as well as all members of i-Tissue Laboratory at the Faculty of Medicine, Chulalongkorn University.

Finally, the author expresses her sincere thanks to her parents and everyone in her family for their unfailing understanding and affectionate encouragement.

จุฬาลงกรณ์มหาวิทยาลัย

CONTENTS

CHAPTER	PAGE
ABSTRACT (IN THAI).....	iv
ABSTRACT (IN ENGLISH).....	v
ACKNOWLEDGEMENTS.....	vi
CONTENTS.....	vii
LIST OF TABLES.....	x
LIST OF FIGURES.....	xi
LIST OF ABBREVIATIONS.....	xiv
CHAPTER	
I. INTRODUCTION.....	1
1.1 Background.....	1
1.2 Objective.....	3
1.3 Scopes of research.....	3
II. RELEVANT THEORY AND LITERATURE REVIEWS.....	5
2.1 Relevant theory.....	5
2.1.1 Biomaterials.....	5
2.1.1.1 Silk.....	5
2.1.1.2 Gelatin.....	9
2.1.1.3 Hydroxyapatite.....	13
2.1.1.4 β -tricalcium phosphate.....	14
2.1.2 Characteristics of three-dimensional scaffold.....	15
2.1.3 Freeze drying techniques.....	16
2.1.4 Bone.....	20
2.1.4.1 Structure of bone.....	20
2.1.4.2 Mineralization.....	22
2.1.5 Bone tissue engineering.....	23
2.1.5.1 Cell based strategies.....	24
2.1.5.2 Growth factor based strategies.....	24
2.1.5.3 Matrix-based strategies.....	25
2.1.6 Perosteum derived cell.....	27

CHAPTER	PAGE
2.2 Literature review.....	28
2.2.1 Gelatin/silk fibroin and collagen/silk fibroin systems.....	28
2.2.2 Silk fibroin and gelatin incorporated with inorganic compound systems.....	33
2.2.3 <i>In vitro</i> and <i>In vivo</i> cell culture using periosteum derived cell.....	33
III. EXPERIMENTAL WORK.....	37
3.1 Materials and reagents.....	37
3.2 Equipments.....	38
3.3 Experimental procedures.....	39
3.3.1 Preparation of Thai silk fibroin solution.....	41
3.3.2 Preparation of gelatin solution.....	41
3.3.3 Scaffold fabrication.....	41
3.3.4 Characterization of received inorganic compound.....	42
3.3.4.1 Morphology observation.....	42
3.3.4.2 Particle size analysis of inorganic compound.....	42
3.3.5 Periosteum derived cell isolation and culture.....	43
3.3.6 Characterization of scaffolds.....	44
3.3.6.1 Physical characterization.....	44
3.3.6.1.1 Morphology.....	44
3.3.6.1.3 Swelling property.....	44
3.3.6.1.4 Porosity.....	44
3.3.6.1.5 Compressive modulus (dry and wet condition).....	45
3.3.6.2 Biological characterization.....	45
3.3.6.2.1 <i>In vitro</i> biodegradability.....	45
3.3.6.2.2 Material cytotoxicity test.....	46
3.3.6.2.3 Cell seeding and cell culture.....	46
3.3.6.2.4 Initial attachment and proliferation tests.....	47
3.3.6.2.5 Osteogenic differentiation test.....	47
3.3.6.2.6 The observation of cultured cell.....	48
3.3.6.2.7 Elemental analysis of cell after culture.....	48

CHAPTER	PAGE
3.3.7 Statistical analysis.....	49
IV. RESULTS AND DISCUSSION.....	50
4.1 Morphology and particle size of inorganic compounds	50
4.2 Effect of incorporated β -tricalcium phosphate and hydroxyapatite on Thai silk fibroin/gelatin based scaffolds.....	52
4.2.1 Physical properties.....	52
4.2.1.1 Morphology.....	52
4.2.1.2 Swelling property.....	56
4.2.1.3 Porosity.....	58
4.2.1.4 Compressive modulus (dry and wet condition).....	60
4.2.2 Biological properties.....	62
4.2.2.1 <i>In vitro</i> biodegradability.....	62
4.2.2.2 Material cytotoxicity test using L929.....	64
4.2.2.3 <i>In vitro</i> biocompatibility using periosteum derived cell.....	65
4.2.2.3.1 Periosteum derived cells initial attachment and proliferation tests.....	65
4.2.2.3.2 Osteogenic differentiation test.....	69
4.2.2.3.3 Cell and scaffold observation after culture in osteogenic medium.....	74
4.2.2.3.4 Elemental analysis of periosteum derived cells culture in osteogenic medium	76
V. CONCLUSIONS AND RECOMMENDATIONS.....	77
5.1 Conclusions.....	77
5.2 Recommendations.....	78
REFERENCES.....	79
APPENDICES.....	87
BIOGRAPHY.....	101

LIST OF TABLES

TABLE	PAGE
2.1 Amino acid composition (%) of silk fibroin extracted from different <i>Bombyx mori</i> cocoons.....	7
2.2 Amino acid composition in gelatin.....	12
2.3 Relationships between vapor pressure and temperature in freeze drying System.....	19
2.4 Composition of adult human and bovine cortical bone.....	22
3.1 Weight ratio of inorganic compound/protein (silk fibroin and gelatin) in scaffold.....	42
3.2 Cell surface marker analysis of isolated periosteum derived cells.....	43
4.1 Notation and pore size of Thai silk fibroin/gelatin based scaffolds incorporated with β -TCP and HA.....	53
4.2 Elemental analyses on cell surface after 28 days cultured in osteogenic Medium.....	76
A-1 Mean and SD of compressive modulus of Thai silk fibroin/gelatin scaffolds based scaffold incorporated with inorganic compound, β -TCP and HA.....	88
A-2 Mean and SD of porosity of Thai silk fibroin/gelatin scaffolds based scaffold incorporated with inorganic compound, β -TCP and HA.....	88
B-1 Mean and SD of compressive modulus of Thai silk fibroin/gelatin scaffolds based scaffold incorporated with inorganic compound, β -TCP and HA, in dry condition.....	89
B-2 Mean and SD of compressive modulus of Thai silk fibroin/gelatin scaffolds based scaffold incorporated with inorganic compound, β -TCP and HA, in wet condition.....	89
C-1 Mean and SD of remaining weight (%) of Thai silk fibroin/gelatin scaffolds based scaffold incorporated with inorganic compound, β -TCP and HA, in dry condition during the enzymatic degradation for 28 days.....	90

LIST OF FIGURES

FIGURE	PAGE
2.1 Structure of raw silk.....	5
2.2 Structure of silk fibroin.....	6
2.3 Schematic representation of the primary structure of <i>Bombyx mori</i> silk fibroin.....	8
2.4 Applications of silk.....	9
2.5 Structure of gelatin.....	10
2.6 Preparation processes for acidic and basic gelatins from collagen.....	11
2.7 Application of gelatin.....	13
2.8 Structure of hydroxyapatite.....	14
2.9 Formula structure of β -tricalciumphosphate.....	15
2.10 A typical phase diagram.....	18
2.11 Structure of bone.....	20
2.12 Characteristics of compact bone and cancellous bone.....	21
2.13 Differentiation progression from a multipotent mesenchymal stem cell to a committed osteoblast.....	24
2.14 Bone tissue-engineered scaffolds.....	26
2.15 Location of periosteum.....	27
3.1 Summary of experimental procedures.....	40
4.1 Morphology of (a) β -tricalcium phosphate and (b) hydroxyapatite.....	50
4.2 Size distributions of (a) β -tricalcium phosphate and (b) hydroxyapatite.....	51
4.3 Morphology of Thai silk fibroin/gelatin based scaffolds incorporated with β -TCP and HA. (a) 0/100, (b) 30 β -TCP/70, (c) 50 β -TCP/50, (d) 70 β -TCP/30, (e) 30HA/70, (f) 50HA/50 and (g) 70HA/30.....	54
4.4 Surface morphology of Thai silk fibroin/gelatin based scaffolds incorporated with β -TCP and HA.(a) 0/100, (b) 30 β -TCP/70, (c) 50 β -TCP/50, (d) 70 β -TCP/30, (e) 30HA/70, (f) 50HA/50 and (g) 70HA/30.....	55
4.5 Percentage of water absorption of Thai silk fibroin/gelatin scaffolds incorporated with inorganic compounds, β -TCP and HA.....	57

FIGUR	PAGE
4.6 Porosity of Thai silk fibroin/gelatin scaffolds incorporated with inorganic compound.....	59
4.7 Compressive modulus of Thai silk fibroin/gelatin scaffolds incorporated with inorganic compound; (a) in dry condition, (b) in wet condition.....	61
4.8 The remaining weight (%) of Thai silk fibroin/gelatin scaffolds incorporated with inorganic compounds; β -TCP and HA, after immersion in 1 U/ml collagenase (pH 7.4) at 37°C containing 0.01% w/v sodium azide for 1, 3, 5, 7, 14, 21 and 28 days.....	63
4.9 The number of cells from cytotoxicity test of Thai silk fibroin/gelatin scaffolds incorporated with inorganic compound, β -TCP and HA.....	64
4.10 Number of periosteum derived cell attached and proliferated on Thai silk fibroin/gelatin based scaffolds incorporated with β -TCP and HA under proliferating medium for 1, 3 and 5 days, determined by DNA assay (seeding: 5×10^5 cells/scaffold) a, b represent the significant difference ($p < 0.05$) within the same culture period.....	67
4.11 Morphology of periosteum derived cell cultured under proliferating medium for 5 days on Thai silk fibroin/gelatin based scaffolds incorporated with inorganic compound. (a) 0/100, (b) 30 β -TCP/70, (c) 50 β -TCP/50, (d) 70 β -TCP/30, (e) 30HA/70, (f) 50HA/50 and (g) 70HA/30.....	68
4.12 Number of periosteum derived cells on Thai silk fibroin/gelatin based scaffolds incorporated with β -TCP and HA under osteogenic medium for 3, 5, 7, 14, 21, and 28 days (seeding: 1×10^6 cells/scaffold).....	71
4.13 ALP activity of periosteum derived cells cultured on Thai silk fibroin/gelatin based scaffolds incorporated with β -TCP and HA under osteogenic medium for 3, 5, 7, 14, 21, and 28 days. (seeding: 1×10^6 cells/scaffold).....	72
4.14 Calcium content of periosteum derived cell cultured on Thai silk fibroin/gelatin based scaffolds incorporated with β -TCP and HA under osteogenic medium for 7, 14, 21, and 28 days (seeding: 1×10^6 cells/scaffold).....	73

FIGURE	PAGE
4.15 Morphology of periosteum derived cell cultured under proliferating medium for 28 days on Thai silk fibroin/gelatin base scaffolds incorporated with inorganic compound. (a) 0/100, (b) 30 β -TCP/70, (c) 50 β -TCP/50, (d) 70 β -TCP/30, (e) 30HA/70, (f) 50HA/50 and (g) 70HA/30.....	75
D-1 Standard curve of number of cells for DNA assay.....	91
D-2 Standard curve of p-nitrophenol standard solution for ALP activity.....	92
D-3 Standard curve of CaCO ₃ standard solution for calcium content.....	92
E-1 Elemental analysis using EDX of periosteum derived cell after 28 day culture in osteogenic media; 0/100.....	94
E-2 Elemental analysis using EDX of periosteum derived cell after 28 day culture in osteogenic media; 30 β -TCP/70.....	95
E-3 Elemental analysis using EDX of periosteum derived cell after 28 day culture in osteogenic media; 50 β -TCP/50.....	96
E-4 Elemental analysis using EDX of periosteum derived cell after 28 day culture in osteogenic media; 70 β -TCP/30.....	97
E-5 Elemental analysis using EDX of periosteum derived cell after 28 day culture in osteogenic media; 30HA/70.....	98
E-6 Elemental analysis using EDX of periosteum derived cell after 28 day culture in osteogenic media; 50HA/50.....	99
E-7 Elemental analysis using EDX of periosteum derived cell after 28 day culture in osteogenic media; 70HA/30.....	100

LIST OF ABBREVIATIONS

α -MEM	Minimum Essential Medium Alpha
β -TCP	Beta-tricalcium phosphate
ALP	Alkaline phosphatase
DMEM	Dulbecco's Modified Eagle Medium
DMSO	Dimethyl Sulfoxide
EDC	N-(3-dimethyl aminopropyl)-N'-ethylcarbodiimide- hydrochloride
EDX	Energy-dispersive X-ray spectroscope
FBS	Fetal bovine serum
G	Gelatin
HA	Hydroxyapatite
L929	Mouse fibroblast cells
MC3T3-E1	Mouse Osteoblastic Cells
MTT	3-(4,5-Dimethylthiazol-2-yl)-2,5-diphenyltetrazolium bromide
MSC	Mesenchymal stem cell
NSH	N-hydroxy succimide
PBS	Phosphate buffered saline
pI	Isoelectric point
RGD	Amino acid sequence Arg-Gly-Asp
SEM	Scanning Electron microscope
SF	Silk fibroin

CHAPTER I

INTRODUCTION

1.1 Background

Tissue Engineering is a multidisciplinary field which applies the principles of biology, materials, engineering, and medicine to develop tissue substitutes that can assist the regeneration and repair damaged tissues. Scaffolds play an important role in an accomplishment of tissue regeneration. Different tissues required biodegradable scaffolds with different physical and chemical characteristics. Collagen and silk fibroin are examples of natural biodegradable materials that have been used as tissue engineered scaffolds due to their biocompatible and biodegradable characteristics.

Silk has been investigated as a biomaterial due to the successful use of silk fibers from *Bombyx mori* as suture material for centuries [1]. Silk fibroin is a major constituent of raw silk fiber, which has been widely explored for many biomedical applications, because of its biocompatibility and biodegradability, minimal inflammatory reactions, and favorable mechanical properties. For example, silk fibroin from *Bombyx mori* silkworms is reported to support matrices and ligament using osteoblast, hepatocyte and fibroblast cell for tissue engineering [2]. Thai silk is one of *Bombyx mori* silkworms. Characteristics of cocoon Thai silk are its yellow color and coarse filament. In the recent years, there are a few reports of Thai silk scaffolds for tissue engineering such as electrospun silk fibroin fiber mats as bone scaffolds [3] and biocompatibility of freeze-dried and salt-leached Thai silk fibroin scaffolds [4-7]. To enhance the biological properties of Thai silk fibroin-based scaffolds, Chamchongkaset et. al. [7] have introduced the concept of blending Thai silk fibroin with gelatin. This was due to the fact that gelatin, a derivative of collagen, contains arginine-glycine-aspartic acid (RGD)-like sequence that promotes cell adhesion and migration. Jetbumpenkul [5] has reported that the chemical crosslinked Thai silk fibroin/gelatin scaffolds using EDC/NHS showed lower weight loss (%) and higher compressive modulus than those of non-crosslinked scaffolds. Interestingly, non-crosslinked Thai silk fibroin/gelatin scaffold at the weight blending ratio of 50/50

showed the lowest weight loss (%) with excellent mechanical strength as good as the crosslinked scaffold due to the suitable electrostatic interactions between silk fibroin and gelatin. The incorporation of hydroxyapatite into freeze dried Thai silk fibroin/gelatin scaffold was also preliminarily reported to enhance the mechanical properties. Vachiraroj et.al. [4] have reported the biocompatibility of hybrid scaffolds developed from silk fibroin, gelatin and hydroxyapatite. The *in vitro* results using MC3T3-E1 and rat bone marrow derived stem cells (rMSC) for cell attachment/proliferation and osteogenic differentiation proved that the scaffold had high potential to promote cell attachment and proliferation while hydroxyapatite hybrid scaffolds supported osteogenic differentiation. Takahashi et. al. [8] have reported the gelatin sponges incorporating β -tricalcium phosphate (β -TCP) prepared by chemical crosslinking of gelatin with glutaraldehyde. The obtained scaffolds showed the average pore size of 180–200 μm and well suspension of β -TCP. The *in vitro* study using rMSC show that the cell attachment, proliferation, and osteogenic differentiation in the sponges depended on the β -TCP composition. The presence of β -TCP at 50 wt% showed the best results on cell attachment, proliferation, and osteogenic differentiation. Recently, the integration of two type of materials, inorganic compound and biodegradable materials, such as hydroxyapatite/poly(L-lacticacid)[9],hydroxyapatite/poly-DL-lactide[10],hydroxyapatite/titania/poly(lactide-co-glycolide)[11], β -TCP/gelatin [8] and hydroxyapatite/silk[4], was used to develop a new material with desirable properties. The result on the integration of biodegradable polymer or protein with inorganic compound showed the enhancement of biocompatibility, biodegradability, ability to initiate osteogenesis and mechanical properties.[12] However, the presence of hydroxyapatite and β -TCP in Thai silk fibroin/gelatin system has not been investigated and compared.

It is the aim of this research to investigate the effects of inorganic compounds on the properties of Thai silk fibroin/gelatin scaffolds. Two types of inorganic compounds selected for this study are hydroxyapatite and β -TCP. Different ratios of inorganic compound added in Thai silk fibroin/gelatin solution will be investigated in order to find out the appropriate ratio between inorganic compound and Thai silk fibroin/gelatin which can enhance the mechanical properties and the osteoconduction of the scaffold. The scaffolds will be fabricated via freeze drying. The mechanical properties, swelling property, porosity and pore size will be characterized. The *in vitro* biocompatibility including cell attachment, proliferation and osteogenic

differentiation will be studied using periosteum derived cell. The applicability of Thai silk fibroin/gelatin scaffolds incorporated with inorganic compounds as alternative materials in bone tissue engineering will be evaluated.

1.2 Objective

To investigate the effects of hydroxyapatite and β -tricalcium phosphate on the physical and biological properties of Thai silk fibroin/gelatin scaffolds for bone tissue engineering.

1.3 Scopes of Research

1. Prepare silk fibroin solution from Thai silk cocoon “Nangnoi-Srisaket 1”.
2. Prepare the blended solution of silk fibroin/gelatin (SF/G) at the weight ratio of 50/50 incorporated with inorganic compounds.

Parameters to be investigated are :

- Type of inorganic compound : β -tricalcium phosphate and hydroxyapatite
- Blending weight ratio of each inorganic compound/protein:

0/100,30/70,50/50,70/30

3. Fabricate the scaffold from blended solution by freeze drying technique
4. Investigate the properties of obtained scaffolds

4.1 Physical properties

4.1.1 Morphology by scanning electron microscope (SEM).

4.1.2 Compression modulus (dry and wet condition).

4.1.3 Swelling property

4.1.4 Porosity

4.2 Biological properties

4.2.1 *In vitro* biodegradability

4.2.3 Material cytotoxicity test

4.2.3 *In vitro* biocompatibility using Periosteum derived cell

4.2.3.1 Cell attachment at 1 day and proliferation at 3 and 5 day by DNA assay.

4.2.3.2 Cell differentiation by alkaline phosphatase (ALP) activity and calcium contents.

4.2.3.3 Cell morphology by scanning electron microscopy (SEM) and Energy-dispersive X-ray spectroscopy (EDX)



ศูนย์วิทยทรัพยากร
จุฬาลงกรณ์มหาวิทยาลัย

CHAPTER II

RELEVANT THEORY AND LITERATURE REVIEWS

2.1 Relevant theory

2.1.1 Biomaterials

2.1.1.1 Silk [1, 13-15]

The nature of silk

Silk is naturally occurring protein produced by *Lepidoptera larvae* species including silkworms, spiders, scorpions, mites, butterflies and moths, which form their cocoons. Silk especially from silkworms, has been used commercially as biomedical sutures for decades and used in textile production for centuries. Silk is a fibrous protein synthesized in specialized epithelial cells that line glands in these organisms, followed by secretion into the lumen of these glands where the protein is stored prior to spinning into fibers. The most widely studied silks are cocoon silk from *Bombyx mori* silkworms and dragline silk from *Nephila clavipes* spiders, due to their impressive mechanical properties which are the advantage for textile and biomedical applications.

Silk in its natural form is composed of a filament core protein, silk fibroin, and a glue-like coating consisting of a family of sericin proteins, as shown in Figure 2.1.

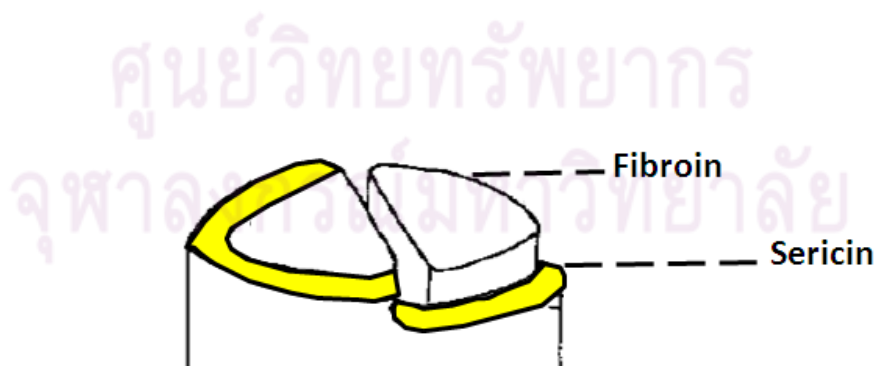


Figure 2.1 Structure of raw silk fiber

Sericin is the water-soluble glue-like protein that binds the fibroin fibers together. It is brittle, and inelastic. The amount of sericin ranges from 20-25wt% of raw silk fiber depending

on the type of cocoon. Sericin is a macromolecular protein which has the molecular weight ranges vary from 10 to over 300 kDa. Removal of the sericin from silk fibroin is accomplished by a process called “degumming” using acid or soap.

A major constituent of raw silk fiber, about 75-80wt%, is silk fibroin. It is an insoluble fibrous protein that is biocompatible with living tissues. Its structure is composed of layers of antiparallel beta pleated sheets (Figure 2.2) which run parallel to the silk fiber axis. Silk fibroin fibers are about 10-25 μm in diameter and composed of heavy (~350 kDa) and light (~25 kDa) polypeptide fractions connected by disulfide linkages. The disulfide linkage between the Cys-c20 (20th residue from the carboxyl terminus) of the heavy chain and Cys-172 of the light chain holds the fibroin together and a P25 (a 25 kDa glycoprotein) is noncovalently linked to these proteins. The heavy chains consist of 12 repetitive regions interspersed with 11 non-repetitive regions. The repetitive regions are responsible for the formation of crystalline β -sheet structures where the non-repetitive regions are amorphous.

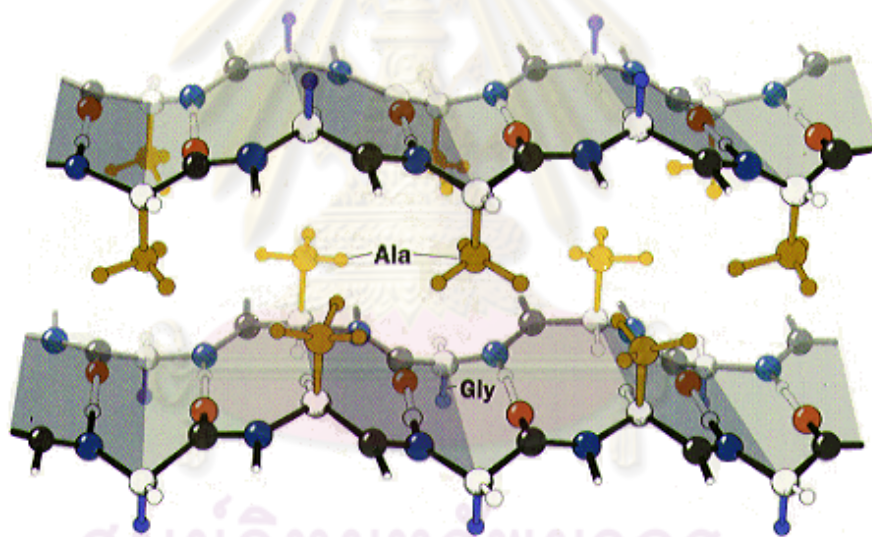


Figure 2.2 Structure of silk fibroin [16].

ศูนย์วิทยทรัพยากร
จุฬาลงกรณ์มหาวิทยาลัย

Amino acid compositions and molecular structure of *Bombyx mori* silk fibroin

Bombyx mori silk fibroin consists of 18 amino acids (Table 2.1) and most of which have strongly polar side groups such as hydroxyl, carboxyl, and amino groups. The isoelectric point is around 3.

Table 2.1 Amino acid compositions (%) of silk fibroins extracted from different *Bombyx mori* cocoons [17].

Amino acid	Silk fibroins			
	Yellow	White	Pink	Green
Glycine, Gly*	50.0	48.8	51.0	47.0
Alanine, Ala*	24.7	27.0	24.5	25.4
Serine, Ser*	10.8	9.8	9.6	10.9
Tyrosine, Tyr*	4.7	5.0	4.8	1.4
Valine, Val*	2.7	2.7	2.9	2.8
Threonine, Thr^o	0.9	1.0	1.0	0.9
Isoleucine, Ile+	2.0	1.2	1.6	1.7
Phenylalanine, Phe+	0.7	0.7	0.8	0.9
Lysine, Lys^o	0.8	1.1	0.9	1.2
Aspartic Acid, Asp^o	0.5	0.7	0.6	1.4
Leucine, Leu+	0.5	0.6	0.6	0.7
Arginine, Arg^o	0.4	0.5	0.5	0.4
Glutamic Acid, Glu^o	0.7	0.5	0.6	1.4
Proline, Pro+	0.5	0.5	0.5	0.4
Methionine, Met+	Nd	Nd	Nd	Nd
Histidine, His^o	Nd	Nd	Nd	Nd
Cysteine, Cys	Nd	Nd	Nd	Nd
Tryptophan, Trp	Nd	Nd	Nd	Nd

*Amino acid forming the repetitive exapeptides (H-chain): Gly, Ala, Ser, Tyr, Val +Non-polar amino acid: Ile, Leu, Phe, Met, Pro ^oBasic amino acid: Asp, Glu, Arg, Thr, Lys, His Nd: not detected.

The primary structure of *Bombyx mori* silk fibroin was generally divided into four regions as shown in Figure 2.3 Region 1 is the highly repetitive Gly-Ala-Gly-Ala-Gly-Ser sequence which constitutes the crystalline part of the fibroin (94% of total chain). Region 2 is the relatively less repetitive Gly-Ala-Gly-Ala-Gly-Tyr and/or Gly-Ala-Gly-Ala-Gly-Val-Gly-Tyr sequences consisting of the semi-crystalline parts. Region 3 is Gly-Ala-Gly-Ala-Gly-Ser-

Gly-Ala-Ala-Ser and Region 4 is the amorphous part containing charged and aromatic residues.

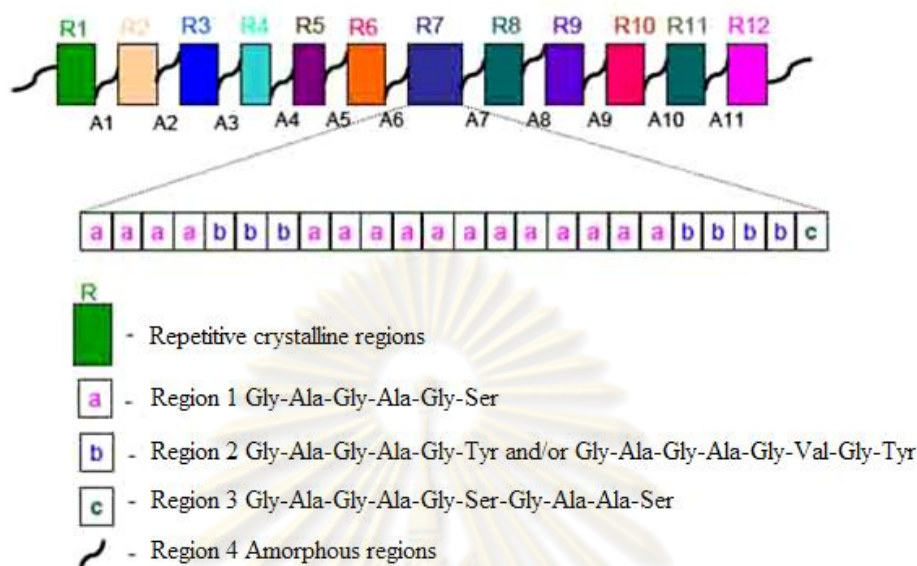


Figure 2.3 Schematic representation of the primary structure of *Bombyx mori* silk fibroin [17].

Thai silk [18]

Thai silk is one of *Bombyx mori* silkworms which mainly produced for textile industry in the northern and north-eastern parts of Thailand. Characteristics of Thai silk are yellow color and coarse filaments. It also contains more silk gum (up to 38%) than other types of *Bombyx mori* silk (20-25%). There are around 28 species of Thai silk such as Nangnoi Srisaket 1, Nangline and other species of blended-Thai silk such as blended-Sakolnakorn and blended-Ubonratchathani 60-35 (lotus).

- Nangnoi Srisaket 1

This specy is easily cultivated. The life cycle is short, approximately 18 days and the color of the cocoon is dark yellow.

- Nangline

This specy is easily degummed. The color of cocoon is dark yellow. The weight of cocoon is 0.68 – 1.64 g and the length of silk fiber is about 311 m/cocoon.

- Blended-Ubonratchathani 60-35

This specy is the blend between Ubonratchathani 60 and Nangnoi Srisaket 1. The color of cocoon is yellow. The weight of cocoon is 1.4 g and the length of silk fiber is about 519 m/cocoon.

Applications of silk

It is well known that silk thread has been used clinically as sutures. In addition, it is used in many applications including textile industry, cosmetics and medical applications. Attractive properties of silk fibroin include its robust mechanical properties when hydrated, biocompatibility, biodegradability, high dissolved-oxygen and water-vapor permeability, and resistance against enzymatic degradation. Examples of products made from silk in medical applications are wound covering materials, gauze pads and bandaged, silk clothes for protecting affected parts (incised wound, burn, tumor, bedsore, etc.), artificial skin, cell-growth substrates, oxygen-permeable membranes, and tissue-engineered scaffolds, as shown in Figure 2.4.



Figure 2.4 Applications of silk [19]

2.1.1.2 Gelatin [20-22]

The nature of gelatin

Gelatin is a protein which does not occur in nature. It is derived from collagen, a main component found in connective tissue, skin and bone of human and animals such as fish, bovine and porcine. Gelatin can be obtained by partial hydrolysis of collagen with subsequent purification, concentration, and drying operations. Gelatin is a polypeptide, i.e. a series of amino acids joined together by peptide bonds as shown in Figure 2.5.

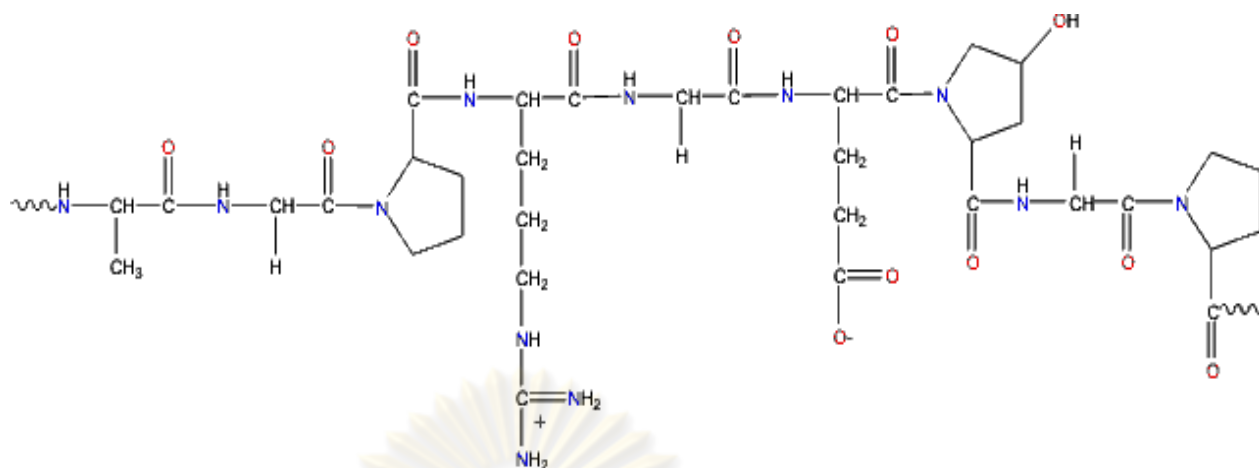


Figure 2.5 Structure of gelatin [22]

Types of gelatin

Gelatin can be divided into 2 types depending on the production process (Figure 6.)

Type A gelatin is produced from an acid process. This process is mainly applied to porcine skin, in which the collagen molecule is young. The isoelectric points (pI) of type A gelatin are in the range of 6-9. High gel strength (bloom strength) gelatins normally have the higher pI and the low bloom strength gelatins have a pI closer to 6.

Type B gelatin is formed from an alkaline process. It is mainly applied to cattle skin and bone, in which the triple helix collagen molecule is more densely crosslinked and complex. Type B gelatin has a pI value around 5.

ศูนย์วิทยทรัพยากร
จุฬาลงกรณ์มหาวิทยาลัย

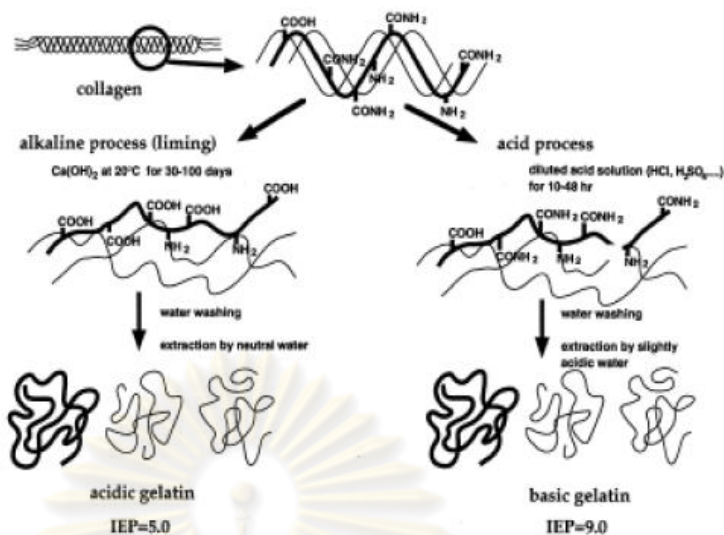


Figure 2.6 Preparation processes for acidic and basic gelatins from collagen [23]

Properties of gelatin

Gelatin is nearly tasteless and odorless. It is colorless or slightly yellow, transparent and brittle. It is soluble in hot water, glycerol, and acetic acid, and insoluble in organic solvents. Gelatin swells and absorbs 5-10 times its weight of water to form a gel in aqueous solutions at low temperature. The viscosity of the gel increases under stress (thixotropic) and the gelation is thermally reversible. Gelatin has a unique protein structure that provides a wide range of functional properties. These proteins can form a triple helix in aqueous solution.

Gelatin is amphoteric, meaning that it is neither acidic nor alkali, depending on the nature of the solution. The pH at which charge of gelatin in solution is neutral is known as the isoelectric point (pI).

The isoelectric point (pI) of a protein is the pH at which the protein will not migrate in an electric field. This is due to the fact that at that pH the molecule carries an equality of positive and negative charges. Gelatin, is rather unique as it can have an isoelectric point anywhere between pH 9 and pH 5, depending upon the source and method of production.

The properties of gelatin from various sources can be different, for example, fish gelatin is distinguished from bovine or porcine gelatin by its low melting point, low gelation temperature, and high solution viscosity.

Amino acid composition

Gelatin is a high molecular weight protein. On a dry weight basis, gelatin consists of 98 to 99% of protein. The molecular weight of these large protein structures typically ranges between 20,000 and 250,000, with some aggregates weighing in the millions. Coils of amino acids are joined together by peptide bonds (Table 2.2). As a result, gelatin contains relatively high levels of amino acids.

Table 2.2 Amino acid composition in gelatin [24]

Amino Acid	%
Alanine	8.9%
Arginine	7.8%
Asperic acid	6.0%
Glutamic acid	10.0%
Glycine	21.4%
Histidine	0.8%
Hydoxylysine	1.0%
Hydroxyproline	11.9%
Isoleucine	1.5%
Leucine	3.3%
Lycine	3.5%
Methionine	0.7%
Phenylanine	2.4%
Proline	12.4%
Serine	3.6%
Theronine	2.1%
Tyrosine	0.5%
Valine	2.2%

Applications of gelatin

Gelatin is biocompatible, biodegradable and nonimmunogenic, which makes it a suitable compound for biomedical applications, such as vascular prosthetic sealants, wound dressing formulation, tissue engineering scaffolds (Figure 2.7), and in drug delivery, e.g., as hard and soft capsules, hydrogel, or microspheres. In addition, it has been commonly used as pharmaceutical, photography, cosmetic manufacturing. It is used extensively in foods as a gelling agent, stabilizer, thickener and clarification of juices. Common examples of foods that contain gelatin are gelatin desserts, jelly, trifles, aspic, marshmallows, ice cream, jams, yogurt and margarine etc.



Figure 2.7 Application of gelatin [25]

2.1.1.3 Hydroxyapatite [26-29]

The nature of hydroxyapatite

Hydroxyapatite, also called hydroxylapatite (HA), is a naturally occurring mineral. It has a occurring form of calcium apatite with the formula of $\text{Ca}_5(\text{PO}_4)_3(\text{OH})$, but is usually written as $\text{Ca}_{10}(\text{PO}_4)_6(\text{OH})_2$ to denote that the crystal unit cell comprises two molecules. Some commercially available hydroxylapatite particles have a size range between 10-40 μm with a Ca/P ratio of 1.62, while other sources had a size range of 160-200 μm with a Ca/P ratio of 1.66 to 1.69. Its crystallized structure has a hexagonal form. The structure of hydroxyapatite is shown in Figure 2.8. Hydroxyapatite is also the main mineral component of bones and hard tissues in mammals; 70% of bone is made up of the inorganic mineral hydroxyapatite.

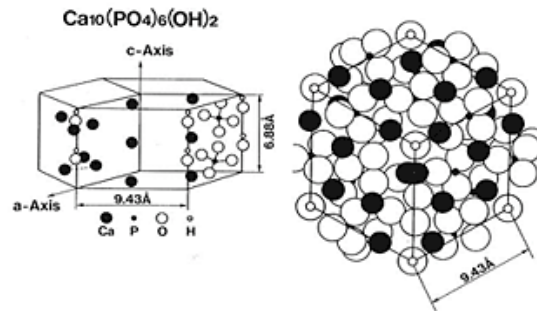


Figure 2.8 Structure of hydroxyapatite [30].

Properties of hydroxyapatite

Naturally occurring apatite is brown, yellow or green while the pure hydroxyapatite is white. Hydroxyapatite has a specific gravity of 3.08 and its Mohs hardness scale is 5. It is decomposed at the temperature of 800 - 1200°C depending on its stoichiometry.

Applications of hydroxyapatite

Hydroxyapatite is a compound of great interest in catalysis, in the industry of fertilizers, protein chromatography, bioceramic coatings and water treatment procedures. It is also used in the preparation of bioactive materials because it is the inorganic crystalline constituent in vertebrates calcified hard tissues such as bone and teeth. Hydroxyapatite may be employed in forms of powders, porous blocks or beads to fill bone defects or voids when large sections of bone are removed (e.g. bone cancers) or when bone augmentations are required (e.g. maxillofacial reconstructions or dental applications). The bone filler acts as a scaffold and encourages the rapid filling of the void by naturally forming bone. Treatment using bone filler can reduce healing times compared to the case of empty defect.

2.1.1.4 β -tricalcium phosphate [31-33]

Natural of β -tricalcium phosphate

β -tricalcium phosphate (β -TCP) is a beta crystal form of tricalcium phosphate (Figure 2.9). The formula of β -TCP is $\text{Ca}_3(\text{PO}_4)_2$. It is also known as calcium orthophosphate, tertiary calcium phosphate, tribasic calcium phosphate, or bone ash because tricalcium phosphate is the main combustion products of bone.

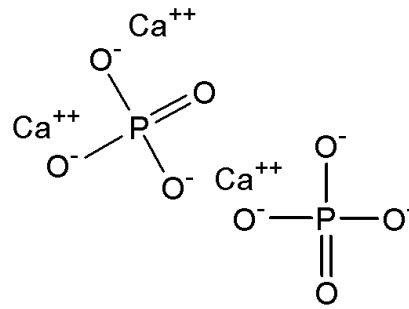


Figure 2.9 Formula structure of β -tricalcium phosphate [33]

In minerals, calcium phosphate refers to minerals containing calcium ions (Ca^{2+}) together with orthophosphates (PO_4^{3-}), metaphosphates or pyrophosphates ($\text{P}_2\text{O}_7^{4-}$) and occasionally hydrogen or hydroxide ions. Most of the tricalcium phosphate on the market is actually in powder form.

Properties of β -tricalcium phosphate

Its appearance of β -tricalcium phosphate is white amorphous powder. β -tricalcium phosphate has a density of 3.14 g/cm^3 . Its melting point is 1391°C . The molecular weight of β -tricalcium phosphate is 310.78 g/mol . It is found in nature as a rock in Morocco, Israel, Philippines, Egypt, and Kola (Russia) and in smaller quantities in some other countries. The natural form is not completely pure, and there are some other components like sand and lime which can change the composition.

Application of β -tricalcium phosphate

Tricalcium phosphate in both alpha and beta crystal form is used in powder form as an anti-caking agent. It is an important raw material for the production of phosphoric acid and fertilizers.

It is commonly used in porcelain and dental powders medically as an antacid or calcium supplement and as a tissue replacement for repairing bony defects when autogenous bone graft is not feasible or possible. It may be used alone or in combination with a biodegradable, resorbable polymer such as polyglycolic acid and also be combined with autologous materials for a bone graft.

2.1.2 Characteristics of three-dimensional scaffold [34]

Growing cells in three-dimensional scaffold has been of great interest. In this approach, scaffold plays an important role. It guides cells to grow, synthesizes extracellular matrix and other biological molecules, and facilitates the formation of functional tissues.

Ideally a scaffold should possess the following characteristics to bring about the desired biologic responses [35]:

- 1) Three-dimensional and highly porous with an interconnected pore network for cell/tissue growth and flow transport of nutrients and metabolic waste
- 2) Biodegradable or bioresorbable with a controllable degradation and resorption rate to match cell/tissue growth *in vitro* and/or *in vivo*
- 3) Suitable surface chemistry for cell attachment, proliferation and differentiation
- 4) Mechanical properties to match those of tissues at the site of implantation
- e) Easily processed to form a variety of shapes and sizes

2.1.3. Scaffold fabrication by freeze drying technique

Principles of freeze drying [36-37]

Freeze drying has been used in a number of applications for many years, most commonly in food and pharmaceutical industries. There are also some other uses for the processes including the stabilization of living materials such as microbial cultures, preservation of whole animal specimens for museum display, restoration of books and other items damaged by water, and recovery of reaction products. Freeze drying involves the removal of water or other solvent from a frozen sample by a process called sublimation. Sublimation occurs when a frozen liquid goes directly to gas phase without passing through liquid phase. In contrast, drying at ambient temperatures from the liquid phase usually results in changes in the product, and may be suitable only for some materials.

The freeze drying process consists of three stages involving prefreezing, primary drying, and secondary drying.

Prefreezing

Since freeze drying is a state change from solid to gas phase, material to be freeze dried must first be adequately frozen. The method of prefreezing and the final temperature of the frozen sample have a direct effect on freeze dried material. Rapid cooling rate results in small ice crystals, useful in preserving structures to be examined microscopically, but more difficult to freeze dry. Slower cooling rate results in larger ice crystals and lesser restrictive channels in the matrix during the drying process. A low final freezing temperature can increase the rate of cooling as well as the rate of ice crystal nucleation and decreases the rate of heat and protein diffusion, leading to small ice crystals. Samples that are subjected to freeze drying consist primarily of water or solvent, materials dissolved or suspended in water or solvent. Most samples used to be freeze dried are eutectics which are a mixture of substances that freeze at lower temperatures than surrounding water. When the aqueous

suspension is cooled, changes occur in the solute concentrations of the matrix. As cooling proceeds, water is separated from solutes as it changes to ice, creating more concentrated areas of solute. These pockets of concentrated materials have a lower freezing temperature than water. Although a product may be frozen because of all the ice presented, it is not completely frozen until all of the solute in the suspension is frozen. It is very important in freeze drying to freeze the sample to below the eutectic temperature before beginning the freeze drying process. Small pockets of unfrozen material remaining in the sample expand and compromise the structural stability of the freeze dried sample.

Primary drying

Several factors can affect the ability to freeze dry a frozen suspension. While these factors can be discussed independently, it must be remembered that they interact in a dynamic system, and it is delicate balance between these factors that results in a properly freeze dried sample. After prefreezing the product, conditions must be established in which ice can be removed from the frozen sample via sublimation, resulting in a dry, structurally intact sample. This requires very careful control of two parameters, temperature and pressure. The rate of sublimation of ice from a frozen sample depends upon a difference in the vapor pressure of the product compared to the vapor pressure of the ice collector. Molecules migrate from a higher pressure area to a lower pressure area. Since vapor pressure is related to temperature, it is necessary that the sample temperature is warmer than the cold trap (ice collector) temperature. The balance between the temperature that maintains the frozen integrity and the temperature that maximizes the vapor pressure of the sample is extremely important, since it is the key to optimum drying. The typical phase diagram shown in Figure 8. illustrates this point. Most samples are frozen well below their eutectic temperature (Point A), and then the temperature is raised to just below this critical temperature (Point B) and they are subjected to a reduced pressure. At this point the freeze drying process is started.

ศูนย์วิทยทรัพยากร
จุฬาลงกรณ์มหาวิทยาลัย

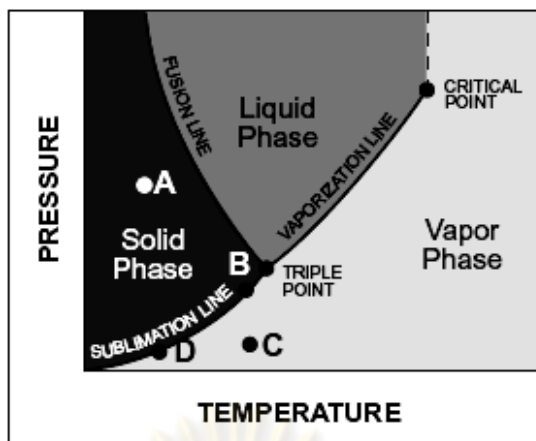


Figure 2.10 A typical phase diagram [36].

Freeze drying conditions must be created to encourage the free flow of water molecules from the sample. Therefore, a vacuum part is essentially needed to lower the pressure of the environment (to Point C). Another essential part is a collecting system, which is a cold trap used to collect moisture that leaves the frozen sample. The collector condenses all condensable gases, i.e. water, and the vacuum part removes all non-condensable gases. It is important to understand that the vapor pressure of the sample forces the sublimation of the water vapor molecules from the frozen sample matrix to the collector. The molecules have a natural affinity to move toward the collector because its vapor pressure is lower than that of the sample. Therefore, the collector temperature (Point D) must be significantly lower than the sample temperature. In addition, raising the sample temperature has more effect on the vapor pressure than lowering the collector temperature. The relationships between vapor pressure and temperature are shown in Table 2.3.

ศูนย์วิทยทรัพยากร
จุฬาลงกรณ์มหาวิทยาลัย

Table 2.3 Relationships between vapor pressure and temperature in freeze drying system [36].

Vapor Pressure (mBar)	Temperature (°C)
6.104	0
2.599	-10
1.034	-20
0.381	-30
0.129	-40
0.036	-50
0.011	-60
0.0025	-70
0.0005	-80

The last essential part in a freeze drying system is energy. Energy is supplied in form of heat. Energy required to sublime a gram of water from the frozen to gas phase is almost 10 times greater than that required to freeze a gram of water. Therefore, with all other conditions being adequate, heat must be applied to the sample to encourage the removal of water in the form of vapor from the frozen sample. The heat must be very carefully controlled, since applying more heat than the evaporative cooling in the system can warm the sample above its eutectic temperature. Heat can be applied by several methods. One is to apply heat directly through a thermal conductor shelf such as in tray drying. Another method is to use ambient heat as in manifold drying.

Secondary drying

After primary freeze drying is complete and all ice has sublimed, bound moisture is still presented in the sample. The residual moisture content may be as high as 7-8%. Continued drying is necessary at a higher temperature to reduce the residual moisture content to optimum values. This process is called isothermal desorption as the bound water is desorbed from the sample.

Secondary drying is normally operated at a sample temperature higher than ambient but compatible with the sensitivity of the sample. All other conditions, such as pressure and collector temperature, remain the same. Secondary drying is usually carried out for approximately 1/3 to 1/2 the time required for primary drying.

2.1.4 Bone

2.1.4.1 Structure of bone [38]

Bones are rigid organs that form part of the endoskeleton of vertebrates. They function to move, support, and protect the various organs of the body and store minerals. The structure of bone shown in Figure 2.11 can be grouped into 4 levels.

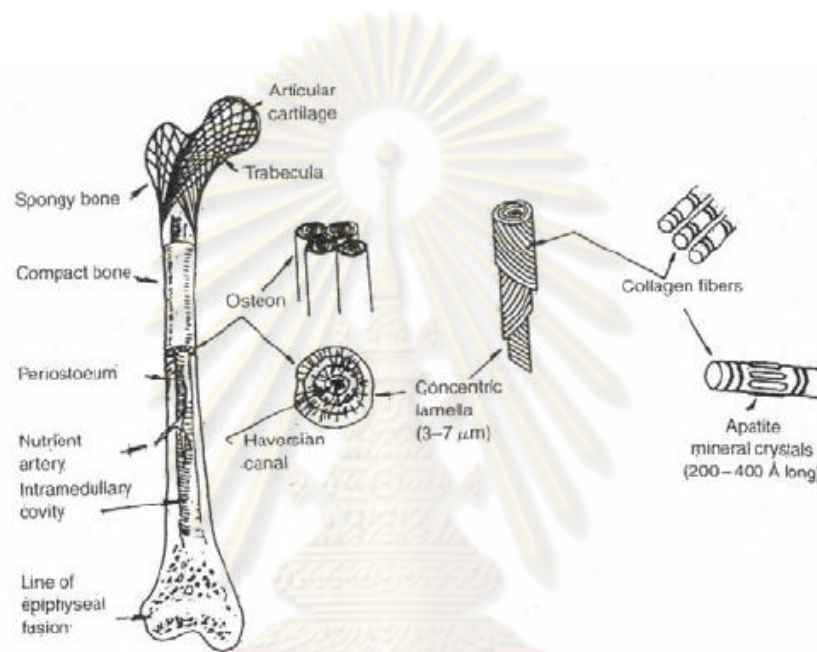


Figure 2.11 Structure of bone [38]

Molecular level

The smallest unit of structure is the tropocollagen molecule and the associated apatite crystallites. The former is approximately $1.5 \times 280 \text{ nm}^2$, made up of three individual left-handed helical polypeptide chains coiled into a right-handed triple helix. Apatite crystallites have been found to be carbonate-substituted hydroxyapatite. The crystallites appear to be about $4 \times 20 \times 60 \text{ nm}^3$ in size.

Ultrastructural level

The collagen and apatite are intimately associated and assembled into a microfibril composite, several of which are then assembled into fibers from approximately 3 to 5 μm thick.

Microstructural level

These collagen fibers are either randomly arranged (woven bone) or organized into concentric lamellar groups (osteons in the case of human) or linear lamellar groups (plexiform bone in the case of mammals). In addition to the differences in lamellar organization at this level, there are also two different types of architectural structures as shown in Figure 2.12.

- Compact or cortical bone

The hard outer layer of bone is composed of compact and dense bone tissue, due to its minimal gaps and spaces. This tissue gives bones their smooth, white, and solid appearance, and accounts for 80% of the total bone mass of an adult skeleton.

- Cancellous or trabecular bone

Cancellous bone is more porous or spongy. It is composed of a network of rod and plate-like elements that make the overall organ lighter and allowing room for blood vessels and marrow. Cancellous bone accounts for the remaining 20% of total bone mass.

Compact Bone & Spongy (Cancellous Bone)

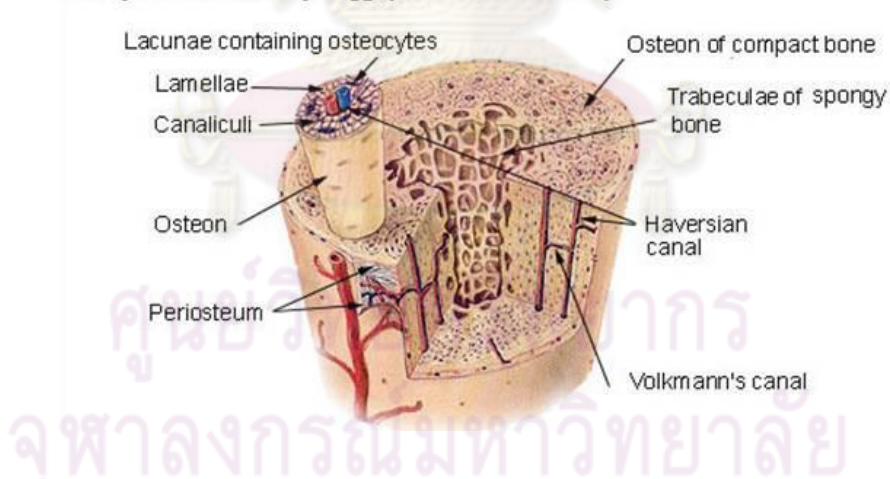


Figure 2.12 Characteristics of compact bone and cancellous bone [39]

Macrostructural level

Finally, the whole bone constructs of osteons and portions of older, partially destroyed osteons or plexiform bone. The elastic properties of the whole bone results from the hierarchical contribution of each of this level.

Composition of bone

The composition of bone depends on a large number of factors: the location from which the sample is taken, age, sex, and type of bone tissue, for example, woven, cancellous, cortical. However, a rough estimate for overall composition by volume is one-third apatite, one-third collagen and other organic components, and one-third H₂O. The compositions of adult human and bovine cortical bone are given in Table 2.4.

Table 2.4 Composition of adult human and bovine cortical bone [38].

Species	%H ₂ O Apatite	%dry weight	collagen	Glycosaminoglycan (GAG)
Bovine	9.1	76.4	21.5	Not determined
Human	7.3	67.2	21.2	0.34

2.1.4.2 Mineralization [40]

Bone development can be divided into three stages: proliferation, extracellular matrix maturation and mineralization. There are two phases for mineralization. In the first phase, osteoblasts secrete an organic matrix which is considered to be a preosseous matrix (osteoid). The osteoid consists of type I collagen, proteoglycans, glycoproteins and non-collageneous proteins. During the second phase, mineralization occurs and osteoid is transformed into bone.

Osteoblastic cells derived from human and rodent bone tissue were used for the mineralization studies. In primary cultures, isolated osteoblasts have been shown to synthesize several proteins and enzymes which are known to be localized in bone such as alkaline phosphatase (ALP), osteocalcin and type I collagen. Primary human bone cells are cultured for sufficient lengths of time (about 30 days), nodules is formed by the cells. Nodules are a dense matrix which cells lay down and develop a granular appearance. These nodules appear to consist of calcium phosphate crystals

embedded in matrix. The process is usually associated with the release of vesicle-type structures from the cells and this may initiate mineral deposition.

Culture conditions contribute the ability of cells to differentiate and calcify. The addition of agents such as calcium β -glycerophosphate, glucocorticoids, sodium β -glycerophosphate, calcium hexose monophosphate and dexamethasone are used to promote mineralization of osteoblasts in culture.

2.1.5 Bone Tissue Engineering [41-42]

Sometimes injured bone cannot be healed by the natural healing process. In traditional, there are several methods for treating the severe fractures. The most common method involves placing a bone graft, which can be derived from own patient (autograft bone marrow and bone matrix) or from a registered bone bank (allograft bone matrix without cells) into the defect site. However, there are some limitations of these methods. For example, size of the defect, autologous bone supply and viability of the host bed can be problems of autograft. In large defects, autologous bone graft can often be resorbed before osteogenesis is complete. Technically, it can be difficult to shape bone grafts to fit the defect well. For these reasons, tissue engineering offers great potential for the construction and regeneration of bone. The emerging field of tissue engineering aims to combine engineering technology and the principles of biological science to develop strategies for the repair and regeneration of lost or damaged tissue. Tissue engineering concept is consisting of three general strategies: (1) cell-based strategies, (2) growth factor-based strategies and (3) matrix-based strategies. In practice, most experimental works combine two or more of these strategies together towards a solution. In the realm of bone tissue engineering, these strategies require interaction between osteogenic, osteoinductive, and osteoconductive elements. Osteogenic components include cells capable of bone production such as osteoprogenitor cells, stem cells or differentiated osteoblasts. Osteoinductive factors include bioactive chemicals that induce recruitment, differentiation, and proliferation of the proper cell types at an injury. A material that supports bone growth demonstrates osteoconductivity. An osteoconductive scaffold may provide mechanical support, sites for cell attachment and vascular ingrowth. It can also be served as a delivery vehicle for implanted growth factors and cells.

2.1.5.1 Cell based strategies [43-45]

Cell-based strategies for bone regeneration by tissue engineering approach involve the implantation of cells with osteogenic potential directly into a defect site. Cell transplantation is particularly beneficial to patients with a low number of cells, as in the case of vascular disease or irradiated tissue around the site of tumor resection. The choice of cell type is important and various cells have been employed for bone regeneration. These include transplantation of fresh marrow containing osteoprogenitor cells, differentiated osteoblasts or chondrocytes, and purified mesenchymal stem cells. These cells may not be capable of synthesizing bone matrix themselves but instead are expected to stimulate differentiation to an osteogenic phenotype through delivery of bioactive factors. Populations of differentiated osteoblasts are typically derived from mesenchymal stem cells found in bone marrow or periosteum using osteogenic cell culture supplements including β -glycerophosphate, dexamethasone, and L-ascorbic acid. Figure 2.13 illustrates the progression from multipotent mesenchymal stem cells to committed osteoblasts. The proliferative capacity of the cells decreases as they differentiate toward a specific matrix-producing phenotype.

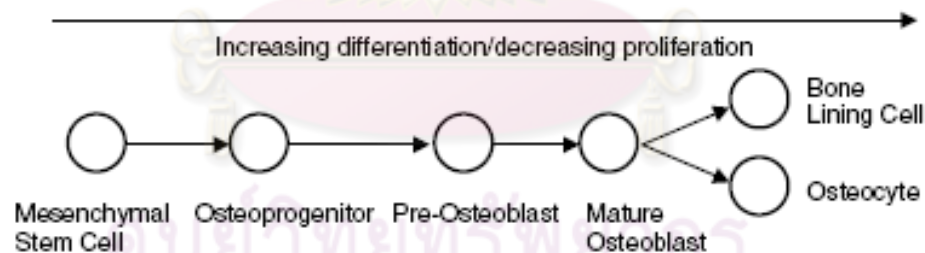


Figure 2.13 Differentiation and progression from a multipotent mesenchymal stem cell to a committed osteoblast [44]

2.1.5.2 Growth factor based strategies [41]

Osteoinductive growth factors have been identified, two of the most common groups in the transforming growth factor- β superfamily are the bone morphogenic proteins (e.g., BMP-2, BMP-7) and the transforming growth factor- β s (e.g. TGF- β 1). BMPs are growth factors that stimulate differentiation of mesenchymal stem cells into

osteoblasts as well as proliferation and function of both chondrocytes and osteoblasts. TGF- β s are growth factors that stimulate differentiation of mesenchymal stem cells towards chondrocytes and proliferation of osteoblasts and chondrocytes. Both types of growth factors have been shown to enhance bone resorption at certain concentrations. Other growth factors with similar effects are fibroblast growth factors (FGFs), insulin-like growth factors (IGFs), platelet-derived growth factors (PDGFs), and epidermal growth factors (EGFs). Vascular endothelial growth factor (VEGF) is also as important as osteoinductive growth factors for bone applications because it promotes vascularization and angiogenesis by encouraging endothelial cell proliferation and migration. In fact, VEGF is unique among most angiogenic growth factors since it acts directly upon endothelial cells. Another important osteoinductive substance is dexamethasone, a potent synthetic member of the glucocorticoid class of steroid hormones. It is also known to induce osteogenic differentiation of mesenchymal stem cells *in vitro*.

2.1.5.3 Matrix-based strategies [41,44,46]

Osteoconductive material has ability to act as a substrate for cell adhesion and function while facilitating bone growth throughout a three-dimensional scaffold across a defect. Functional modification of biomaterial surfaces is another promising strategy being investigated to improve the efficacy of scaffolds for bone tissue engineering. The conformation of the absorbed proteins or protein fragments on material surfaces can be utilized to direct integrin receptor binding and thereby control cell proliferation and differentiation. The engineering of rationally designed surfaces that control cell function may endow osteoconductive scaffolds with the additional ability to induce osteoblast differentiation and subsequent bone regeneration

Biodegradable materials are highly preferred over nondegradable materials, though they are generally weaker. Controlled degradation of a scaffold allows gradual load transfer to bone, increasing space for bone growth, and eventual filling of a defect with natural bone. This opposed to a permanent biomaterial which may cause stress-shielding or infection. Furthermore, predictable degradation time of the scaffold is also crucial. If a scaffold degrades very slowly, as is the case with many hydroxyapatite formulations, it will restrict bone regeneration and may fail

mechanically due to repetitive loading. In contrast, a scaffold that degrades very fast may lose their mechanical integrity before the defect site can be stabilized by newly formed bone. The degradation mechanism may also be important since scaffolds may experience hydrolytic, enzymatic, bulk, or surface degradation.

Mechanical properties of a scaffold should initially match the properties of the target tissue in order to provide structural stability to an injury site (Figure 2.14). The chosen biomaterial must be strong enough to support the physiological load of the body without absorbing the mechanical stimuli required for natural growth in the affected area.

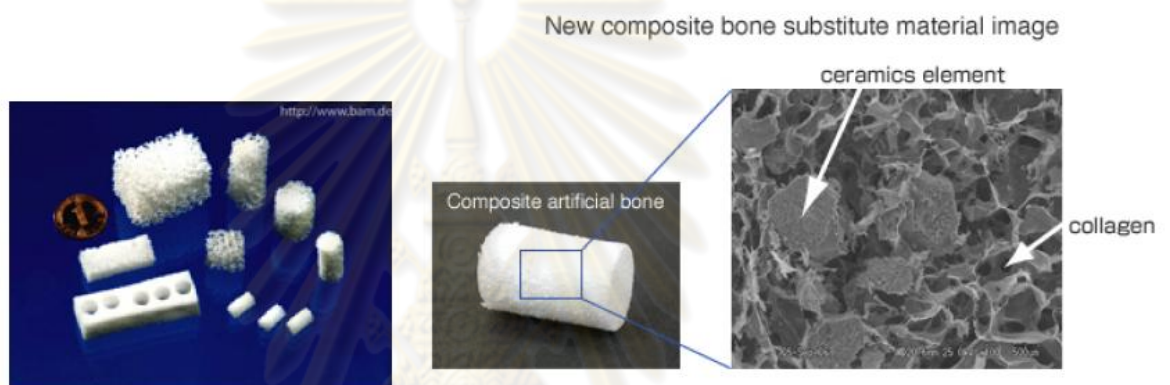


Figure 2.14 Bone tissue-engineered scaffolds. [47,48]

ศูนย์วิทยทรัพยากร
จุฬาลงกรณ์มหาวิทยาลัย

2.1.6. Periosteum derived cell [49-50]

Periosteum derived cell is a cell which isolated from membrane that lines the outer surface of all bones cell periosteum (Figure 2.15).

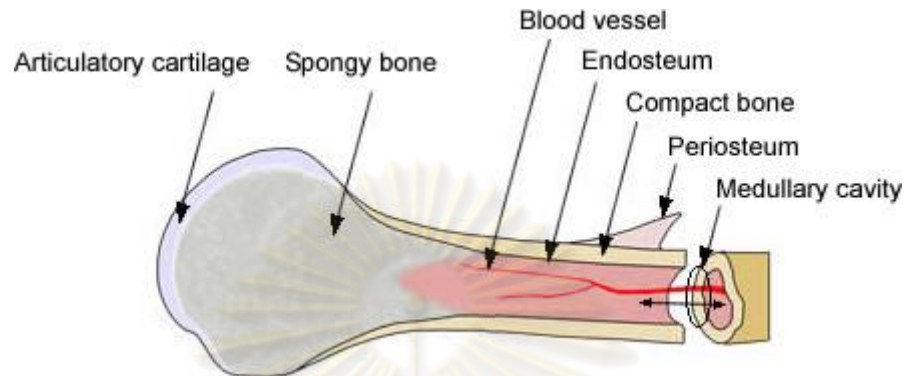


Figure 2.15 Location of periosteum [50]

Periosteum is divided into an outer fibrous layer and inner cambium layer or osteogenic layer. The fibrous layer contains fibroblasts, while the cambium layer contains progenitor cells that develop into osteoblasts. These osteoblasts are responsible for increasing the width of a long bone and the overall size of the other bone types. After a bone fracture the progenitor cells develop into osteoblasts and chondroblasts, which are essential to the healing process.

Periosteum can be described as an osteoprogenitor cell-containing bone envelope, which can be activated to proliferate by trauma, retroviruses, tumors, and lymphocyte mitogens. Activated periosteum produces cartilage and bone, and is colonized by osteoclasts. The osteogenic activity of periosteum is maintained in heterotrophic sites and *in vitro*.

ศูนย์วิทยุทันตกรรม
จุฬาลงกรณ์มหาวิทยาลัย

2.2 Literature review

2.2.1 Gelatin/silk fibroin and collagen/silk fibroin systems

Meinel, L. et.al. [51]

In 2004, Lorenz Meinel *et.al.* compared porous scaffolds made of silk (slow degrading), silk-RGD (slow degrading, enhanced cell attachment), and collagen (fast degrading) for tissue-engineered human bone using human bone marrow derived mesenchymal stem cells (hMSCs). Histological analysis and microcomputer tomography (micro-CT) showed the development of up to 1.2-mm-long interconnected and organized bone-like trabeculae with cuboid cells on the silk-RGD scaffolds, features still present but to a lesser extent on silk scaffolds and absent on the collagen scaffolds. Biochemical analysis showed increased mineralization on silk-RGD scaffolds compared with either silk or collagen scaffolds after 4 weeks. Expression of bone sialoprotein, osteopontin, and bone morphogenetic protein 2 was significantly higher for hMSCs cultured in osteogenic than control medium both after 2 and 4 weeks in culture. The results suggest that RGD-silk scaffolds are particularly suitable for autologous bone tissue engineering, because of their stable macroporous structure, tailorable mechanical properties matching those of native bone, and slow degradation.

Gil, E.S. et.al. [52]

In 2005, Eun S. Gil *et.al.* examined the swelling and protein release kinetics of gelatin/silk fibroin (G/SF) hydrogels varying in composition at temperatures below and above the helix \rightarrow coil (h \rightarrow c) transition of gelatin. G/SF hydrogels have been prepared by blending gelatin with amorphous *Bombyx mori* silk fibroin and promoting β -crystallization of silk fibroin via subsequent exposure to aqueous MeOH solutions. The mass of protein released was acquired from the basis of an intensity-concentration calibration curve. These were determined by colorimetric assay with a bicinchoninic acid protein assay and spectrophotometry. The swelling behavior of these hydrogels reveals that β -crystallization is virtually complete after only 5 min of exposure to 75/25 w/w MeOH/water solution and sensitive to MeOH concentration in the aqueous MeOH solutions. The results demonstrated that at 20°C, gelatin and gelatin-rich mixed hydrogels display moderate swelling with negligible mass loss in

aqueous solution, resulting in porous polymer matrices upon solvent removal. When the solution temperature is increased beyond the h→c transition of gelatin to body temperature (37°C), these gels exhibit much higher swelling with considerable mass loss, indicating that the dissolved triple-helix conformation of gelatin permits greater water sorption and protein as gelatin molecules are slowly released into the surrounding aqueous solution.

Gil, E.S. et.al. [53]

In 2005, Eun S. Gil *et.al.* investigated the effect of β -sheet crystals on the thermal and rheological behavior of gelatin/silk fibroin (G/SF) hydrogels. G/SF hydrogels with various contents have been prepared by blending type A gelatin with amorphous *Bombyx mori* silk fibroin and subsequently inducing crystallization of silk fibroin upon exposure to 75/25 w/w MeOH/water solution for 2 h at 20°C. Thermal calorimetry and dynamic rheology results showed that if the silk fibroin chains possess a random-coil conformation within the G/SF gels, they have little effect on the helix→coil (h→c) transition of gelatin. Silk fibroin serves to dilute the stabilizing efficacy of the triple-helix crosslink sites, thereby reducing the dynamic elastic modulus of G/SF gels. On the other hand, the silk fibroin chains possess a β -sheet conformation, they can, at sufficiently high concentration, shift the h→c transition of gelatin to higher temperature, increase the dynamic elastic modulus of the G/SF gels and also stabilize the hydrogels to much higher temperatures than the untreated gels. Even in the presence of silk fibroin β -crystalline network, the h→c transition of gelatin is found to be thermally reversible between ambient and body temperature.

Gil, E.S. et.al. [71]

In 2006, Eun S. Gil *et.al.* studied the effects of solvent-induced crystallization and composition in G/SF hydrogels. After exposure to aqueous MeOH solutions, silk fibroin undergoes a conformational change from random coil to β -sheet. According to infrared spectroscopy (FTIR) and wide-angle x-ray diffraction (WAXD), this transformation occurred in pure silk fibroin as well as in each of the G/SF blends quickly, typically within a few minutes. Thermal calorimetry (DSC) reveals the existence of relatively low temperature thermal transitions (glass transition temperature, T_g and crystallization temperature, T_c) in untreated silk fibroin and silk fibroin-rich blends with gelatin. These transitions disappear entirely upon MeOH

treatment. Thermal gravimetric analysis (TGA) indicates that the formation of the β -sheet structure generally improved thermal stability at elevated temperatures, enhances the mechanical properties, such as tensile modulus, elongation, and tensile strength of the blends, and also used to stabilize gelatin-based hydrogels for biomaterial and pharmaceutical purposes.

Lv, Q. et.al. [54]

In 2007, Qiang Lv *et.al.* prepared silk fibroin/collagen hydrogels by crosslinking silk fibroin/collagen solutions with different contents of 1-ethyl-3-(3-dimethylaminopropyl)carbodiimide, hydrochloride (EDC). The hydrogels were formed via freeze-drying method. The weight percentage of silk fibroin and collagen in dried blend scaffolds was fixed as 80% and 20%, respectively. It was found that, when the weight percentage of EDC was above 10%, especially 20% and 30%, compared with silk fibroin/collagen dried scaffolds without EDC, the stiff silk fibroin/collagen hydrogels were formed (storage modulus >10 kPa by rheological analysis). Furthermore, these hydrogels can maintain their configuration above 80°C and still maintain the mobility of silk fibroin molecules. The growth of vascular smooth muscle cells (VSMCs) in silk fibroin/collagen gels indicates that the crosslinking reaction has no negative influence on the biocompatibility of these gels. Therefore the stiff silk fibroin/collagen hydrogel has better cytocompatibility than silk fibroin/collagen scaffold, an excellent biomaterial for tissue engineering.

2.2.2 Silk fibroin and gelatin incorporated with inorganic compound systems.

Chang, M.C. et.al. [55]

In 2003, Myung Chul Chang *et.al.* developed biomimetic process, for the formation of organized hydroxyapatite (HA) – gelatin (G) nanocomposites. The HA nanocrystals were precipitated in aqueous solution of G at pH 8 and 38°C. The coprecipitated HA–G nanocomposites showed chemical bonding between calcium ions of HA and carboxyl ions of G molecules induced a red shift of the 1339 cm^{-1} band of G in FT-IR analysis. A self-organization of HA nanocrystals along G fibrils was observed in TEM images and electron diffraction patterns. The concentration ratio of G to HA greatly influenced the nucleation and the development of HA

nanocrystals. A higher concentration of G induced the formation of tiny crystallites (4nm×9 nm size), while a lower concentration of G contributed to the development of bigger crystallites (30nm×70nm size). From TGA-DTA data, the HA-G nanocomposites showed typically three exothermic temperatures consist of the thermal degradation and pyrolyzation of G molecules, and the final thermal degradation of the residual organics. The increase in decomposition temperatures indicates the formation of a primary chemical bond between HA and G.

Takahashi, Y. et.al.[8]

In 2004, Yoshitake Takahashi et.al. Study the osteogenic differentiation of mesenchymal stem cells in biodegradable sponges composed of gelatin. In this study gelatin sponges incorporating β -TCP were prepared by chemical crosslinking of gelatin with glutaraldehyde in the presence of β -TCP. The 3 wt% aqueous solution of gelatin containing different amounts of β -TCP was mixed at 5000 rpm at 37°C for 3 min by using a homogenizer. After 0.16 wt% of glutaraldehyde aqueous solution was added to the mixed solution, the β -TCP dispersed gelatin solution was further mixed for 15 s by the homogenizer. The resulting formy solution was cast and followed by leaving at 4°C for 12 h for gelatin crosslinking .Then the crosslinked gelatin was washed with glycine solution to block the residual aldehyde groups of glutaraldehyde. The obtained scaffolds showed the average pore size of 180–200 mm and well suspension of β -TCP. The *in vitro* study using mesenchymal stem cells show that the cell attachment, proliferation, and osteogenic differentiation in the sponges depended on the β -TCP composition. The presence of β -TCP at 50 wt% showed the best results on osteogenic differentiation.

Wang, L. et.al. [45]

In 2005, Li Wang et.al. prepared hydroxyapatite (HA)-based nanocomposite solid via a wet-mechanochemical route with either untreated and alkali pretreated silk fibroin powders (USF and ASF). Silk fibroin powders were treated using an alkali solution (NaOH 0.05 M) attempting to disentangle their surface fibrils and to enhance the effective contact between the mineral and the organic particles. With the ASF involved, Vickers microhardness of the composite increases by 57% and a more enhanced three-dimensional porous network with a homogenous particle form and a uniform pore size distribution is formed through the intimate crosslinkage between HA clusters and silk fibroin fibrils. In addition, ASF increased the viscosity and the

rigidity of the composite solid, and promotes its gelation process, which is favorable for healing bone defects by an injection technique.

Du, C. et.al. [56]

In 2008, Chunling Du *et.al.* fabricated *bombyx mori* silk fibroin (SF) and hydroxyapatite (HA) composite films, with glycerin as an additive, by means of coprecipitation, where the theoretical HA content was varied from 2 w/w% to 31 w/w%. The results showed that the SF/HA composite films were smooth and transparent with the uniform distribution of HA into the composites at a low level of HA content (the HA content was lower than 21 w/w%). XRD and TGA data showed that the SF in the composites was predominantly in a β -sheet crystalline structure, which was induced not only by the addition of glycerin, also by the HA crystal growth during the composite fabrication, leading to the thermal stable composite films. On the other hand, the HA crystals had the anisotropic growth with high extent of lattice imperfection and the preferential orientation along c-axis, probably promoted by the SF. The mechanical testing results showed that both break strain and stress were declined with the increase of HA content in the composites, presumably due to the original brittleness of HA compound.

Peter, M. et.al.[57]

In 2010, Mathew Peter *et.al.* studied the preparation and characterization of chitosan–gelatin/nanohydroxyapatite composite scaffolds for tissue engineering applications. In this work, chitosan–gelatin/nanophase hydroxyapatite composite scaffolds were prepared by blending chitosan and gelatin with nanophase hydroxyapatite (nHA). The prepared nHA was characterized using TEM, XRD and FT-IR. The prepared composite scaffolds were characterized using SEM, FT-IR and XRD. The composite scaffolds were highly porous with a pore size of 150–300 μm . In addition, density, swelling ratio, degradation, biomineralization, cytotoxicity and cell attachment of the composite scaffolds were studied. The scaffolds showed good swelling characteristic, which could be modulated by varying ratio of chitosan and gelatin. Composite scaffolds in the presence of nHA showed a decreased degradation rate and increased mineralization in simulated body fluid (SBF). The biological response of MG-63 cells (human osteosarcoma cell line) on nanocomposite scaffolds was superior in terms of improved cell attachment, higher proliferation, and spreading compared to chitosan–gelatin (CG) scaffold.

Zhang, Y. et.al/[58]

In 2010, Yufeng Zhang et.al. developed the porous CaP/silk composite scaffolds with a CaP-phase distribution and pore architecture suited to facilitate osteogenic properties of human bone mesenchymal stromal cells (BMSCs) and *in vivo* bone formation abilities. This was achieved by first preparing CaP/silk hybrid powders which were then incorporated into silk to obtain uniform CaP/silk composite scaffolds, by means of a freeze-drying method. The CaP incorporated in silk scaffold was 5% and 10%. The composition, microstructure and mechanical properties of the CaP/silk composite scaffolds were ascertained by X-ray diffraction (XRD), Fourier transform infrared spectra (FTIR), scanning electron microscope (SEM) and a universal mechanical testing machine. Bone marrow stromal cells (BMSCs) were cultured in these scaffolds and cell proliferation analyzed by confocal microscopy and MTS assay. Alkaline phosphatase (ALP) activity and osteogenic gene expression were assayed to determine if osteogenic differentiation had taken place. A calvarial defect model in severe combined immunodeficiency (SCID) mice was used to determine the *in vivo* bone forming ability of the hybrid CaP/silk scaffolds. The result showed that incorporating the hybrid CaP/silk powders into silk scaffolds improved both pore structure architecture and distribution of CaP powders in the composite scaffolds. By incorporating the CaP phase into silk scaffolds *in vitro* osteogenic differentiation of BMSCs was enhanced and there was an increase *in vivo* cancellous bone formation.

2.2.3 *In vitro* and *In vivo* cell culture using periosteum derived cell.

Zhang, C. et.al. [59]

In 2006, Chao Zhang et.al. studied on a tissue-engineered bone using rhBMP-2 induced periosteal cells with a porous nano-hydroxyapatite/collagen/poly(L-lactic acid) scaffold. In this study the cell–scaffold construct was cultured *in vitro* for 2 weeks, followed by subcutaneous implantation in nude mice. The assessment of the cell viability and osteogenesis function was performed both *in vitro* and *in vivo* to determine the clinical potential of this kind of cell–material system for bone repair. The result on scanning electron microscopy proved that the scaffold supported adhesion and proliferation of periosteal cells. Histological bone formation was observed only in experimental groups with cell transplants 8 weeks post-implantation.

The animals of the control groups did not show bone formation. The results strongly encourage the approach of the transplantation of rhBMP-2 induced periosteal cells within a suitable carrier structure for bone regeneration.

Alexander, D. et.al.[60]

In 2007, Dorothea Alexander et.al. analyzed the suitability of commercially available 3D open-cell polylactic acid(OPLA) scaffolds compared with calcium phosphate scaffold (CaP) and collagen composite scaffold (Coll) for the growth and osteoinductive potential of human jaw periosteal cells (JPC) using proliferation assays, scanning electron microscopy, real-time oxygen consumption measurements and EDX spectrometry. Furthermore, osteoinductive effects of OPLA scaffolds were also examined by analysis of gene expression in seeded JPC using quantitative real-time PCR. The result showed that JPC growing within open-cell polylactic acid scaffolds presented the highest proliferation rates among the analyzed scaffold types. Scanning electron micrographs illustrated the denser colonization of JPC-seeded OPLA scaffolds and formation of nodules after initiation of osteogenesis. EDX spectrometry demonstrated that JPC growing within OPLA scaffolds are able to form CaP particles.

Yamauchi, K. et.al[61].

In 2008, Kensuke Yamauchi et.al. investigated the periosteal expansion osteogenesis using highly purified β -tricalcium phosphate (β -TCP) blocks. In this study three beagle dogs weighing 10 to 12 kg were used. The β -TCP block was placed at the lateral surface of the mandibular bone. Two titanium screws were inserted from the lingual aspect to push the block to the buccal side. After a latency period of 8 days, during which primary wound healing occurred, the lingual screws were advanced by 0.5 mm/day for 8 days. Specimens were taken 8 weeks after lingual screw adjustments ceased and were analyzed by hematoxylin and eosin, tartrate-resistant acid phosphatase (TRAP), and Villanueva bone staining. The result showed that newly formed bone was observed in the gap between the bone and the β -TCP block, as well as on the lateral surface of the block. Moreover, the replacement of large parts of β -TCP with newly formed bone was observed in the β -TCP block area. However, newly formed bone was not observed over the upper parts of the block, and multinucleated TRAP positive cells were attached to the β -TCP in the periphery of this area. It can be concluded that the highly purified β -TCP block worked as an

activator for the soft tissue, including the periosteum, as well as a space maker to induce an osteoblastic response in the periosteum.

Mare' chal, M. et.al.[62]

In 2008 Marina Mare' chal et.al. studied the bone augmentation with autologous periosteal cells and two different calcium phosphate scaffolds under an occlusive titanium barrier in rabbits. In this study, 38 rabbits were divided into five groups. The first four groups are two different scaffolds with and without cells. The blood clot only was used as the last group as a negative control. Prior to implantation, autologous periosteal cells were harvested from the tibia by stripping the periosteum. Cells were cultured, and 1 day before the implantation 20 million cells were collected and seeded onto the scaffolds. Two preformed dome-shaped full titanium barriers were placed subperiosteally onto the frontal and parietal bones of each rabbit. Before placement of the barriers, the different scaffolds, seeded with or without cells, were put on top of the skull. As a negative control, autologous blood was injected into the barriers. Histological evaluation and histomorphometric analysis were performed after 12 weeks of undisturbed bone growth. Measurements involved the amounts of newly formed tissue and of new bone distinguishing between trabecular bone and osteoid. The result showed that there are no significant differences were found between the four treatment groups (scaffolds with or without cells). However, the amount of new bone tissue found underneath the titanium barriers with scaffolds was significantly higher than with a blood clot only.

Kawase, T. et.al[63]

In 2010, Kawase, T. et.al. studied the combination of human periosteum-derived Cells and superporous hydroxyapatite (HA) blocks for osteogenic bone substitute in periodontal regenerative therapy. In this study commercially available superporous HA blocks were acid treated and subjected to a three-dimensional (3D) culture for periosteal cell cultivation. Cells in the pore regions of the treated HA block were observed on the fracture surface by scanning electron microscopy. After osteogenic induction, the cell-HA complexes were implanted subcutaneously in nude mice. Osteoid formation was histologically evaluated. The result showed that acid treatment enlarged the interconnection among pores, resulting in the deep penetration of periosteal cells. Under these conditions, cells were maintained for longer than 2 weeks without appreciable cell death in the deep pore regions of the HA block. The cell-HA complexes that received *in vitro* osteogenic induction formed osteoids in

pore regions of the treated HA blocks *in vivo*. In contrast, most pore regions in the nonpretreated, cell-free HA blocks that were evaluated *in vivo* remained cell free. Their findings suggest that an acid-treated HA block could function as a better scaffold for the 3D high-density culture of human periosteal cells *in vitro*, and this cell–HA complex had significant osteogenic potential at the site of implantation *in vivo*. Compared with the cell-free HA block, the cell–HA complex using periosteal cells showed promising results as a bone substitute in periodontal regenerative therapy.



ศูนย์วิทยทรัพยากร
จุฬาลงกรณ์มหาวิทยาลัย

CHAPTER III

EXPERIMENTAL WORK

The experimental work can be divided into three main parts:

1. Materials and reagents
2. Equipments
3. Experimental procedures

3.1 Materials and reagents

- 3.1.1 *Bombyx mori* cocoon (Nangnoi Srisaket 1 from Queen Sirikit Sericulture Center, Nakhornratchsima, Thailand)
- 3.1.2 Type A gelatin powder (pI 9, Nitta gelatin Inc., Japan)
- 3.1.3 β -tricalcium phosphate (β -TCP, Fluga, Germany)
- 3.1.4 Hydroxyapatite (HA, Fulga, UK)
- 3.1.5 Sigmacote (Sigma-Aldrich, Germany)
- 3.1.6 Sodium carbonate (Na_2CO_3 , Ajax Finechem, Australia)
- 3.1.7 Lithium bromide (LiBr, Sigma-Aldrich, Germany)
- 3.1.8 Chloroform (Analar, England)
- 3.1.9 Dulbecco's phosphate buffer saline without calcium and magnesium (PBS(-) powder, Nissui Pharmaceutical Co. Ltd)
- 3.1.10 Sodium azide (Labchem, APS, Australia)
- 3.1.11 Collagenase from *Clostridium histolyticum* (2.69 units/ml, Fluka, Biochemika, USA)
- 3.1.12 Ethanol (99.7-100%, VWR International Ltd., UK)
- 3.1.13 70% ethanol (RCM, store at RT)
- 3.1.14 α -modified eagle powder medium (α -MEM(s), Hyclone, USA)
- 3.1.15 Dulbecco's modified eagle powder medium (D-MEM, Hyclone, USA)
- 3.1.16 Fetal bovine serum (FBS, Hyclone or Biochrom or ICP)
- 3.1.17 Penicillin-Streptomycin solution (10,000 units/ml, Hyclone, USA)
- 3.1.18 L-glutamine (200 mM, Hyclone, USA)

- 3.1.19 Sodium hydrogen carbonate (Fluka)
- 3.1.20 Trypsin/EDTA (0.25% Trypsin in EDTA.4Na, Hyclone, USA)
- 3.1.21 Trypan blue solution (0.4%, Sigma-Aldrich, Germany)
- 3.1.22 Dimethyl sulfoxide for cell freezing (Cell culture tested DMSO, Sigma-Aldrich, Germany)
- 3.1.23 Glutaraldehyde solution (50% GTA, Fluka)
- 3.1.25 SDS lysis buffer
- 3.1.26 Hoechst 33258 solution (1 mg/ml DMSO)
- 3.1.27 p-Nitrophenol standard solution (10 mM, Sigma-Aldrich, Germany)
- 3.1.28 p-Nitrophenyl phosphate liquid substrate (pNPP, Sigma-Aldrich, Germany)
- 3.1.29 Sodium hydroxide (0.02 N NaOH, Analar, England)
- 3.1.30 1M HCl
- 3.1.31 Calcium carbonate (CaCO₃, Analar, England)
- 3.1.32 O-cresolphthalein complex substrate (OCPC, MW 636.62)
- 3.1.33 Ethanolamine buffer (0.88 mol/l, pH 11)
- 3.1.33 MTT [3-(4,5-dimethylthiazol-2-yl)-2,5-diphenyltetrazolium bromide]

3.2 Equipments

- 3.2.1 Centrifuge (Kubota corporation 6500, Tokyo, Japan)
- 3.2.2 -80°C freezer (Heto, PowerDry LL3000, USA)
- 3.2.3 Lyophilizer (Christ Loc-1m, Alpha 1-4, Germany)
- 3.2.4 Homogenizer (T 25 digital, Ultra-turrex, Ika Co., Germany)
- 3.2.5 Fine coating machine (JFC-1100E, JEOL Ltd., Japan)
- 3.2.6 Scanning Electron Microscope (JSM-5410LV, JEOL Ltd., Japan)
- 3.2.7 Universal Testing Machine (Instron, No. 5567, USA)
- 3.2.8 Laminar Flow (HWS Series 254473, Australia)
- 3.2.9 CO₂ incubator (Series II 3110 Water Jacketed Incubator, Thermo Forma, USA)
- 3.2.10 Fluorescence microplate reader (Perkin elmer, 1420 multilabel)
- 3.2.11 Energy-dispersive X-ray spectroscopy (EDX, Philip Model XP 30 CP)
- 3.2.12 Mastersizer 2000 (Malvern Instruments Ltd., UK)

3.3 Experimental procedures

All experimental and procedures are summarized in Figure 3.1. In brief, there are three main steps comprised in this work; preparation of Thai silk fibroin and gelatin solutions; fabrication of Thai silk fibroin/gelatin incorporated with β -tricalcium phosphate and hydroxyapatite; characterization of scaffolds including morphology, swelling property, porosity, compressive modulus (dry and wet condition), *in vitro* biodegradability, material cytotoxicity and *in vitro* biocompatibility using periosteum derived cell.



ศูนย์วิทยทรัพยากร
จุฬาลงกรณ์มหาวิทยาลัย

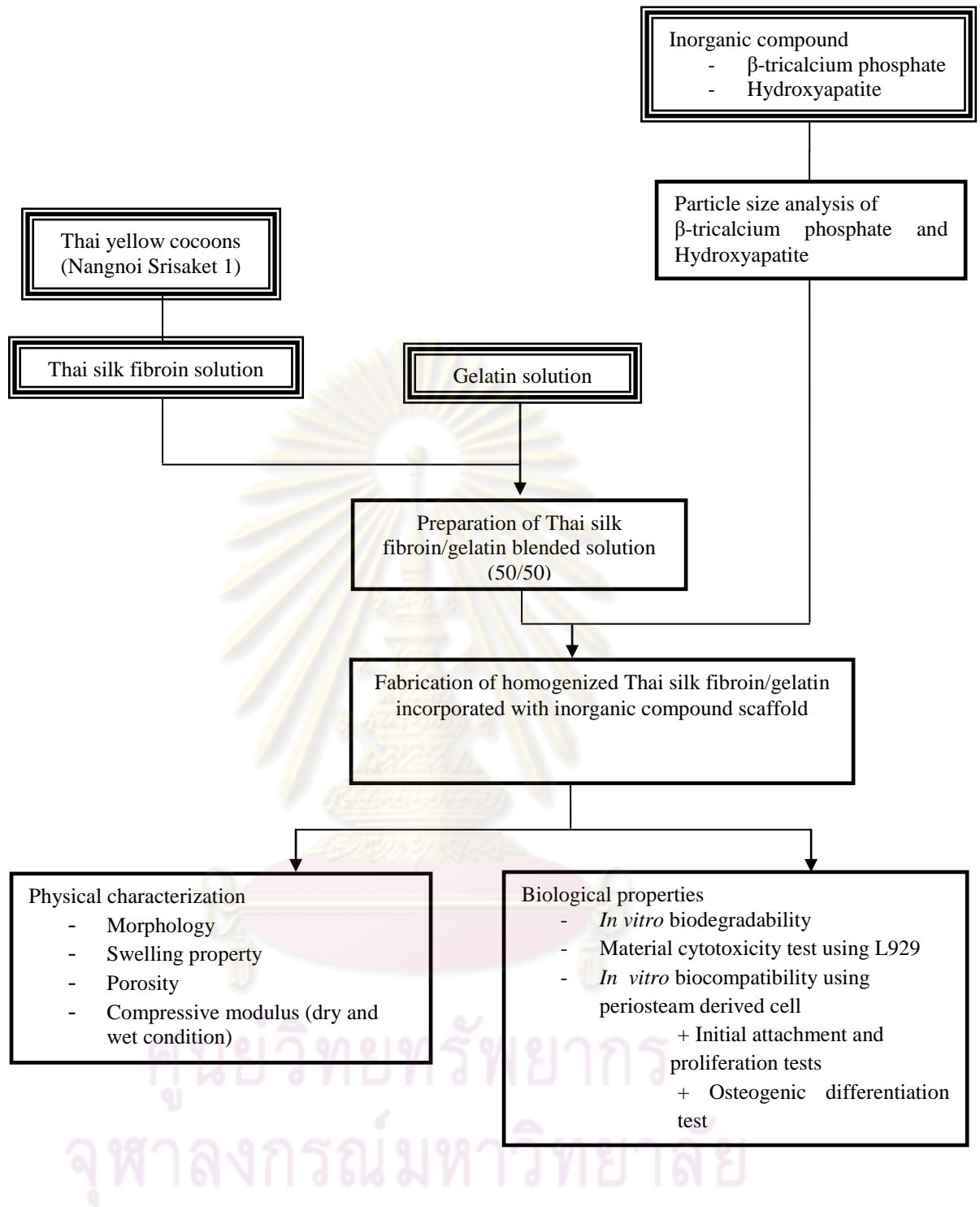


Figure 3.1 Summary of experimental procedures

3.3.1 Preparation of Thai silk fibroin solution

Thai silk fibroin solution was prepared as described by Kim *et.al.* [14]. Cocoons were boiled for 20 min in an aqueous solution of 0.02 M Na₂CO₃ and then rinsed thoroughly with deionized water to remove sericin. The degummed Thai silk fibroin was dissolved in 9.3 M LiBr solution at 60°C for 4 h to form 25wt% solution. The solution was dialyzed against deionized water using seamless cellulose tubing (MWCO 12000-16000, Viskase Companies, Inc., Japan) at room temperature for 2 days until the conductivity of dialyzed water was the same as that of deionized water. The final concentration of Thai silk fibroin aqueous solution was about 6-6.5wt%, determined by weighing the remaining solid after drying.

3.3.2 Preparation of gelatin solution

To prepare gelatin solution, type A gelatin was suspended in deionized water for 30 min. The suspension was subsequently stirred at 40°C for 60 min to obtain gelatin solution 2.1-2.9 wt%.

3.3.3 Scaffold fabrication

Silk fibroin solution was blended with gelatin solution at the weight blending ratio of 50/50. Various type and amount of inorganic compounds were added in the blended solution of silk fibroin/gelatin as shown in Table 3.1.

Briefly, 4 wt% aqueous solution of blended Thai silk fibroin/gelatin was mixed with inorganic compound using a homogenizer at 10000 rpm for 1.75 min. After that, 5 ml of chloroform solution was slowly added into the solution in order to stabilize the foamy solution. The solution was further homogenized for 15 s. The resulting foamy solution was quickly poured into a prefrozen tray and frozen at -80°C overnight prior to lyophilization at -55°C for 48 hr. After the lyophilization, all scaffolds were immersed in 70% ethanol for 1 hour, rinsed with PBS (-), and re-lyophilized .

Table 3.1 Weight ratio of inorganic compound/protein (silk fibroin and gelatin) in scaffolds.

Inorganic compound	Weight blending ratio of inorganic compound and protein (silk fibroin and gelatin 50/50)
β -tricalcium phosphate	0/100,30/70,50/50,70/30
Hydroxyapatite	0/100,30/70,50/50,70/30

3.3.4 Characterization of received inorganic compound

3.3.4.1 Morphology observation

The morphology of both inorganic compounds, β -tricalcium phosphate and hydroxyapatite, was investigated by scanning electron microscopy (SEM, JSM-5410LV, JEOL Ltd., Japan). The inorganic compound particles were placed on the copper mount and coated with gold prior to SEM observation.

3.3.4.2 Particle size analysis of inorganic compound

The particle size of inorganic compounds, β -tricalcium phosphate and hydroxyapatite, was investigated by Mastersizer 2000 (Malvern Instruments Ltd., UK). The inorganic compound particles, approximately 0.5 g, was suspended in 0.1% w/v sodium pyrophosphate in deionization water. The solution was suspended by ultrasonic for 5 min and stirred at 1,750 rpm during the particle size analysis.

3.3.5 Periosteum derived cell isolation and culture [64]

The periosteum derived cells used in the *in vitro* study were isolated from the periosteum explants of 6-year-old female patient. The sample from the patients was used in accordance with the approval of Faculty of Medicine, Chulalongkorn University ethical committee.

Periosteal explants approximately 3×3 mm² were harvested by careful dissection and placed in a 25-mm culture flask. The explants were cultured in minimum essential medium alpha powder medium (α -MEM, Hyclone, USA), supplemented with 10% fetal bovine serum at 37°C and penicillin (100IU/mL) and streptomycin (100 g/mL) in humidified atmosphere with 5% CO₂. After 4 to 6 days of culture, cells started to migrate from the periosteal explants. After 3 weeks of confluence. The expanded periosteal cells were then trypsinized, recovered by centrifugation at 1,500 rpm for 5 minutes, and expanded in a second passage.

Periosteum derived cells (passage 3) was analyzed for the expression of mesenchymal stem cells (MSC) by cell surface marker using flow cytometry technique. The result of analysis was provided by Department of Biochemistry, Faculty of Medicine, Chulalongkorn University and confirmed that the isolated periosteum derived cells expressed the MSC makers, including CD29, CD44, CD90, and CD105. CD34, CD45 which are hematopoietic stem cell marker were hardly detected, as presented in Table 3.2.

Table 3.2 Cell surface maker analysis of isolated periosteum derived cells

Marker	Percentage of maker expression (%)
CD29	98.48
CD44	99.58
CD90	99.4
CD105	49.34
CD34	7.11
CD45	0.01

3.3.6 Characterization of scaffolds

3.3.6.1 Physical characterization

3.3.6.1.1 Morphology

The morphology of scaffolds was investigated by scanning electron microscopy (SEM, JSM-5410LV, JEOL Ltd., Japan). In order to observe the inner structure of scaffolds, the scaffolds were cut vertically with razorblades. The cut scaffolds were placed on the copper mount and coated with gold prior to SEM observation.

The pore diameter of the scaffold was determined from SEM micrographs using ImageJ Launcher (n=100).

3.3.6.1.2 Swelling property [65]

A dried scaffold with known weight was immersed in phosphate buffered saline (PBS) at 37 °C for 24 hr. After blotting the excess PBS with lint-free paper, the wet weight of scaffold was determined. The percentage of water swelling (W_{sw}) of the scaffold was calculated from the following equation.

$$W_{sw} = \left[\frac{W_{24} - W_0}{W_0} \right] \times 100 \dots \dots \dots (3.1)$$

Where W_{24} represents the wet weight of scaffold after 24 hours of immersion, and W_0 is the initial weight of the scaffolds. The values were expressed as mean \pm standard deviation (n = 5).

3.3.6.1.3 Porosity

The porosity of the scaffolds was measured by liquid displacement [14]. Ethanol was used as the displacement liquid as it could permeate through the scaffolds. The weight of 1 ml ethanol was recorded as W_l . The scaffolds were immersed in the ethanol under vacuum for 5 min and the weight of scaffolds in

ethanol was recorded as W_2 . The ethanol impregnated-scaffolds were then taken out and the weight of residue ethanol was recorded as W_3 . The porosity of the scaffold (ε) was obtained by the following equation.

$$\varepsilon(\%) = \frac{(W_1 - W_3)}{(W_2 - W_3)} \times 100 \dots \dots \dots (3.2)$$

3.3.6.1.4 Compressive modulus (dry and wet condition) [4]

To determine the mechanical properties of the scaffolds, the compression tests were performed in dry and wet conditions using a universal testing machine (Instron, No. 5567) at the constant compression rate of 0.5 mm/min. The size of the scaffolds used for this test was 12 mm in diameter and 3 mm in height. For the test in wet condition, sample was immersed in PBS (-) under vacuum for 24 h at room temperature before the measurement. The compressive modulus of the scaffolds was determined from the slope of the compressive stress-strain curves during the strain range of 5%-30%. The reported values were the mean \pm standard deviation (n=5).

3.3.6.2 Biological characterization

3.3.6.2.1 *In vitro* biodegradability [66, 67]

To investigate the *in vitro* biodegradation behavior of scaffolds, the scaffolds were punched into 12 mm in diameter and 3 mm in thickness. These scaffolds were incubated in 1.5 ml solution of 1 U/ml collagenase (pH 7.4) at 37°C containing 0.01% w/v sodium azide [67] for 1, 3, 5, 7, 14, 21 and 28 days. The solution was refreshed every 2 days to ensure continuous enzyme activity. After each of interval time, the degraded scaffolds were taken out from the solution, rinsed with deionized water, centrifuged at 5,000 rpm for 15 min and freeze dried. The % remaining weight of each scaffold was determined using the following equation. The number of scaffolds used for each experimental group was three (n=3), where W_{re} is remaining weight and W_{int} is initial weight.

$$\% \text{ Remaining weight} = \frac{W_{re}}{W_{int}} \times 100 \dots\dots\dots 3.3$$

3.3.6.2 Material cytotoxicity test

The test was modified based on the biological evaluation of medical devices-Part 5 (ISO 10993-5: 1999).

Sample preparation: The scaffold was soaked in 2 ml of DMEM containing 10% fetal bovine serum (FBS) and kept in an incubator at 37 °C for 24 hours. After that, the scaffold was removed and the left media, so called “sample extract”, would be used in cytotoxicity test. DMEM containing 10% FBS and DMEM containing 10% FBS and 20 ppm of zinc acetate were used as negative and positive controls, respectively.

Test procedure: L-929 were used in the cytotoxicity test. 50,000 cells of L-929 suspended in DMEM containing 10% FBS were seeded into 24-well plate and incubated at 37 °C with 5% CO₂ for 24 hours. After that, the medium from each well was discarded and replaced with sample extract, negative control and positive control. All wells were further incubated for 24 hours. The cells viability was measured after incubation by MTT assay [68].

To measure the cell viability, 5 mg/ml of MTT in PBS (-) were added into the well containing cells and incubated in a CO₂ incubator at 37 °C for 30 min. After that, MTT solution were removed and replaced by DMSO to dissolve the formazan crystals. All samples were transfer to the 96-well plate and measured the absorbance at 570 nm.

3.3.6.2.3 Cell seeding and cell culture

Before cell seeding, scaffolds (dimension: d=12mm, h=2mm) were placed into 48-well tissue culture plates and sterilized using ethylene oxide. The scaffolds were immersed in the culture medium overnight prior to cell seeding.

Periosteum derived cells (passage 4) were seeded into the scaffolds by anagitated seeding method [8]. Briefly, 5×10⁵ and 1×10⁶ periosteum derived cells were seeded into the scaffold placed in 48-well tissue culture plates for proliferation and osteogenic differentiation tests, respectively. The scaffolds were agitated at

250 rpm for 6 h using an orbital shaker at 37°C in 5% CO₂ incubator. After that, the cells-seeded scaffolds were transferred into new 6-well tissue culture plates and cultured in α -MEM supplemented with 10% FBS at 37°C in 5% CO₂ incubator. In case of osteogenic differentiation test, the medium was changed into osteogenic medium (α -MEM supplemented with 10% FBS, 10 mM β -glycerophosphate, 50 μ g/ml L-ascorbic acid, and 10 nM dexamethasone) after 1 day of seeding [54]. Along the cell culture period, the medium was refreshed every 2 days.

3.3.6.2.4 Initial attachment and proliferation tests

To monitor cell adhesion and proliferation on scaffolds, the number of cells was determined by fluorometric DNA assay [8]. After the cells were cultured for a desired period of time (1, 3, and 5 days), the cell-seeded scaffolds were washed with PBS (-). Then the samples were lysed in SDS lysis buffer at 37°C overnight to prepare cell lysate and stored at -20°C until assay. When performing the assay, standard cell lysate prepared from the known amount of cells, and samples were thawed at room temperature. After thawing, standard cells were lysed in SDS lysis buffer at 37°C for 1 h and diluted with SDS for calibration curve (SDS was used as a blank test). Then 20 μ l of Hoechst solution (1 mg/ml DMSO) was diluted at room temperature with 19 ml deionized water and 1 ml of sodium citrate-buffered saline solution (SSC) 20X. After that, 100 μ l of diluted Hoechst solution was added into standard cells and samples. The fluorescent intensity of mixed solution was measured using a fluorescence microplate reader (Perkin elmer, 1420 multilabel counter) at the excitation and emission wavelengths of 355 and 460 nm, respectively. All data were expressed as mean \pm standard deviation (n = 3).

3.3.6.2.5 Osteogenic differentiation test

To assess the osteogenic differentiation of periosteum derived cell cultured on the scaffolds under osteogenic induction after 3, 5, 7, 14, 21, and 28 days of the culture, the alkaline phosphatase (ALP) activity and calcium content were used as the early and late marker for osteogenic differentiation test, were determined, respectively [69, 70].

To determine ALP activity, 10 mM p-nitrophenol solution was diluted with deionized water for calibration curve (deionized water was used as a blank test). Then 20 μ l of each deionized water, p-nitrophenol standard solution, and supernatant of cell lysate prepared using the procedure described in section 3.3.6.2.4 was reacted with 100 μ l p-nitrophenyl phosphate liquid substrate (pNPP) at 37°C for 15 min to converse p-nitrophenyl phosphate to p-nitrophenol. To stop reaction, 80 μ l of 0.02 N NaOH solution was added. Finally, the solution was measured spectrophotometrically at 405 nm using a UV-VIS spectrophotometer (Thermo Spectronic, Genesys 10UV scanning).

To measure the calcium content, 1 M HCl was added into the cell lysate samples with equal volume and incubated at 4 °C overnight. For standard solution preparation, 20 mg/ml CaCO₃ was diluted with 1 M HCl for calibration curve (1 M HCl was used as a blank test). Then 1 ml of 0.88 M ethanolamine buffer and 100 μ l of 0.63 M o-cresolphthalein complex substrate (OCPC) was added into 10 μ l of each 1 M HCl, CaCO₃ standard solution, and the samples. Thereafter, calcium contents were determined spectrophotometrically at 570 nm using a UV-VIS spectrophotometer. At each time interval, the number of cells were also determined by DNA assay and used to normalize the ALP activities and calcium content. All data were expressed as mean \pm standard deviation (n = 3).

3.3.6.2.6 The observation of cultured cells

After 5 and 28 days for proliferation and osteogenic differentiation tests, respectively, the scaffolds seeded with cells were washed with PBS (-) to remove non-adherent cells and then fixed in 2.5wt% glutaraldehyde solution in PBS (-) at 4°C for 1 hr. The scaffolds were then dried by critical point dry technique. Dried scaffolds were cross-sectional cut and observed under SEM.

3.3.6.2.7 Elemental analysis of cultured cell after culture

Elements, particularly calcium (Ca) and phosphorous (P), on the surface of cells after 28-day cultured in osteogenic media were analyzed by EDX (Philip Model

XP 30 CP). The same cell seeded constructs used in SEM observation were used for EDX analysis.

3.3.7 Statistical analysis

Significant levels of each result were determined by an independent two-sample t-test. All statistical calculations were performed on the Minitab system for Windows (version 14, USA). P-values of <0.05 was significantly considered.



ศูนย์วิทยทรัพยากร
จุฬาลงกรณ์มหาวิทยาลัย

CHAPTER IV

RESULTS AND DISCUSSION

4.1 Morphology and particle size of inorganic compounds

Morphology of both inorganic compounds, β -TCP and HA, was shown in Figure 4.1. From SEM micrograph, an individual particle of β -TCP was observed while an aggregated group of HA particle was noticed. From the particle size analysis by laser diffraction technique using a Mastersizer (Malvern Instruments Ltd., UK), the results on size distribution were shown in Figure 4.2. It was observed that the average particle size of β -TCP and HA are 5.66 μm and 7.56 μm , respectively. The smallest of β -TCP and HA size are approximately 0.3 μm and 0.4 μm , respectively, while largest the larger size of both are approximately 44 μm .

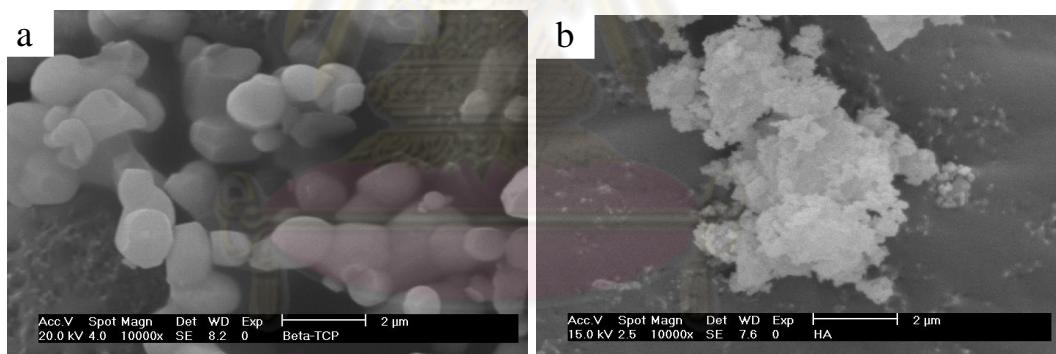


Figure 4.1 Morphology of (a) β -tricalcium phosphate and (b) hydroxyapatite

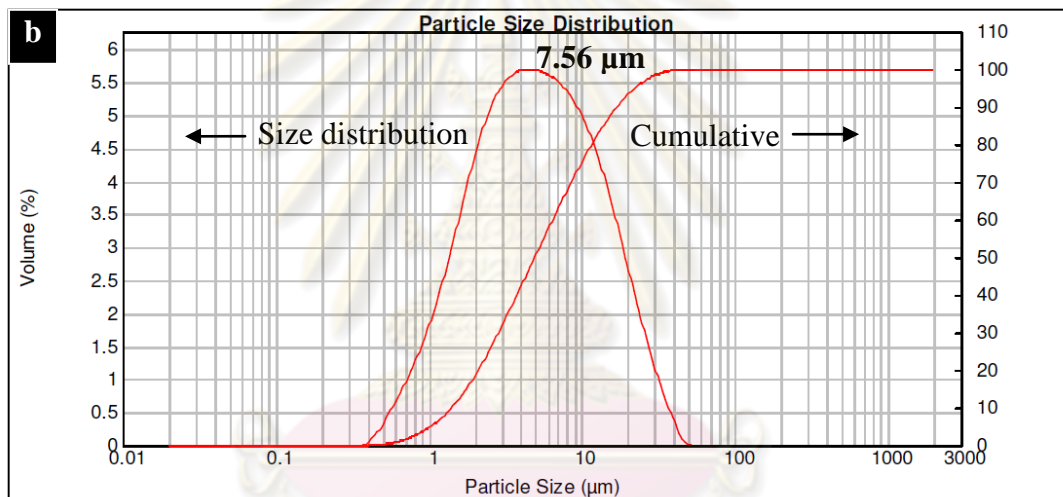
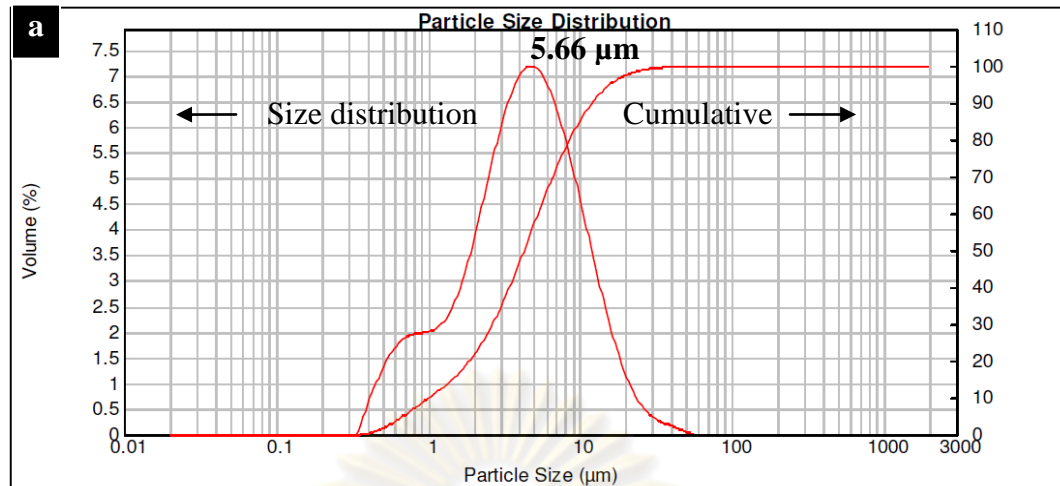


Figure 4.2 Size distributions of (a) β -tricalcium phosphate and (b) hydroxyapatite

ศูนย์วิทยทรัพยากร
จุฬาลงกรณ์มหาวิทยาลัย

4.2 Effect of incorporated β -tricalcium phosphate and hydroxyapatite on Thai silk fibroin/gelatin based scaffolds

In this section, physical and biological characteristics of Thai silk fibroin/gelatin (50/50) based scaffold incorporated with each inorganic compound, β -TCP and HA, were reported and discussed.

4.2.1 Physical properties

4.2.1.1 Morphology

The Thai silk fibroin/gelatin based scaffolds incorporated with β -TCP and HA were vertically cut in order to observe the inner structure under SEM. The pore morphology and surface morphology were showed in Figure 4.3 and 4.4, respectively. The pore sizes of Thai silk fibroin/gelatin based scaffolds incorporated with inorganic compound were shown in Table 4.1.

From the pore morphology illustrated in Figure 4.3, all Thai silk fibroin/gelatin based scaffolds showed porous network. The smaller pore size was observed when the amount of both inorganic compound particles increased. This might be because the inorganic particle inhibited the accumulation of the ice crystal in freeze-drying process.

When comparing the pore size of scaffolds containing inorganic compounds to pure protein scaffold, the incorporation of 30%, 50% and 70% of β -TCP could decrease the pore size of pure protein scaffold by approximately 39%, 39% and 63%, respectively. At the present of 30% and 50% of β -TCP, some very small pores were observed between the irregularly elongated pores. The incorporation of HA could decrease the pore size of pure protein scaffold by approximately 32% to 46%. The smallest pore size was found at the present of 70% β -TCP.

Comparing the effect of each inorganic compound, β -TCP and HA, at the same weight blending ratio, the present of β -TCP resulted in the smaller pore size of Thai silk fibroin based scaffold than HA. This might be because β -TCP particle is smaller than HA. Thus, it could better distribute in protein matrix and inhibit the accumulation of ice crystal more than HA.

Owing to high speed used to mix the solution and high freezing rate used in the scaffold fabrication, small bubble was formed and embedded in the wall of pure protein scaffold, as seen in Figure 4.4 (a). The uniform distribution of β -TCP and HA in the surface of Thai silk fibroin based scaffold was observed, resulting in non-smooth surface. It was also noticed that larger HA granules localized in the surface of scaffold resulted in the rougher surface compared to that with smaller β -TCP particles.

Table 4.1 Notation and pore size of Thai silk fibroin/gelatin based scaffolds incorporated with β -TCP and HA.

Scaffold Type	Inorganic/Protein (wt/wt)	Notation	Pore size (μm)
Silk fibroin/gelatin (50/50) scaffold or pure protein scaffold	0/100	0/100	150 \pm 26
Silk fibroin/gelatin based scaffold incorporated with β -TCP	30/70	30 β -TCP/70	92 \pm 15
Silk fibroin/gelatin based scaffold incorporated with β -TCP	50/50	50 β -TCP/50	92 \pm 12
Silk fibroin/gelatin based scaffold incorporated with β -TCP	70/30	70 β -TCP/30	56 \pm 6
Silk fibroin/gelatin (50/50) based scaffold incorporated with HA	30/70	30HA/70	102 \pm 13
Silk fibroin/gelatin (50/50) based scaffold incorporated with HA	50/50	50HA/50	105 \pm 16
Silk fibroin/gelatin (50/50) based scaffold incorporated with HA	70/30	30HA/70	81 \pm 12

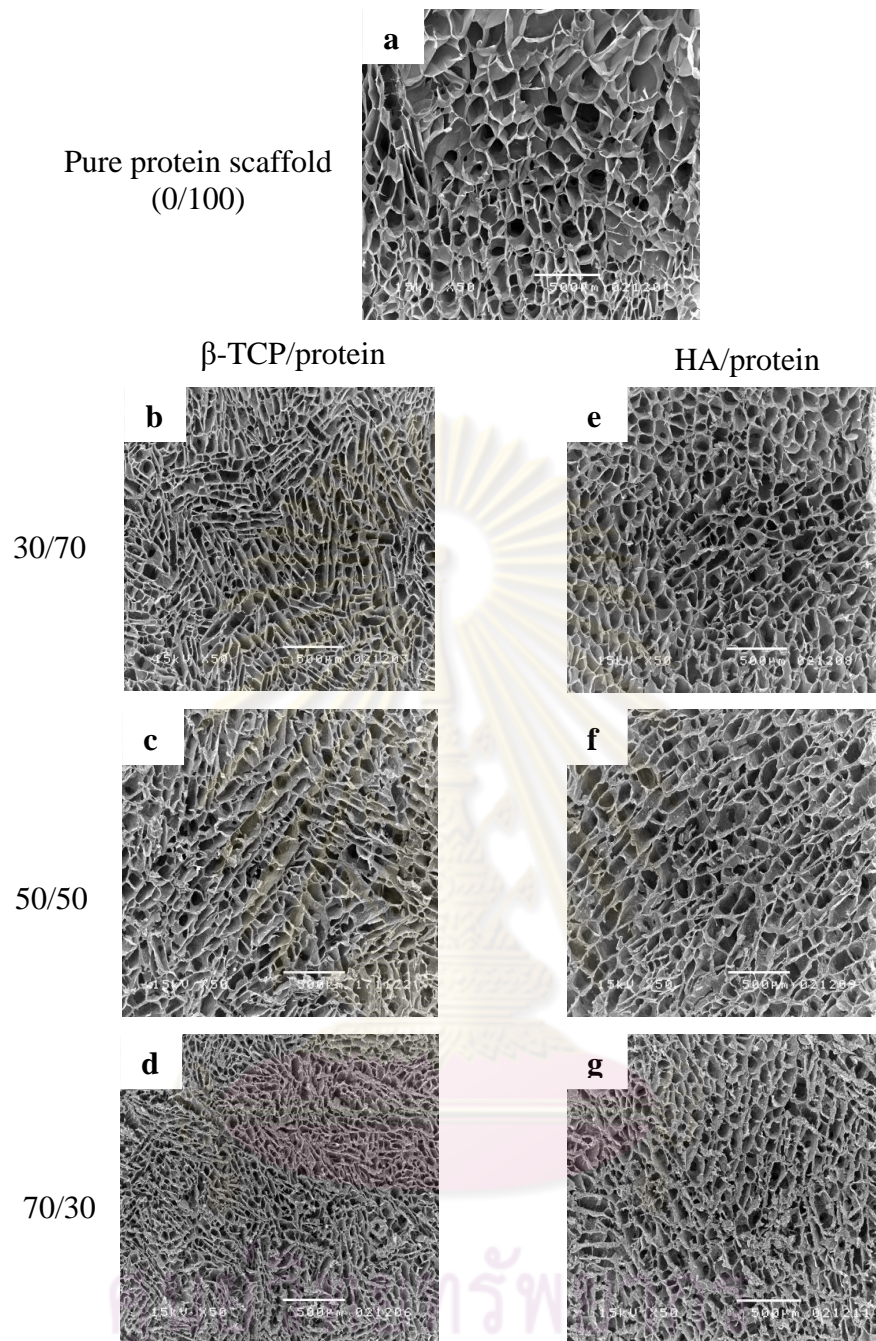


Figure 4.3 Morphology of Thai silk fibroin/gelatin based scaffolds incorporated with β -TCP and HA. (a) 0/100, (b) 30 β -TCP/70, (c) 50 β -TCP/50, (d) 70 β -TCP/30, (e) 30HA/70, (f) 50HA/50 and (g) 70HA/30 (scale bar =500 μ m)

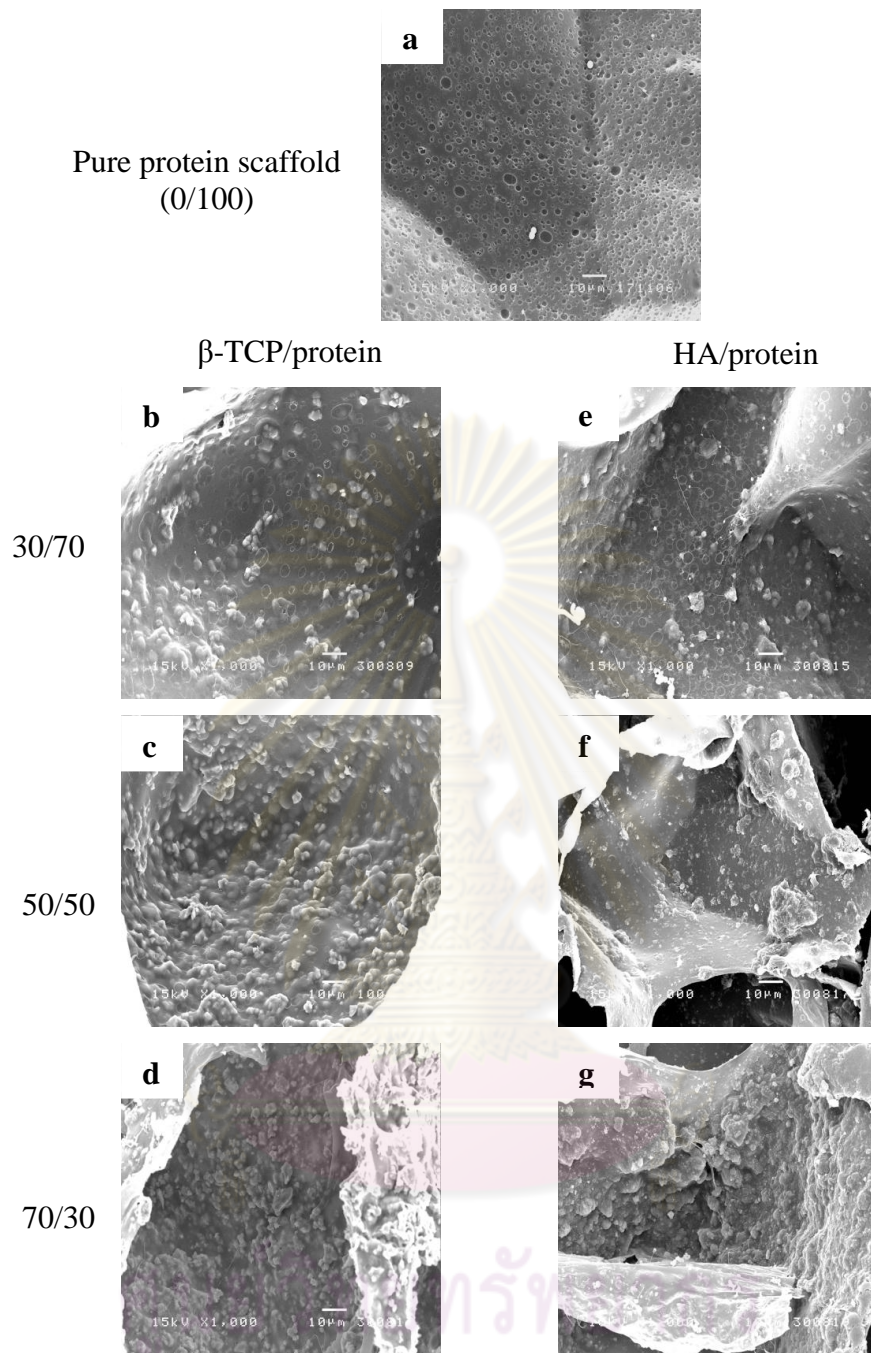


Figure 4.4 Surface morphology of Thai silk fibroin/gelatin based scaffolds incorporated with β -TCP and HA. (a) 0/100, (b) 30 β -TCP/70, (c) 50 β -TCP/50, (d) 70 β -TCP/30, (e) 30HA/70, (f) 50HA/50 and (g) 70HA/30 (scale bar = 10 μ m)

4.2.1.2 Swelling property

The swelling ability is an important property of scaffold. The higher swelling ability could increase the bioactivity between cell and culture medium [71].

The result on water absorption of Thai silk fibroin/gelatin scaffold incorporated with both inorganic compounds, β -TCP and HA, was demonstrated in Figure 4.5. The highest percentage of water absorption, 93.5%, was found in pure protein scaffold. It was observed that the higher amount of inorganic compound incorporated in protein scaffold resulted in the significantly lower swelling ability compared to the pure protein scaffold. At the present of 30%-50% of β -TCP and HA, no significant difference in the water absorption of each pair of scaffolds at the same percentage of inorganic compound. However, the scaffold with 70% HA showed significantly lower water absorption than that having 70% of β -TCP. The incorporation at 70% of β -TCP and HA could decrease the swelling ability of pure protein scaffold by 5.2% and 7.7%, respectively. The lowest percentage of water absorption also showed in the case of composited scaffold with 70% incorporation of HA.

The decreasing of water absorption might be due to the smaller pore size of scaffold with inorganic added, Furthermore this might be because of the hydrophobic effect of inorganic compound that inhibited the water absorption, resulting in the drop of water absorption ability. Peter et.al. [57] had studied the preparation and characterization of chitosan–gelatin/nanohydroxyapatite composite scaffolds for tissue engineering applications. They found that nanohydroxyapatite decreased the swelling of chitosan–gelatin/nanohydroxyapatite network because nanohydroxyapatite formed cross link between the chains and decreased the hydrophilicity of gelatin by binding calcium and phosphate to the hydrophilic –COOH or NH₂ groups. Since some of the NH₂ are bound to Ca groups the OH groups cannot form hydrogen bonds, hence swelling properties decreases.

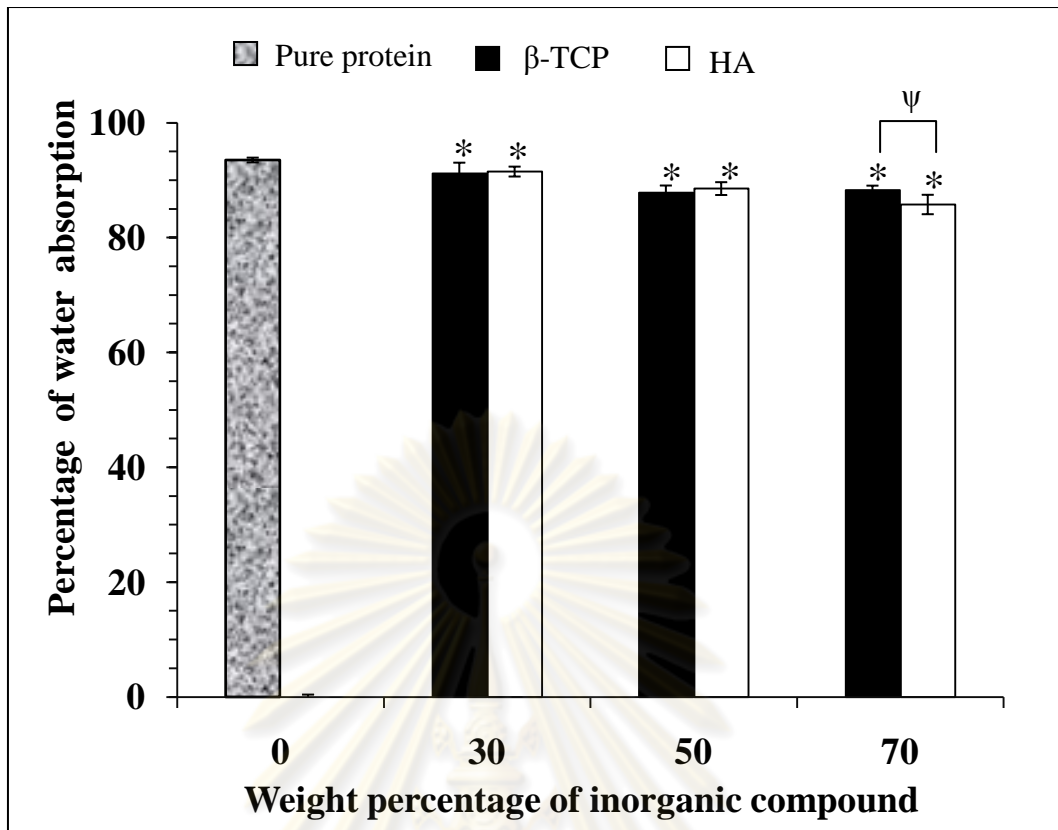


Figure 4.5 Percentage of water absorption of Thai silk fibroin/gelatin scaffolds incorporated with inorganic compounds, β -TCP and HA.

* represent the significant difference ($p < 0.05$) relative to Thai silk fibroin/gelatin scaffolds without inorganic compound.

Ψ represent the significant difference ($p < 0.05$) between the pair at the same percentage of inorganic compound

ศูนย์วิทยทรัพยากร
จุฬาลงกรณ์มหาวิทยาลัย

4.2.1.3 Porosity

Porous structure is one of the main design criteria for bone tissue engineering scaffolds [72]. The highly porous structures could improve mass transfer rate of oxygen and nutrients into the inner pores and also efficiently remove metabolic products [73].

In this study, the porosity of scaffolds measured by liquid displacement method was illustrated in Figure 4.6. The result showed that all scaffolds showed high porosity. The highest porosity at 94% was found in pure Thai silk fibroin/gelatin scaffold. It was observed that the higher amount of inorganic compound resulted in the significantly lower porosity compared to the pure protein scaffold. The addition of 70% β -TCP and HA could reduce the porosity of Thai silk fibroin/gelatin based scaffold by 4% and 7%, respectively. The lowest porosity of scaffold, 87%, was observed at the present of 70% HA.

The decreasing of porosity could possibly result from the inorganic particles localized in the pore wall of scaffold. This decreased the pore volume of the scaffold, resulting in the decreasing of porosity. This finding corresponded to our previous study by Tritanipakul [74]. She studied the deposition of hydroxyapatite on salt leached Thai silk fibroin scaffold and found that the deposited hydroxyapatite on the pore wall of scaffold resulted in the lower porosity of the scaffold.

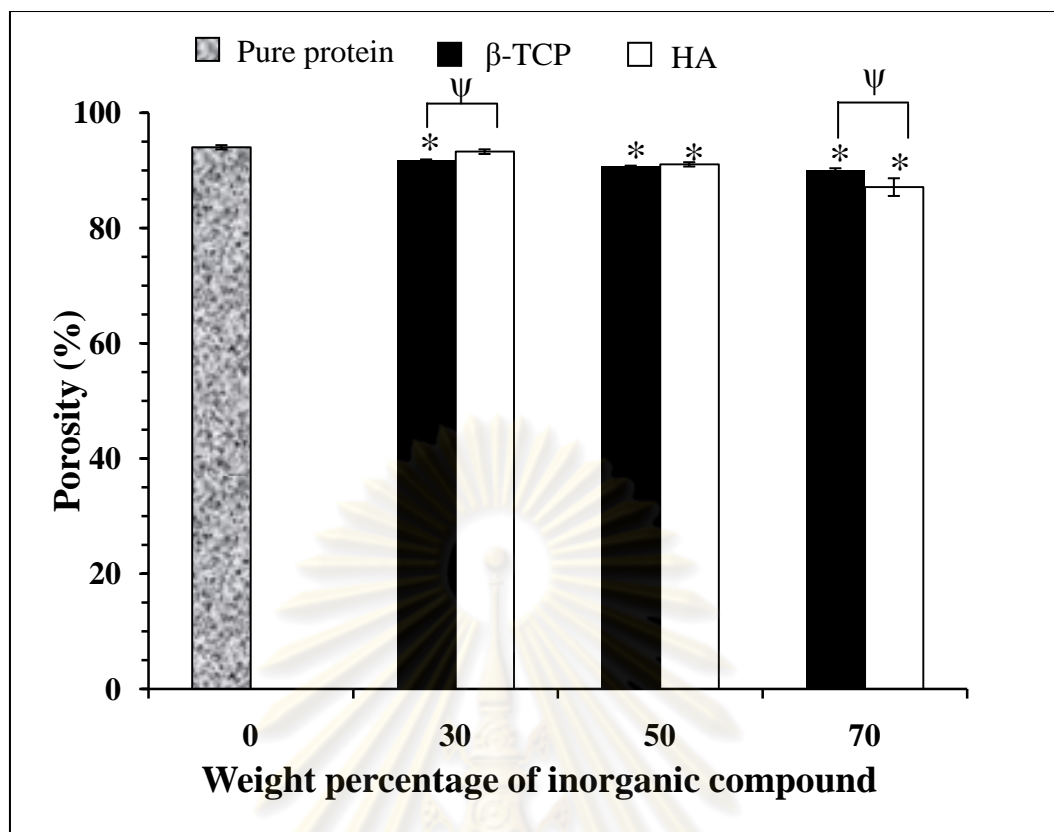


Figure 4.6 Porosity of Thai silk fibroin/gelatin scaffolds incorporated with inorganic compound.

* represent the significant difference ($p < 0.05$) relative to Thai silk fibroin/gelatin scaffolds without inorganic compound.

Ψ represent the significant difference ($p < 0.05$) between the pair at the same percentage of inorganic compound

ศูนย์วิทยทรัพยากร
จุฬาลงกรณ์มหาวิทยาลัย

4.2.1.4 Compressive modulus (dry and wet condition)

The compressive modulus of Thai silk fibroin/gelatin scaffolds incorporated with inorganic compound at various weight blending ratios of both inorganic compounds, β -TCP and HA, tested in dry and wet condition was illustrated in Figure 4.7.

For dry condition (Figure 4.7(a)), the compressive modulus of Thai silk fibroin/gelatin scaffolds incorporated with inorganic compound was higher than Thai silk fibroin/gelatin scaffolds without inorganic compound. The compressive modulus was slightly higher when incorporated 30%-50% of both inorganic compounds. The significantly higher compressive modulus was noticed when 70% of inorganic compound was incorporated. The highest compressive modulus, 1082 kPa, was found at the presence of 70% β -TCP. The result revealed that both inorganic compounds, β -TCP and HA, promoted the mechanical strength of scaffolds. For this system, β -TCP and HA act as the reinforcing agents. Comparing at the same weight percentage of inorganic compound, β -TCP could enhance the compressive modulus of Thai silk fibroin/gelatin scaffolds greater than HA. This could possibly be due to the smaller pore size of scaffold incorporated with β -TCP compared to that of the scaffold incorporated with HA. The scaffold with smaller pore size can give more paths for distributing to applied stress and result in the greater compressive modulus [14]. Furthermore, Lu *et.al.*[12] had studied the polymer-bioactive glass composite scaffolds with improved mechanical properties. The data of the bioactive glass incorporated with polylactide-co-glycolide (PLGA) showed that bioactive glass particle-reinforcement of the PLGA structure led to a near two-fold increase in compressive modulus.

The compressive modulus of Thai silk fibroin/gelatin based-scaffolds in wet condition was an important mechanical property for tissue engineering to mimic the condition of scaffolds used in the human body. As shown in Figure 4.7(b), the compressive modulus of all scaffolds were significantly decreased, approximately 100 times when compared to that in dry condition. Mostly, the protein based scaffold obtained from freeze-drying presented the high percentage of water absorption. Thus, it acted as the hydrogel when it was wet, leading to a decreasing of mechanical strength [75].

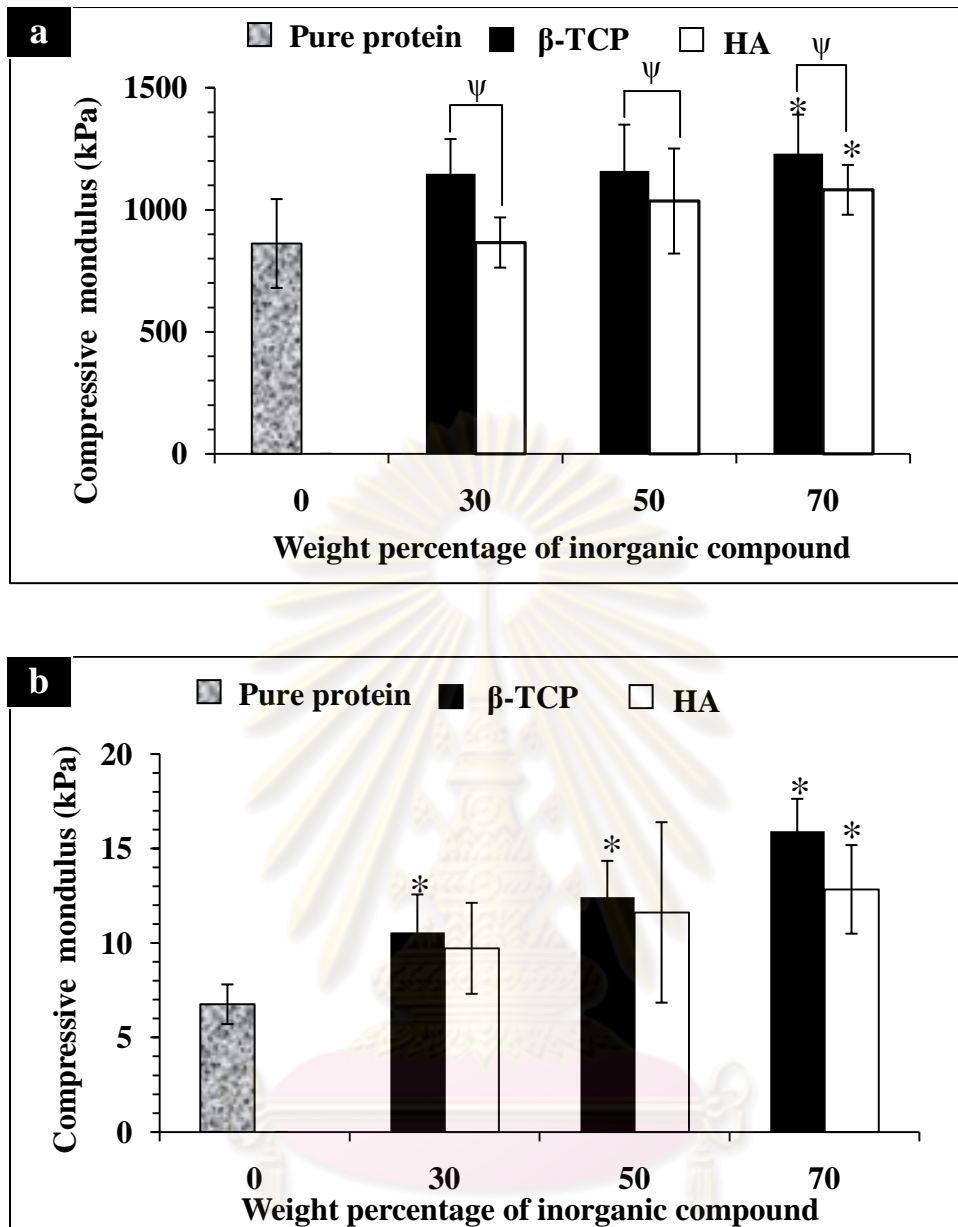


Figure 4.7 Compressive modulus of Thai silk fibroin/gelatin scaffolds incorporated with inorganic compound; (a) in dry condition, (b) in wet condition

* represent the significant difference ($p < 0.05$) relative to Thai silk fibroin/gelatin scaffolds without inorganic compound.

Ψ represent the significant difference ($p < 0.05$) between the pair at the same percentage of inorganic compound.

4.2.2 Biological characterization

In this section, biological characteristics of Thai silk fibroin/gelatin (50/50) based scaffold incorporated with inorganic compounds, β -TCP and HA, were presented and discussed into three parts as follows:

- *In vitro* biodegradability
- Material cytotoxicity test
- *In vitro* biocompatibility

4.2.2.1 *In vitro* biodegradability

To assess the biodegradation behavior of Thai silk fibroin/gelatin based scaffolds incorporated with inorganic compounds, we exposed scaffolds to 1 U/ml collagenase at 37°C, pH 7.4 for various periods of time. Weight changes during degradation test were evaluated and reported in the term of remaining weight (%) of scaffolds.

The remaining weight (%) of Thai silk fibroin/gelatin scaffolds incorporated with HA and β -TCP after incubated in collagenase solution at various periods of time were shown in Figure 4.8. It was observed that the remaining weight (%) of all scaffolds decreased as the degradation time increased. In general, it was noticed that the remaining weight (%) of scaffolds without inorganic compound was completely degraded within 7 days. The remaining weight (%) of scaffold incorporated with both HA and β -TCP were decreased and remained at the weight percentage of incorporated inorganic compound after 7 days. This might be due to the fact that collagenase digested only the protein part (silk fibroin/gelatin) of scaffolds, thus the remaining part of the scaffold would be the inorganic components presented in the scaffolds.

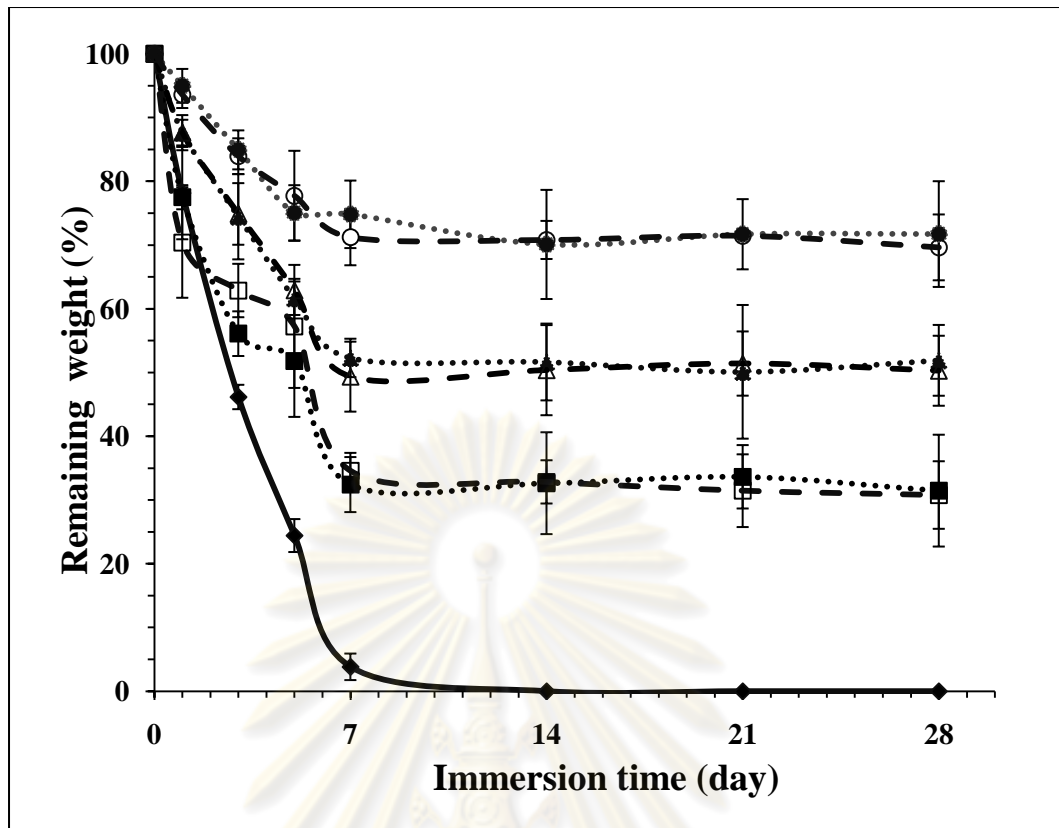


Figure 4.8 The remaining weight (%) of Thai silk fibroin/gelatin scaffolds incorporated with inorganic compounds; β -TCP and HA, after immersion in 1 U/ml collagenase (pH 7.4) at 37°C containing 0.01% w/v sodium azide for 1, 3, 5, 7, 14, 21 and 28 days.

—◆— 0/100, ...■... 30 β -TCP/70, ...▲... 50 β -TCP/50, ...●... 70 β -TCP/30,
 —□— 30HA /70, —△— 50HA /50, —○— 70HA /30.

ศูนย์วิทยทรัพยากร
 จุฬาลงกรณ์มหาวิทยาลัย

4.2.2.2 Material cytotoxicity test using L929

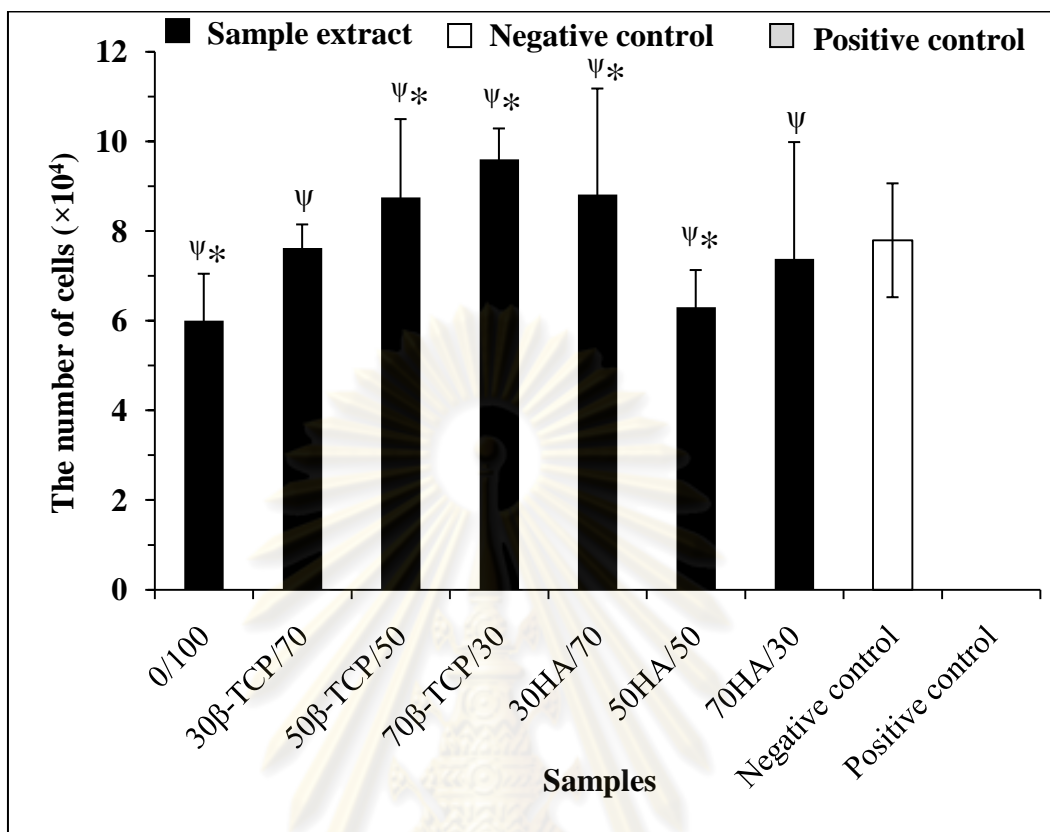


Figure 4.9 The number of cells from cytotoxicity test of Thai silk fibroin/gelatin scaffolds incorporated with inorganic compound, β -TCP and HA.

* represent the significant difference ($p < 0.05$) relative to negative control (DMEM containing 10% FBS).

ψ represent the significant difference ($p < 0.05$) relative to positive control (DMEM containing 10% FBS and 20 ppm of zinc acetate).

An indirect cytotoxicity test was conducted on Thai silk fibroin/gelatin-based scaffolds incorporated with HA and β -TCP using L-929 cell. Figure 4.9 showed the number of viable cell determined by MTT assay. Around 70,000 viable cells were observed when culture in negative control medium (DMEM containing 10% FBS) while no viable cell was noticed in positive control medium (DMEM containing 10% FBS and 20 ppm of zinc acetate). The results (Figure. 4.9) clearly presented that all sample extracts from Thai silk fibroin/gelatin-based scaffolds incorporated with HA

and β -TCP showed low cytotoxicity effect at the similar level to the negative control (DMEM containing 10% FBS).

4.2.2.3 *In vitro* biocompatibility using periosteum derived cells

All Thai silk fibroin/gelatin based scaffolds incorporated with both inorganic compounds, β -TCP and HA, were conducted on *in vitro* biocompatibility tests since it showed low cytotoxicity. Periosteum derived cells isolated from periosteal explants of 6-year-old female patient (passage 4) were cultured on these scaffolds. Cell attachment, proliferation and osteogenic differentiation test were assessed.

4.2.2.3.1 Periosteum derived cells initial attachment and proliferation tests

Periosteum derived cells were seeded and cultured on Thai silk fibroin/gelatin based scaffolds incorporated with both inorganic compounds, β -TCP and HA, for 1, 3 and 5 days. The number of attached and proliferated cells on scaffolds, analyzed by DNA assay, was presented in Figure 4.10

After 1 day of seeding, it could be noticed that there was no significant difference in the number of cells adhered on all scaffolds. After 3 days of seeding, no significant differences in the number of proliferated cells was found. After 5 days of culture, it could be observed that the number of proliferated cell on the scaffold incorporated with both inorganic compounds, β -TCP and HA, tended to be slightly higher than the pure protein scaffold. This could be due to the roughness increasing on the scaffold surface by β -TCP and HA that was able to promote the proliferation of cells [76, 77]. However, there was no significant difference of the cells in the scaffolds during the culture period from 1 day to 5 days.

The morphology of periosteum derived cells cultured on Thai silk fibroin/gelatin based scaffolds incorporated with β -TCP and HA at the weight blending ratios of 70/30, 50/50, and 30/70 (inorganic compound/protein) under proliferating medium for 5 days were depicted in Figure 4.11. Spreaded periosteum derived cells on all scaffolds were observed. There was no significant difference in cell morphology. This cell morphology implied that periosteum derived cell was

active on all Thai silk fibroin/gelatin based scaffolds incorporated with both inorganic compounds, β -TCP and HA.

The results on attachment and proliferation of periosteum derived cells implied that, Thai silk fibroin/gelatin based scaffolds incorporated with both inorganic compounds, β -TCP and HA, could support the attachment and proliferation of periosteum derived cells but could not obviously enhance the attachment and proliferation of periosteum derived cell. The result was in contrast to other reports on inorganic compound/biopolymer system. Han *et.al.* [76] studied the biomimetic chitosan–nanohydroxyapatite composite scaffolds for bone tissue engineering. They found the favorable biological response of pre-osteoblast (MC3T3-E1) on chitosan–nanohydroxyapatite scaffolds, including improved cell adhesion, higher proliferation, and well spreading morphology, when compared to pure chitosan scaffold. Peter, *et.al.* [78] have studied novel biodegradable chitosan–gelatin/nano-bioactive glass ceramic composite scaffolds for alveolar bone tissue engineering. They reported that the cell attachment on chitosan–gelatin/nano-bioactive glass ceramic composite scaffold significantly increased when compared to chitosan–gelatin scaffolds. The SEM micrographs showed flattened morphology of MG-63 cells and formed bridges between pores. Moreover, Liu *et.al.*[79] have studied the biomimetic nanofibrous gelatin/apatite composite scaffolds for bone tissue engineering. In the MC3T3-E1 attachment and proliferation test, gelatin/apatite composite scaffolds were compared with commercially available scaffold, Gelfoam[®]. They reported that more cells were attached on gelatin/apatite composite scaffolds than on Gelfoam[®] after of 1 day cell seeding. After 14 days, there were cells proliferated on both gelatin/apatite composite scaffolds and Gelfoam[®] scaffolds. However, the cell number on gelatin/apatite composite scaffolds remained significantly higher than that on Gelfoam[®] scaffolds. In additional, Takahashi, *et.al.* [8] prepared the biodegradable sponges composed of gelatin and β -tricalcium phosphate. They noticed that the morphology of cells attached depended on the sponge type. The attached cells showed flatter morphology with an increase in the amount of β -TCP. For the gelatin sponge without β -TCP, the shape of mesenchymal stem cell (MSC) attached was spherical. MSC proliferated in every sponge, although the profile depended on the amount of β -TCP. The rate of MSC proliferation increased with the increased β -TCP amount and became significant large when the amount of β -TCP was 75 or 90 wt%.

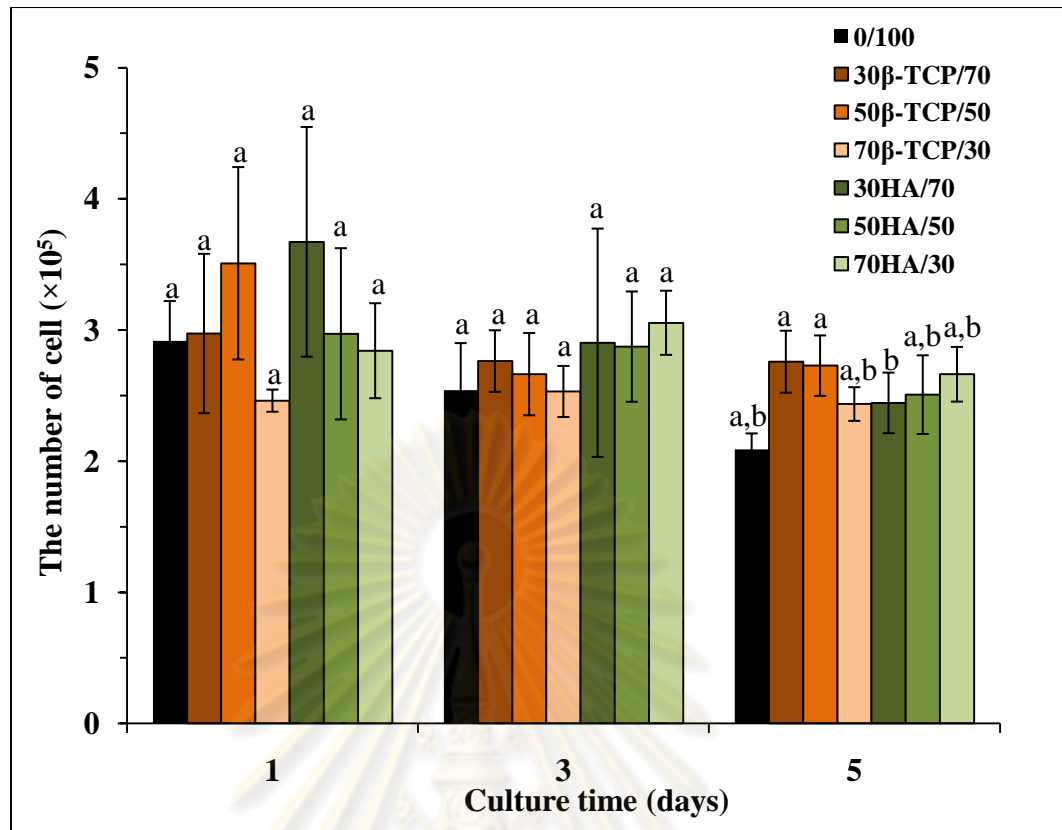


Figure 4.10 Number of periosteum derived cell attached and proliferated on Thai silk fibroin/gelatin based scaffolds incorporated with β -TCP and HA under proliferating medium for 1, 3 and 5 days, determined by DNA assay (seeding: 5×10^5 cells/scaffold).

a, b represent the significant difference ($p < 0.05$) within the same culture period

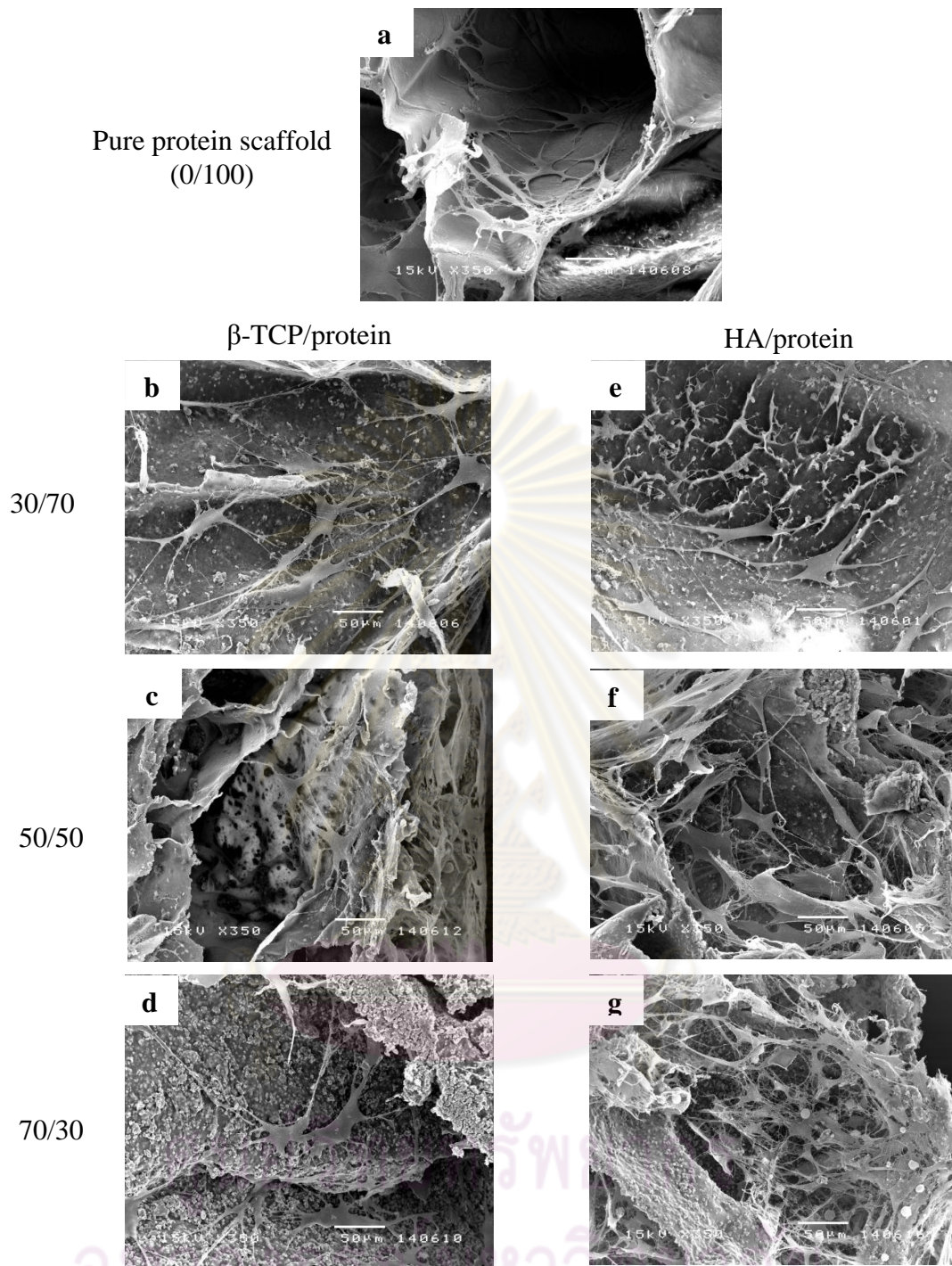


Figure 4.11 Morphology of periosteum derived cell cultured under proliferating medium for 5 days on Thai silk fibroin/gelatin based scaffolds incorporated with inorganic compound. (a) 0/100, (b) 30 β -TCP/70, (c) 50 β -TCP/50, (d) 70 β -TCP/30, (e) 30HA/70, (f) 50HA/50 and (g) 70HA/30 (scale bar = 50 μ m)

4.2.2.3.2 Osteogenic differentiation test

The number of periosteum derived cells on Thai silk fibroin/gelatin scaffolds incorporated with β -TCP and HA under the culture with osteogenic medium was presented in Figure 4.12. It was found that after 3 days of seeding, the number of cells on Thai silk fibroin/gelatin scaffolds with inorganic compound incorporation tended to be more than those on pure protein scaffold. However, during the 5th and 7th day, the number of cells on the Thai silk fibroin/gelatin scaffolds with inorganic compounds seemed to be slightly decreased. After that (at the 14th day onwards) the number of proliferated cells on Thai silk fibroin/gelatin scaffold with HA incorporation under osteogenic medium tended to be slightly higher than the pure protein scaffold. It was interesting that Thai silk fibroin/gelatin scaffold with HA incorporation could promote the proliferation of periosteum derived cell under osteogenic medium. This could be due to the roughness of the scaffold surface caused by inorganic particles which was able to promote the adhesion and proliferation of cells [80, 81, 82].

ALP activity of periosteum derived cell cultured on Thai silk fibroin/gelatin scaffolds incorporated with β -TCP and HA under osteogenic medium for 3, 5, 7, 14, 21, and 28 days was elucidated in Figure 4.13. It was observed that during the culture period of 3 days to 14 days, ALP activity of periosteum derived cells cultured in the scaffolds was gradually increased as increasing the culture period. ALP activity of periosteum derived cells cultured in the scaffolds containing inorganic compounds was generally higher than that in the pure Thai silk fibroin/gelatin scaffold. Remarkably, after 14 days of osteogenic culture, the highest ALP activity was found in the group of scaffolds containing 30-70% of β -TCP and 50% of HA. This result corresponded to the study of ALP activity expression of periosteum derived cell by Park *et.al.* [83]. They investigated the osteogenic phenotypes and mineralization of cultured human periosteal-derived cells cultured for 42 days in an osteogenic induction medium in a 6-well plate. The peak of ALP activity was observed at the 14th day of culture. Comparing among the four types of scaffolds that showed highest ALP activity, ALP activity from the group of scaffold with 30-70% of β -TCP tended to be slightly more than the scaffold with 50% of HA. The explanation of the observation may due to the fact that β -TCP is more resorbable than HA. When the bioactive glass agent like β -TCP and HA was added in materials, it is hydrated in cell

culture media, undergoing a process of continuous calcium and phosphate ion dissolution and reprecipitation. This process can induce osteoblast differentiation and mineralization [84]. In addition, Takahashi, *et.al.* [8] reported the influence of the incorporation of ceramic granules with the same size, such as HA, α -TCP, alumina, and β -TCP in the gelatin sponges at different mixing ratios. When MSCs were cultured in the sponges, the gelatin sponges incorporating β -TCP exhibited the highest ALP activity among all sponges, although the cell density of all sponges was the same. They suggested that β -TCP itself functioned to enhance the osteogenic differentiation of MSC.

Calcium content of periosteum derived cells cultured on Thai silk fibroin/gelatin scaffolds incorporated with β -TCP and HA under osteogenic medium for 7, 14, 21, and 28 days was shown in Figure 4.14. In the 21-day culture period, significantly higher calcium content was found in the case of Thai silk fibroin/gelatin scaffold incorporated with both inorganic compounds, β -TCP and HA, compared to pure protein scaffold. The highest calcium deposited along the culture period was found after 28 days of culture. All scaffolds incorporated with 30-70% β -TCP and HA showed maximum amount of calcium deposited. The result corresponded to the result of ALP activity described earlier, i.e. the group of scaffolds that presented highest ALP activity, the early maker of osteogenic differentiation, also gave the highest calcium content, the later maker of bone formation. This could be due to the osteoinductivity of both inorganic compounds. The result on calcium deposited of periosteum derived cell corresponded to other reports. When periosteum derived cells were cultured in the osteogenic medium, the calcium deposited usually found after 2 weeks of culture period. Subsequently, mineralization gradually increased during the entire duration of the culture period. Arnold *et.al.* [85] studied the *in vitro*-cultivation of human periosteum derived cells in bioresorbable polymer-TCP-composites. In this system, human periosteum derived cells in bioresorbable polymer-TCP-composites scaffold were cultured with osteogenic medium. The calcium deposit was assayed using von-Kossa staining. The result showed that the presence of calcified deposits was formed after 30 days of cultivation.

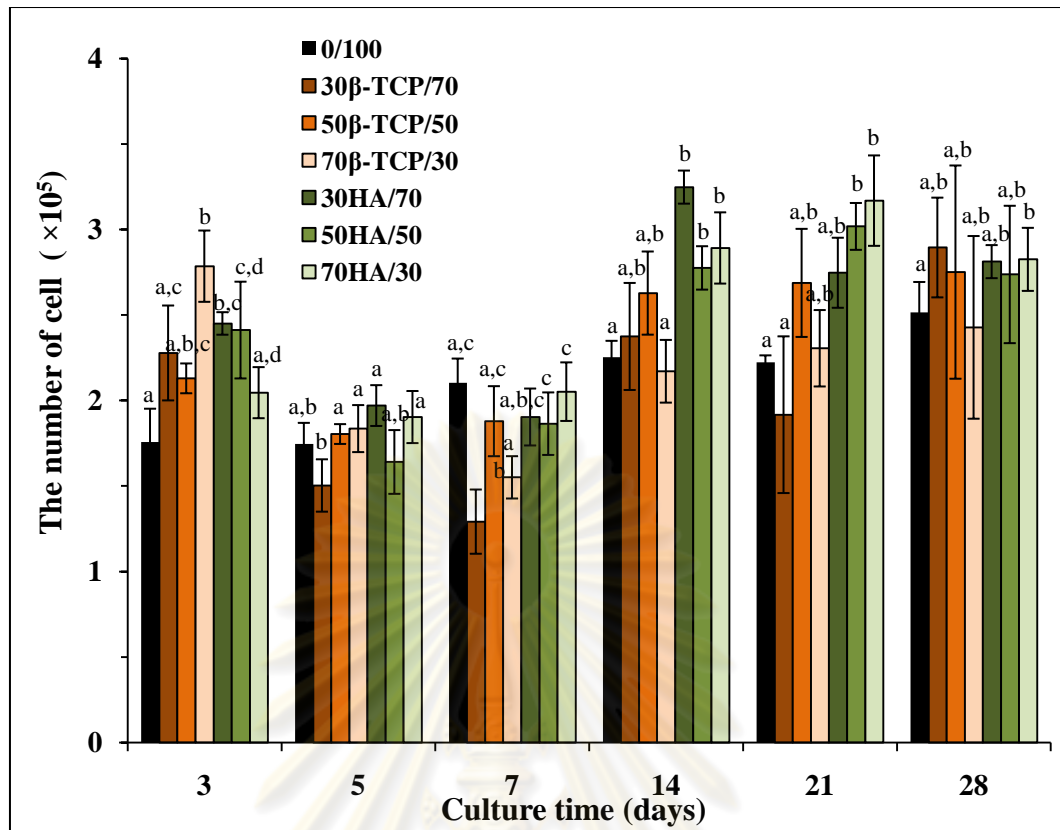


Figure 4.12 Number of periosteum derived cells on Thai silk fibroin/gelatin based scaffolds incorporated with β -TCP and HA under osteogenic medium for 3, 5, 7, 14, 21, and 28 days (seeding: 1×10^6 cells/scaffold).

a, b, c, d represent the significant difference ($p < 0.05$) within the same culture period

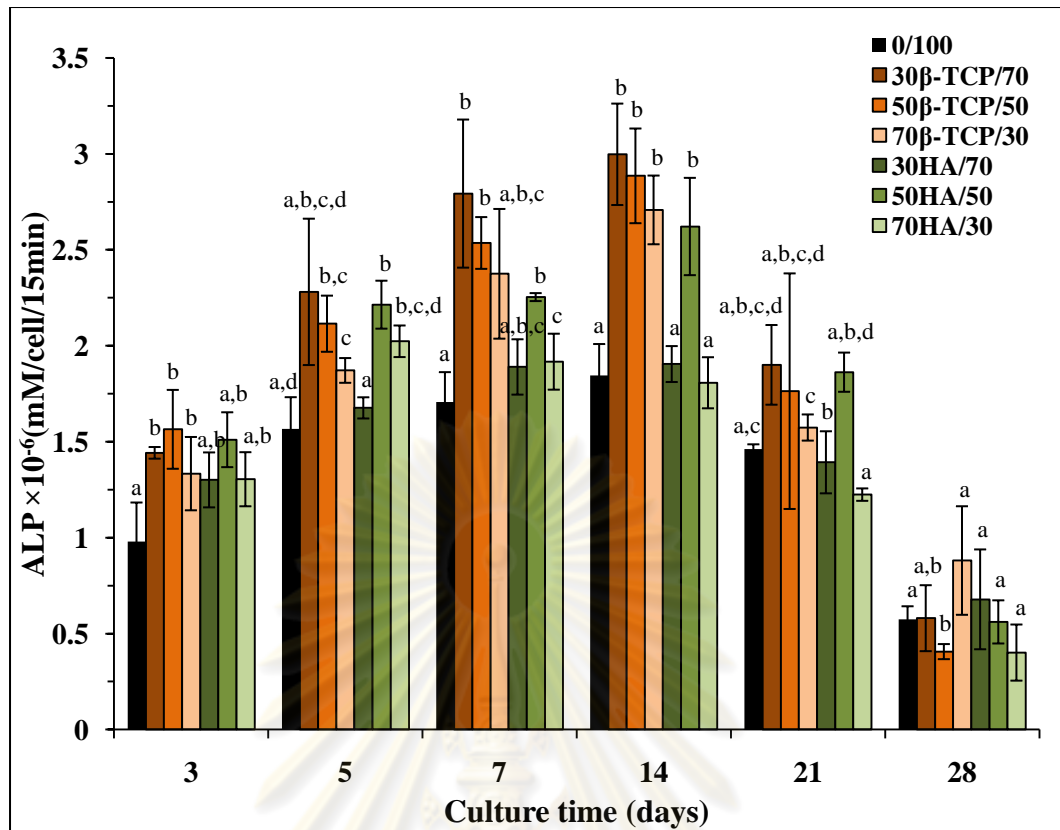


Figure 4.13 ALP activity of periosteum derived cells cultured on Thai silk fibroin/gelatin based scaffolds incorporated with β -TCP and HA under osteogenic medium for 3, 5, 7, 14, 21, and 28 days. (seeding: 1×10^6 cells/scaffold).

a, b, c, d represent the significant difference ($p < 0.05$) within the same culture period

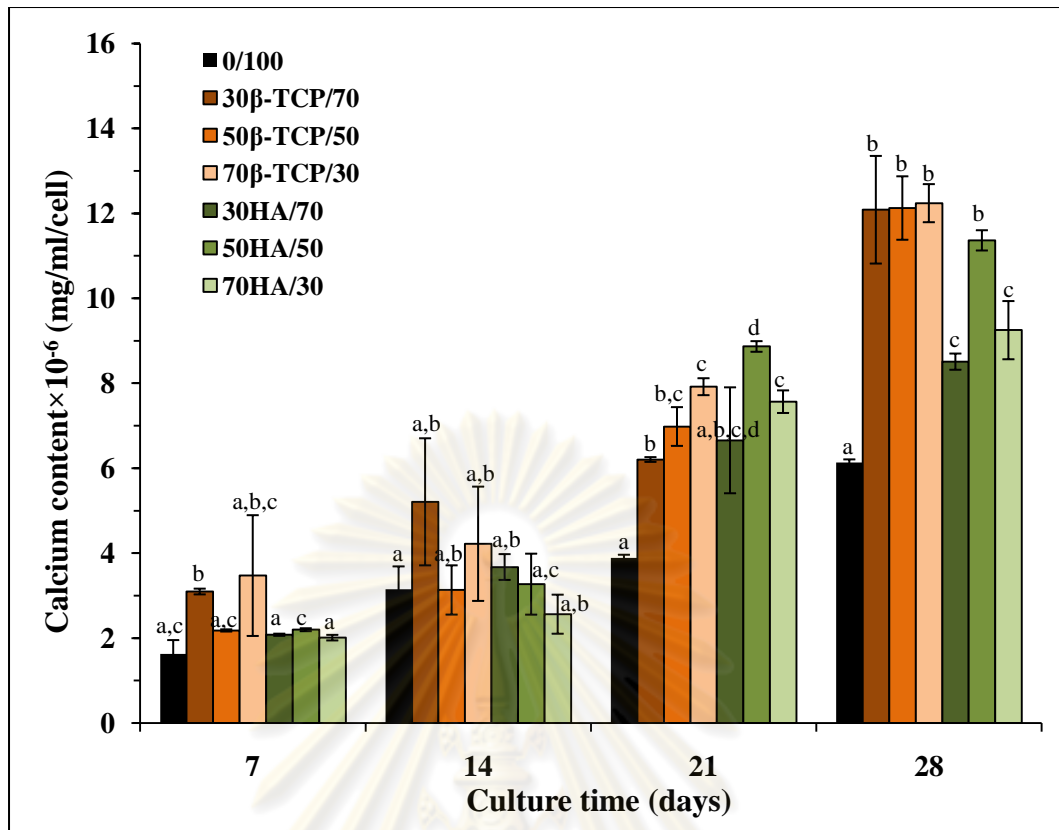


Figure 4.14 Calcium content of periosteum derived cell cultured on Thai silk fibroin/gelatin based scaffolds incorporated with β -TCP and HA under osteogenic medium for 7, 14, 21, and 28 days (seeding: 1×10^6 cells/scaffold).

a, b, c, d represent the significant difference ($p < 0.05$) within the same culture period

4.2.2.3.3 Cell and scaffold observation after cultured in osteogenic medium

The morphology of periosteum derived cells cultured on Thai silk fibroin/gelatin based scaffolds incorporated with β -TCP and HA in osteogenic medium for 28 days was illustrated in Figure 4.15. The SEM micrographs showed that after 28 days of culture, the periosteum derived cells formed multi-layer and the extracellular matrix (ECM) of cells was observed on all scaffolds. The scaffolds incorporated with β -TCP and HA seemed to have more cells and ECM on the surface of scaffolds. This was in agreement with the result on the number of cells determined by DNA assay as shown in section 4.2.2.3.2. The morphology of periosteum derived cells on Thai silk fibroin/gelatin based scaffolds incorporated with β -TCP and HA implied that all scaffolds qualitatively supported the osteogenic differentiation of periosteum derived cell.

Our result corresponded to the other studies of periosteum derived cell, i.e. inorganic compounds could support the cell activity and the osteogenic differentiation. Zhang *et.al* [59] studied on a tissue-engineered bone using rhBMP-2 induced periosteal cells with a porous nano-hydroxyapatite/collagen/poly(L-lactic acid) scaffold. The result on the cell morphology after 2 weeks of culture showed that cells changed to a flat morphology and covered nearly all the surface of the porous nano-HA/collagen/PLA scaffold with a very close intercellular gap and showing the active rate of proliferation. In addition, an abundant extracellular matrix was observed around the cells, which might play an important role in later bone formation. Furthermore, Kawase *et.al.* [63] study the human periosteum derived cells combined with superporous hydroxyapatite blocks used as an osteogenic bone substitute. The result of cell distribution and appearance after 10 days of culture showed that the density and appearance of human periosteal cells in a fractured surface of the superporous HA block were distributed almost equally in most pore regions, even in the deeper regions of the HA block. The cell appearance in pore regions of HA blocks implied that the superporous HA block could induce periosteal cells to form 3D network inside the pores.

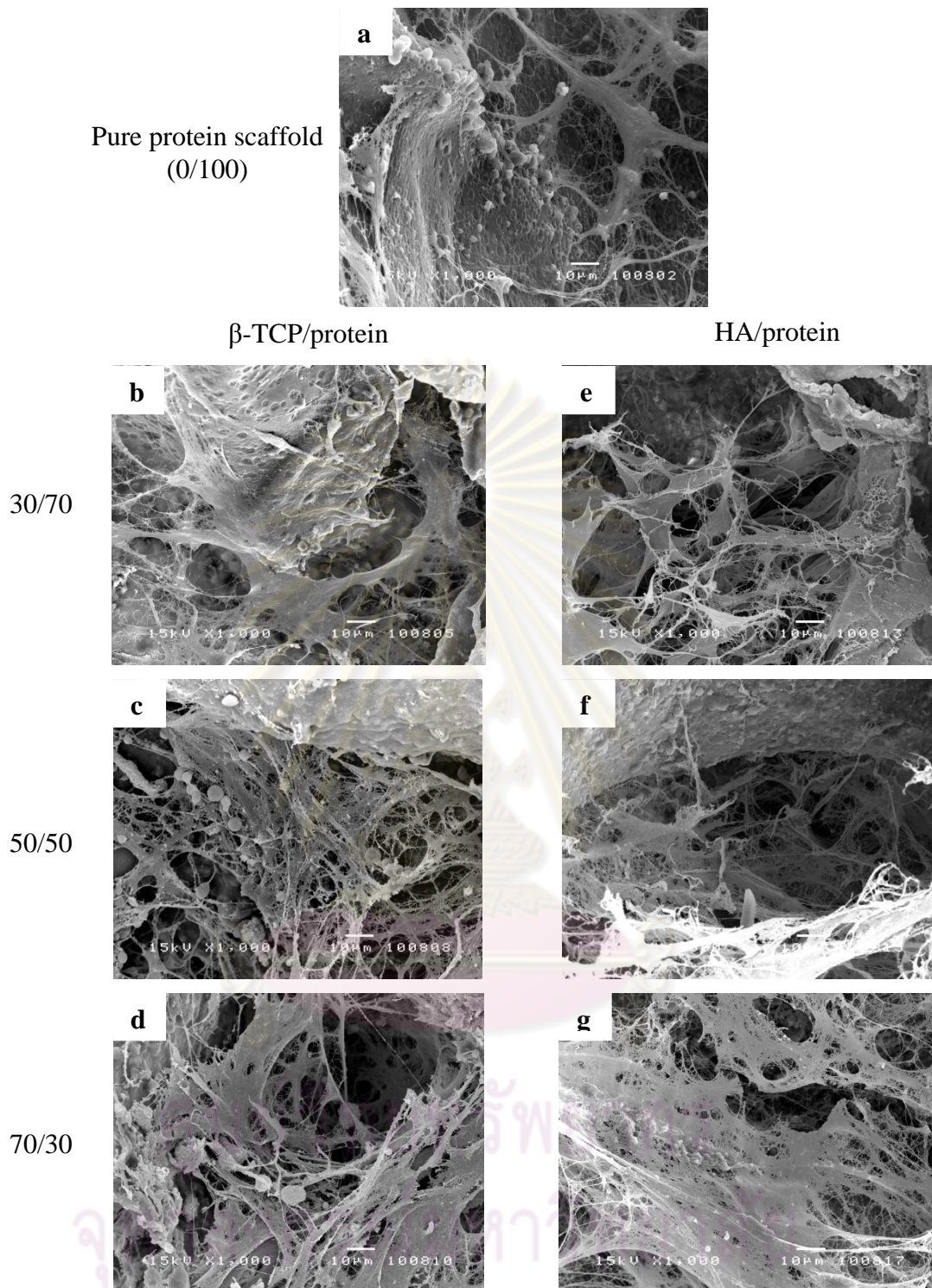


Figure 4.15 Morphology of periosteum derived cells cultured under osteogenic medium for 28 days on Thai silk fibroin/gelatin based scaffolds incorporated with inorganic compounds, β -TCP and HA. (a) 0/100, (b) 30 β -TCP/70, (c) 50 β -TCP/50, (d) 70 β -TCP/30, (e) 30HA/70, (f) 50HA/50 and (g) 70HA/30 (scale bar = 10 μ m)

4.2.2.3.3 Elemental analysis of periosteum derived cells culture in osteogenic medium

After 28 days of culture in osteogenic medium, all scaffolds were analyzed by energy dispersive x-ray spectrometer (EDX) to confirm the production of calcium from periosteum derived cell. EDX results on the cell surface were summarized in Table 4.2. Calcium and phosphate contents on cell surface were found in all scaffolds. For the pure protein scaffold, the calcium deposited was found approximately 11-32%. For the scaffold containing β -TCP, the highest calcium deposited, 53-75%, was found at the incorporation of 50% β -TCP. In the case of scaffold containing HA, the highest calcium deposited, 32- 58%, was also found at the incorporation of 50% HA. The incorporation of both inorganic compounds, β -TCP and HA, showed relatively higher calcium contents deposited compared to the pure protein scaffold. The scaffold incorporated with β -TCP seemed to illustrate the higher calcium content compared to the scaffold incorporated with HA. The EDX results corresponded to the calcium content reported in Figure 4.14.

Table 4.2 Elemental analyses on cell surface after 28 days cultured in osteogenic medium (minimum and maximum values from 3 measurement points were shown.)

Scaffold type	Element (%)		
	O	P	Ca
0/100	48-74	8-20	11-32
30 β -TCP/70	35-59	15-16	15-49
50 β -TCP/50	14-46	7-13	53-75
70 β -TCP/30	27-50	16-22	32-51
30HA/70	61-79	10-15	11-24
50HA/50	22-51	14-20	32-58
70HA/30	45-52	17-19	30-38

CHAPTER V

CONCLUSIONS AND RECOMMENDATIONS

5.1 Conclusions

In this study, the Thai silk fibroin/gelatin based scaffold incorporated with both inorganic compounds, β -TCP and HA, were fabricated via freeze drying technique. The effect of different weight percentages of each inorganic compound incorporated was investigated. The morphology of Thai silk fibroin/gelatin based scaffolds incorporated with β -TCP and HA showed the porous structure with non-smooth surface. The pore size of the scaffolds decreased as the weight blending ratio of inorganic compound was increased. Swelling ability of all scaffolds significantly decreased when the both inorganic compounds, β -TCP and HA, were added. This might be attributable to the hydrophobic effect of both inorganic compounds. At 70% incorporation of β -TCP, the water absorption significantly decreased than that with HA incorporation. All Thai silk fibroin/gelatin based scaffolds incorporated with both inorganic compounds, β -TCP and HA, showed high porosity more than 87%. The incorporation of β -TCP and HA could enhance compressive strength of scaffolds comparing to the pure protein scaffold, both in dry and wet condition. For this system, β -TCP and HA act like the reinforcing agents. However, the compressive modulus of Thai silk fibroin/gelatin based scaffolds incorporated with β -TCP was slightly higher than that with HA incorporation. This could possibly be attributed to the smaller pore size of scaffold incorporated with β -TCP compared to that of the scaffold incorporated with HA. The scaffold with smaller pore size can give more paths for distributing to applied stress.

From the study on biological properties, *in vitro* biodegradability test showed that the scaffolds without inorganic compounds were completely degraded within 7 days. The remaining weight (%) of scaffolds incorporated with both HA and β -TCP were decreased and remained at the weight percentage of incorporated inorganic compound after 7 days. Material cytotoxicity test using L929 clearly presented that all samples showed low cytotoxicity. The results on *in vitro* cell culture indicated that all

Thai silk fibroin/gelatin based scaffolds incorporated with both inorganic compounds, β -TCP and HA, could support the periosteum derived cell attachment and proliferation. In case of periosteum derived cell cultured in osteogenic medium, the results of ALP activity and calcium contents showed that incorporation of both inorganic compounds could enhance osteoconductive potential of the scaffolds. There were four groups of scaffold, 30 β -TCP/70, 50 β -TCP/50, 70 β -TCP/30 and 50HA/50, that gave the significantly higher of ALP activity and calcium contents. Comparing among the four types of scaffolds that showed highest ALP activity and calcium content, ALP activity and calcium content from the group of scaffolds with 30-70% of β -TCP tended to be slightly more than the scaffold with 50% of HA. This result revealed that Thai silk fibroin/gelatin based scaffold incorporated with both inorganic compounds, β -TCP and HA, could serve as a new alternative material for bone tissue engineering.

5.2 Recommendations

Although the effects of inorganic compound incorporation on the physical and biological properties of Thai silk fibroin/gelatin based scaffolds have been investigated in this work, there are other interesting points which should be further considered as follows:

1. The scaffolds that showed osteoconductive potential should be investigated *in vivo*.
2. To ensure the differentiation of periosteum derived cells, the gene expression of osteocalcin and osteopontin should be examined.

References

- [1] Vepari, C.; Kaplan, D. Silk as a biomaterial. **Progress in Polymer Science** 32 (2007) 991–1007.
- [2] Wang, Y.; Kim, H.J.; Novakovic, G.V.; and Kaplan, D.L. Stem cell-based tissue engineering with silk biomaterials. **Biomaterials** 27 (2006): 6064–6082.
- [3] Meechaisue, C.; Wutticharoenmongkol, P.; Warapyt, R.; Huangjing, T.; Ketbumrung, N.; Pavasant, P.; and Supaphol, P. Preparation of electrospun silk fibroin fiber mats as bone scaffolds: a preliminary study. **Biomedical Materials** 2 (2007): 181-188.
- [4] Vachiraroj, N.; Ratanavaraporn, J.; Damrongsakkul, S.; Pichyangkura, R.; Banaprasert, T.; Kanokpanont S. A comparison of Thai silk fibroin-based and chitosan-based materials on *in vitro* biocompatibility for bone substitutes. **International Journal of Biological Macromolecules** 45 (2009): 470–477
- [5] Jetbumpenkul, P. **Effect of chemical crosslink and hydroxyapatite on the properties of Thai silk fibroin/gelatin scaffold.** Master Thesis. Department of Chemical Engineering, Chulalongkorn University 2009.
- [6] Tungtasana, H. **Tissue response and biodegradation of hydroxyapatite-conjugated gelatin/Thai silk fibroin scaffolds.** Master Thesis. Master Program in Biomedical Engineering Chulalongkorn University 2009.
- [7] Chamchongkaset, J.; Kanokpanont, S.; Kaplan, D.L.; and Damrongsakkul, S. Modification of thai silk fibroin scaffolds by gelatin conjugation for tissue engineering. **Advanced Materials Research** 55-57 (2008): 685-688.
- [8] Takahashi, Y.; Yamamoto, M.; and Tabata, Y. Osteogenic differentiation of mesenchymal stem cells in biodegradable sponges composed of gelatin and β -tricalcium phosphate. **Biomaterials** 26 (2005): 3587–3596.
- [9] Fujimoto, M.; Isobe, M.; Yamaguchi, S.; Amagasa, T.; Watanabe, A.; Ooya T and Yui, N. Poly(ethylene glycol) hydrogels cross-linked by hydrolyzable polyrotaxane containing hydroxyapatite particles as scaffolds for bone regeneration. **Journal of Biomaterials Science, Polymer** 6(2005) 1611–1621
- [10] Hasegawa, S.; Tamura, J.; Neo, M.; Goto, K.; Shikinami, Y.; Saito, M.; Kita, M.; and Nakamura, T. *In vivo* evaluation of a porous hydroxyapatite/poly-dl-

- lactide composite for use as a bone substitute. **Journal of Biomedical Materials Research Part A** 75(2005) 567–579.
- [11] Sato, M.; Slamovich, E.B.; and Webster, T.J. Enhanced osteoblast adhesion on hydrothermally treated hydroxyapatite/titania/poly(lactide-co-glycolide)sol-gel titanium coatings. **Biomaterials** 26 (2005) 1349–1357.
- [12] Lu, H.H.; El-Amin, S.F.; Scott, K.D.; and Laurencin, C.T. Three-dimensional, bioactive, biodegradable, polymer-bioactive glass composite scaffolds with improved mechanical properties support collagen synthesis and mineralization of human osteoblast-like cells *in vitro*. **Journal of Biomedical Materials Research Part A** 64(2003) 465–474.
- [13] Gil, E.S.; Frankowski, D.J.; Bowman, M.K.; Gozen, A.O.; Hudson, S.M.; and Spontak, R.J. Mixed protein blends composed of gelatin and bombyx mori silk fibroin: effects of solvent-induced crystallization and composition. **Biomacromolecules** 7 (2006): 728-735.
- [14] Kim, U.J.; Park, J.; Kim, H.J.; Wada, M.; and Kaplan, D.L. Three-dimensional aqueous-derived biomaterial scaffolds from silk fibroin. **Biomaterials** 26 (2005): 2775-2785.
- [15] Sarovart, S.; Sudatis, B.; Meesilpa, P.; Grady, B.P.; and Magaraphan R. The use of sericin as an antioxidant and antimicrobial for polluted air treatment. **Advance Material Science** 5 (2003): 193-198.
- [16] The concord consortium. **Unit VI: Molecular recognition, binding and self-assembly**[online]. (n.d.) Available form: http://www.concord.org/~barbara/workbench_web/unitV_revised/silk/images/silk_beta_sheets.jpg [Nov 14, 2009]
- [17] Drexel university. **Amino acid compositions of silk fibroins**[online]. (n.d.) Available form: <http://dspace.library.drexel.edu/retrieve/4251/CHAPTER+2.pdf> [Mar20, 2008]
- [18] Ministry of Agriculture and Cooperatives. **Thai silk**[online]. (n.d.) Available form: <http://www.moac.go.th/builder/mu/index.php?page=415&clicksub=415&sub=126> [Nov 14, 2009]
- [19] Sumitomo group public affairs committee. **Applications of silk**[online]. (n.d.) Available form: http://www.Sumitomo.gr.jp/english/discoveries/special/images/silk_p16.jpg [Nov 14, 2009]

- [20] Gelatin Manufacturers Institute of America Inc. **Gelatin**[online]. (n.d.) Available form: <http://www.gelatin-gmia.com/> [Nov 14, 2009]
- [21] Wikimedia Foundation. **Gelatin**[online]. (n.d.) Available form: <http://en.wikipedia.org/wiki/Gelatin> [Nov 14, 2009]
- [22] London South Bank University. **The nature of gelatin**[online]. (n.d.) Available form: <http://www.lsbu.ac.uk/.html> [Nov 14, 2009]
- [23] Tabata, Y.; and Ikada, Y. Protein release from gelatin matrices. **Advance drug delivery reviews** 31 (1998): 287-301.
- [24] Gelatin Manufacturers Institute of America Inc. **Gelatin**[online]. (n.d.) Available form: http://www.gelatin-gmia.com/html/gelatine_health.html [Mar 13, 2008]
- [25] Getita medical. **Product fo getita**[online]. (n.d.) Available form: <http://www.gelitamedical.com/content4.asp?SMenuID=1145603510250&DID=2> [Oct 25, 2009]
- [26] Wahl, D.A.; and Czernuszka, J.T. Collagen-hydroxyapatite composites for hard tissue repair. **European cells and materials** 11 (2006): 43-56.
- [27] Azom™.com Pty.Ltd. **Hydroxyapatite**[online]. (n.d.) Available form: <http://www.azom.com/details.asp?ArticleID=107> [Nov 14, 2009]
- [28] Wikimedia Foundation. **Hydroxyapatite**[online]. (n.d.) Available form: <http://en.wikipedia.org/wiki/Hydroxyapatite> [Nov 14, 2009]
- [29] Koutsopoulos, S. **Hydroxyapatite**[online]. (n.d.) Available form: <http://www.chemistry.upatras.gr/studs/sotk/hap.htm> [Nov 14, 2009]
- [30] Hoya Corporation **Structure of hydroxyapatite**[online]. (n.d.) Available form: <http://www.pentax.co.jp> [Nov 14, 2009]
- [31] Kamitakahara, M.; Ohtsuki, C.; Miyazaki, T.; Review Paper: Behavior of ceramic biomaterials derived from tricalcium phosphate in physiological condition. **Journal of biomaterial application** 31 (2008): 197
- [32] Wikimedia Foundation. **Tricalcium phosphate**[online]. (n.d.) Available form: http://en.wikipedia.org/wiki/Tricalcium_phosphate [Nov 14, 2009]
- [33] Chemical book. **Formula structure of β -tricalcium phosphate**[online]. (n.d.) Available form: <http://www.chemicalbook.com/ChemicalProductB3125692.htm> [Nov 14, 2009]
- [34] Ma, X.P.; Scaffolds for tissue fabrication. **Materials Today** 7 (2004):30-40

- [35] Buckley, C. and O'Kelly, K. **Regular scaffold fabrication techniques for investigations in tissue engineering** Dublin: Centre for bioengineering (2004): 147-166
- [36] Snowman, J.W. and Menyhart, L. **Lyophilization: Freeze-Drying a downstream process**. Downstream Processes: Equipment and Techniques (1988): 315-351.
- [37] Labconco Corporation. **Principles of freeze drying**[online]. (n.d.) Available form: <http://www.labconco.com/manual/freeze/FDmanual.pdf> [Nov 14, 2009]
- [38] Bronzino, J.D. Biomedical engineering fundamentals. New York: Taylor & Francis, 2006.
- [39] Wikimedia Foundation. **Cancellous bone**[online]. (n.d.) Available form: http://en.wikipedia.org/wiki/Bone_graft [July 28, 2010].
- [40] Kollar, M.R.; Palsson, B.O.; and Masters, J.R. **Human cell culture**. New York: Kluwer academic publishers, 2002.
- [41] Sharma, P.; Cartmell, S. and Hal, A. J. E. Bone tissue engineering. **Applications of cell immobilisation biotechnology**. Netherlands: Springer, 2006.
- [42] Mistry, A.S. and Mikos, A. G. Tissue engineering strategies for bone regeneration. **Advances in Biochemical Engineering/Biotechnology Journals** 94 (2005): 1-22.
- [43] Bruder, S. P. and Fox, B. S. **Tissue engineering of bone**. Clinical Orthopaedics 367S: S68–S83. 1999.
- [44] Guldberg, R. E. and Duty, A. O. **Design Parameters for Engineering Bone Regeneration**. New York: Springer, 2003.
- [45] Kadiyala, S., Neelam, J. and Bruder, S. P. Culture expanded, bone marrowderived mesenchymal stem cells can regenerate a critical-sized segmental bone defect. **Tissue Engineering** 3 (1997): 173–185.
- [46] García, A. J.; Vega, M. D. and Boettiger, D. Modulation of cell proliferation and differentiation through substrate-dependent changes in fibronectin conformation. **Molecular Biology of the Cell** 10 (1999): 785-798.
- [47] Federal institute for materials research and testing. **Bone tissue-engineered scaffolds**[online]. (n.d.) Available form: <http://www.bam.de/en> [July 28, 2010]
- [48] Olympus corporation. **Bone tissue-engineered scaffolds**[online]. (n.d.) Available form: <http://www.olympus-global.com> [July 28, 2010]

- [49] Dietmar, W.H.; and Sittinger, M. Periosteal Cells in bone tissue engineering. **Tissue engineering** 9 (2003)
- [50] Yayasan Rumah Ilmu Indonesia. **Bone**[online]. (n.d.) Available form:
http://www.rumahilmuindonesia.net/belajarbiologi/wpcontent/uploads/2008/09/lb_horiz.jpg [Nov 14, 2009]
- [51] Meinel, L.; Karageorgiou, V.; Hofmann, S.; Fajardo, R.; Snyder, B.; Li, C.; Zichner, L.; Langer, R.; Vanjak-Novakovic, G.; and Kaplan, D.L. Engineering bone-like tissue *in vitro* using human bone marrow stem cells and silk scaffolds. **Journal of Biomedical Materials Research** 71A (2004): 25-34.
- [52] Gil, E.S.; Frankowski, D.J.; Spontak, R.J.; and Hudson, S.M. Swelling behavior and morphological evolution of mixed gelatin/silk fibroin hydrogels. **Biomacromolecules** 6 (2005): 3079-3087.
- [53] Gil, E.S.; Spontak, R.J.; and Hudson, S.M. Effect of β -sheet crystals on the thermal and rheological behavior of protein-based hydrogels derived from gelatin and silk fibroin. **Macromolecular bioscience** 5 (2005): 702-709.
- [54] Lv, Q.; Hu, K.; Feng, Q.L.; and Cui, F. Fibroin/collagen hybrid hydrogels with crosslinking method: preparation, properties, and cytocompatibility. **Journal of Biomedical Materials Research** 84A (2007): 198-207.
- [55] Wang, L.; Ning, G.L.; and Senna, M. Microstructure and gelation behavior of hydroxyapatite-based nanocomposite sol containing chemically modified silk fibroin. **Colloids and surfaces** 254 (2005): 159–164.
- [56] Du, C.; Jin, J.; Li, Y.; Kong, X.; Wei, K.; and Yao, J. Novel silk fibroin/hydroxyapatite composite films: Structure and properties. **Materials Science and Engineering** 29 (2008): 62-68.
- [57] Peter, M.; Ganesh, N.; Selvamurugan, N.; Nair, S.V.; Furuike, T.; Tamura, H and Jayakumar, R. Preparation and characterization of chitosan–gelatin/nanohydroxyapatite composite scaffolds for tissue engineering applications. **Carbohydrate Polymers** 80 (2010):687–694.
- [58] Zhang, Y.; Wu, C.; Friis, T. and Yin Xiao, The osteogenic properties of CaP/silk composite scaffolds. **Biomaterial** 31 (2010):2848–2856.
- [59] Zhang, C.; Hu, Y.; Cui, F.; Zhang, S. and Ruan, D. study on a tissue-engineered bone using rhBMP-2 induced periosteal cells with a porous nano hydroxyapatite/collagen/poly(L-lactic acid) scaffold. **Biomedical Materials** 1 (2006):56–62.

- [60] Alexander, D.; Hoffmann, J.; Munz, A.; Friedrich, B.; Geis, J. and Reinert G. Analysis of OPLA scaffolds for bone engineering constructs using human jaw periosteal cells **Journal of Materials Science: Materials in Medicine** 19 (2008):965–974.
- [61] Yamauchi, K.; Takahashi, T.; Funaki, K.; and Yamashita Y. Periosteal expansion osteogenesis using highly purified beta-tricalcium phosphate blocks: A Pilot Study in Dogs **Journal of Periodontology** 79 (2008): 999-1005
- [62] Marechal, M.; Eyckmans, J.; Schrooten, J.; Schepers, E.; Luyten, F.P. and Steenberghe, D. Bone augmentation with autologous periosteal cells and two different calcium phosphate scaffolds under an occlusive titanium barrier: An experimental Study in Rabbits **Journal of Periodontology** 79(2008):896-904.
- [63] Kawase, T.; Okuda, K.; Kogami, H.; Nakayama, N.; Nagata, M.; Sato, T.; Wolff, L.F. and Yoshie, H. Human periosteum-derived cells combined with superporous hydroxyapatite blocks used as an osteogenic bone substitute for periodontal regenerative therapy: an animal implantation study using nude mice. **Journal of Periodontology** 81(2010):420-427.
- [64] Kanno, T.; Takahashi, T.; Ariyoshi, W.; Tsujisawa, T.; Haga, M. and Nishihara, T. Tensile Mechanical strain up-regulates Runx2 and osteogenic factor expression in human periosteal cells: implications for distraction osteogenesis. **American Association of Oral and Maxillofacial Surgeons** 63(2005):499-504.
- [65] Banerjee, I.; Mishra, D. and Maiti, T. PLGA Microspheres incorporated gelatin scaffold: microspheres modulate scaffold properties. **International Journal of Biomaterials** 2009 (2009): in press
- [66] Li, M.; Ogiso, M.; and Minoura, N. Enzymatic degradation behavior of porous silk fibroin sheets. **Biomaterials** 24 (2003): 357–365.
- [67] Petrini, P.; Parolari, C.; and Tanzi, M.C. Silk fibroin-polyurethane scaffolds for tissue engineering. **Journal of Materials Science: materials in medicine** 12 (2001): 849-853.
- [68] Mosmann T. Rapid colorimetric assay for cellular growth and survival: Application to proliferation and cytotoxicity assays. **Journal of Immunological Methods** 65(1983):55–63.

- [69] Marolt, D.; Augst, A.; Freed, L. E.; Vepari, C.; Fajardo, R.; Patel, N.; Gray, M.; Farley, M.; Kaplan, D.; and Vunjak-Novakovic, G. Bone and cartilage tissue constructs grown using human bone marrow stromal cells, silk scaffolds and rotating bioreactors. **Biomaterials** 27 (2006): 6138–6149.
- [70] Hofmann, S.; Hagenmuller, H.; Koch, A.M.; Muller, R.; Novakovic, G.V.; Kaplan, D.L.; Merkle, H.P.; and Meinel, L. Control of *in vitro* tissue-engineered bone-like structures using human mesenchymal stem cells and porous silk scaffolds. **Biomaterials** 28 (2007): 1152-1162.
- [71] Hutmacher, D.W. Scaffold design and fabrication technologies for engineering tissues—state of the art and future perspectives. **Journal of biomaterials science polymer edition** 12(2001): 107-124.
- [72] Chen, Q.; Roether, A.J.; and Boccaccini, A.R. Tissue engineering scaffolds from bioactive glass and composite materials. **Tissue Engineering** 4(2008): 1-27.
- [73] Li, J.L.; Pan, J.L.; Zhang, L.G.; and Yu, Y.T. Culture of hepatocytes on fructose modified chitosan scaffolds. **Biomaterials** 24 (2003) : 2317-2322.
- [74] Tritanipakul, S. **Effects of gelatin conjugation and hydroxyapatite deposition on Thai silk fibroin scaffold** Master Thesis. Department of Chemical Engineering, Chulalongkorn University 2009.
- [75] Jeanie L. D.; and David, J. M. Hydrogels for tissue engineering: scaffold design variables and applications **Biomaterials** 24 (2003): 4337–4351.
- [76] Han, T.; and Misra, R.D.K. Biomimetic chitosan nanohydroxyapatite composite scaffolds for bone tissue engineering. **Acta Biomaterial** 5 (2009): 1182-1197.
- [77] Venugopal, J.; Low, S.; Choon, A.T.; Kumar, T.S.; and Ramakrishna, S. Mineralization of osteoblasts with electrospun collagen/hydroxyapatite nanofibers. **Journal of materials science-material in medicine** 19(2008): 2039–2046.
- [78] Peter, M.; Binulala, N.S.; Naira, S.V.; Selvamurugana, N.; Tamurac, H.; and Jayakumara, R. Novel biodegradable chitosan–gelatin/nano-bioactive glass ceramic composite scaffolds for alveolar bone tissue engineering **Chemical Engineering Journal** 158 (2010): 353–361.
- [79] Liu, X.; Smith, A.L.; Hu, J.; and Ma, P.X. Biomimetic nanofibrous gelatin/apatite composite scaffolds for bone tissue engineering. **Biomaterials** 30 (2009): 2252–2258.

- [80] Lauer, G.; Wiedmann-Al-Ahmad, M.; Otten, J.E.; Hubner, U.; Schmelzeisen, R.; and Schilli, W. The titanium surface texture effects adherence and growth of humangingival keratinocytes and human maxillar osteoblast-like cells *in vitro*. **Biomaterials** 22 (2001): 2799–2809.
- [81] Dalby, M.J.; McCloy, D.; Robertson, M.; Wilkinson, C.D.W.; and Oreffo, R.C. Osteoprogenitor response to defined topographies with nanoscale depths. **Biomaterials** 27 (2006): 1306–1315.
- [82] Chastain, S.R.; Kundu, A.K.; Dhar, S.; Calvert, J.W.; and Putnam, A.J. Adhesion of mesenchymal stem cells to polymer scaffolds occurs via distinct ECM ligands and controls their osteogenic differentiation. **Journal of Biomedical Materials Research** 78A (2006) : 73–85.
- [83] Park, B.W.; Hah, Y.S.; Kim, D.R.; Kim, J.R. and Byun, J.H. Osteogenic phenotypes and mineralization of cultured human periosteal-derived cells. **Archives of oral biology** 52 (2007): 983-989.
- [84] Rezwan, K.; Chen, Q.Z.; Blaker J.J.; and Boccaccini A.R. Biodegradable and bioactive porous polymer/inorganic composite scaffolds for bone tissue engineering. **Biomaterials** 27(2006): 3413–3431.
- [85] Arnold, U.; Lindenhayn, K.; and Perka, C. *In vitro*-cultivation of human periosteum derived cells in bioresorbable polymer-TCP-composites **Biomaterials** 23 (2002): 2303–2310.



APPENDICES

ศูนย์วิทยทรัพยากร
จุฬาลงกรณ์มหาวิทยาลัย

APPENDIX A

Raw data of water absorption and porosity

Table A-1 Mean and SD of compressive modulus of Thai silk fibroin/gelatin scaffolds based scaffold incorporated with inorganic compound, β -TCP and HA.

Weight blending ratio of inorganic compound/protein	Water absorption (%)	
	mean	SD
0/100	93.5	0.4
30 β -TCP/70	91.2	1.9
30 β -TCP/70	87.9	0.8
30 β -TCP/70	88.3	1.1
30HA/70	91.5	0.4
50HA/50	88.5	1.9
70HA/30	85.8	0.8

Table A-2 Mean and SD of porosity of Thai silk fibroin/gelatin scaffolds based scaffold incorporated with inorganic compound, β -TCP and HA.

Weight blending ratio of inorganic compound/protein	Porosity (%)	
	mean	SD
0/100	94.0	0.4
30 β -TCP/70	91.7	0.1
30 β -TCP/70	90.6	0.2
30 β -TCP/70	89.9	0.5
30HA/70	93.3	0.4
50HA/50	91.1	0.4
70HA/30	87.1	1.5

APPENDIX B

Raw data of compressive modulus

Table B-1 Mean and SD of compressive modulus of Thai silk fibroin/gelatin scaffolds based scaffold incorporated with inorganic compound, β -TCP and HA, in dry condition.

Weight blending ratio of inorganic compound/protein	Compressive modulus (kPa)	
	mean	SD
0/100	862	181.9
30 β -TCP/70	1148	142.0
30 β -TCP/70	1160	189.1
30 β -TCP/70	1230	160.2
30HA/70	866	102.9
50HA/50	1036	215.1
70HA/30	1082	102.1

Table B-2 Mean and SD of compressive modulus of Thai silk fibroin/gelatin scaffolds based scaffold incorporated with inorganic compound, β -TCP and HA, in wet condition.

Weight blending ratio of inorganic compound/protein	Compressive modulus (kPa)	
	mean	SD
0/100	6.8	1.1
30 β -TCP/70	9.8	2.4
30 β -TCP/70	11.7	4.8
30 β -TCP/70	12.8	2.3
30HA/70	10.6	2.0
50HA/50	12.4	1.9
70HA/30	15.9	1.7

APPENDIX C

Raw data of remaining weight (%)

Table C-1 Mean and SD of remaining weight (%) of Thai silk fibroin/gelatin scaffolds based scaffold incorporated with inorganic compound, β -TCP and HA, during the enzymatic degradation for 28 days

Degradation time (day)	Remaining weight (%)													
	0/100		30 β -TCP/70		50 β -TCP/50		70 β -TCP/30		30HA/70		50HA/50		70HA/30	
	mean	SD	mean	SD	mean	SD	mean	SD	mean	SD	mean	SD	mean	SD
0	100	0.0	100	0.0	100	0.0	100	0.0	100	0.0	100	0.0	100	0.0
1	78.1	7.2	77.5	1.9	87.6	2.8	94.99	2.7	70.4	8.7	87.6	2.0	93.6	2.0
3	46.6	1.9	56.1	3.5	74.4	6.7	84.93	3.1	62.9	4.2	74.9	4.8	83.9	2.8
5	23.2	2.6	51.8	8.8	61.7	2.6	75.05	4.3	57.2	9.7	62.9	1.8	77.7	7.1
7	3.8	2.0	32.4	4.3	52.3	3.0	74.81	5.3	34.6	2.8	49.4	5.5	71.2	4.4
14	0.0	0.0	32.6	7.9	51.7	6.0	70.09	8.6	32.8	3.4	50.4	7.1	70.8	2.9
21	0.0	0.0	33.6	4.9	50.1	10.5	71.69	5.5	31.5	5.7	51.4	5.0	71.5	0.4
28	0.0	0.0	31.5	8.8	51.9	5.6	71.72	8.3	30.8	5.3	50.3	5.5	69.6	5.1

APPENDIX D

Standard curve of *in vitro* cell culture test

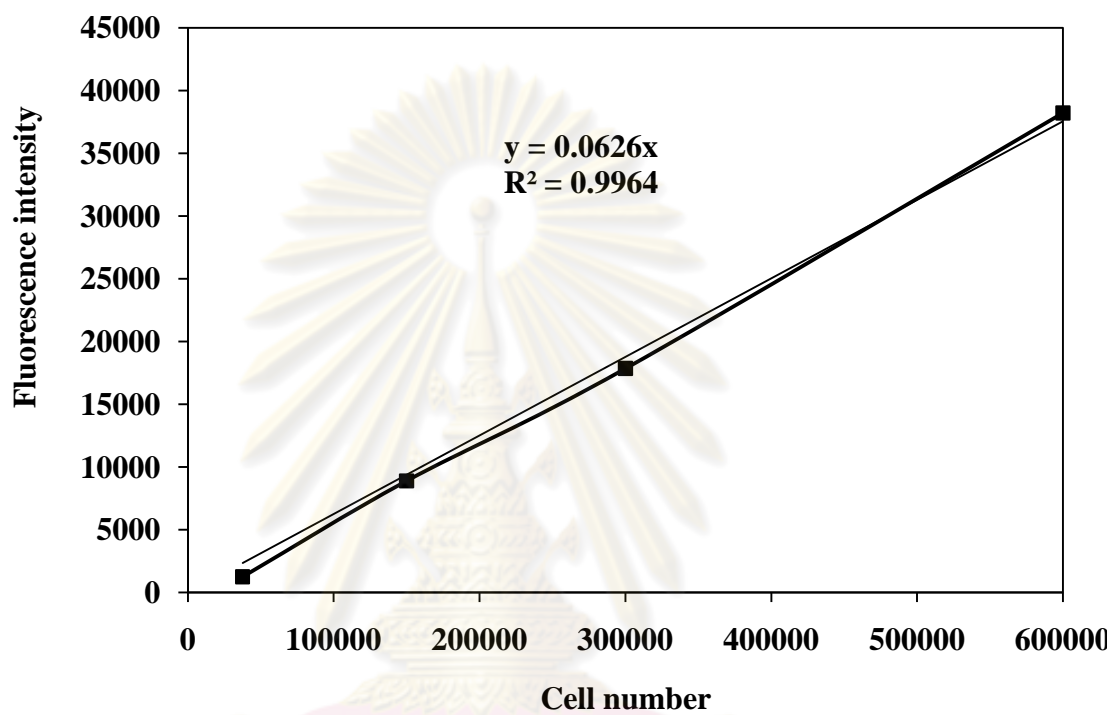


Figure D-1 Standard curve of number of cells for DNA assay.

ศูนย์วิทยทรัพยากร
จุฬาลงกรณ์มหาวิทยาลัย

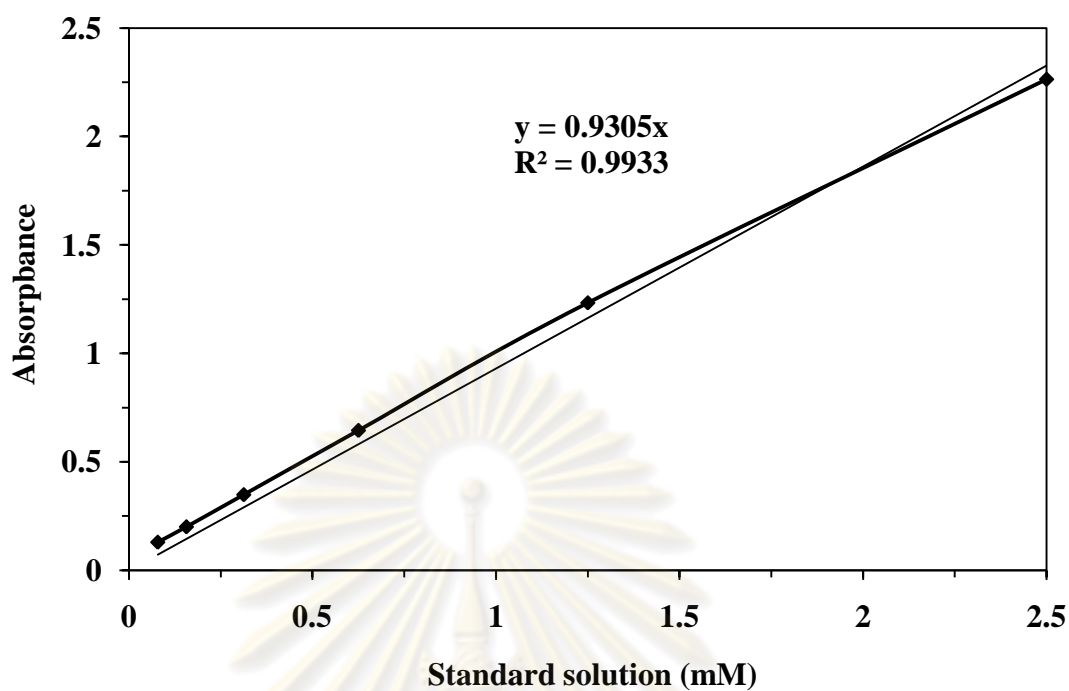


Figure D-2 Standard curve of p-nitrophenol standard solution for ALP activity.

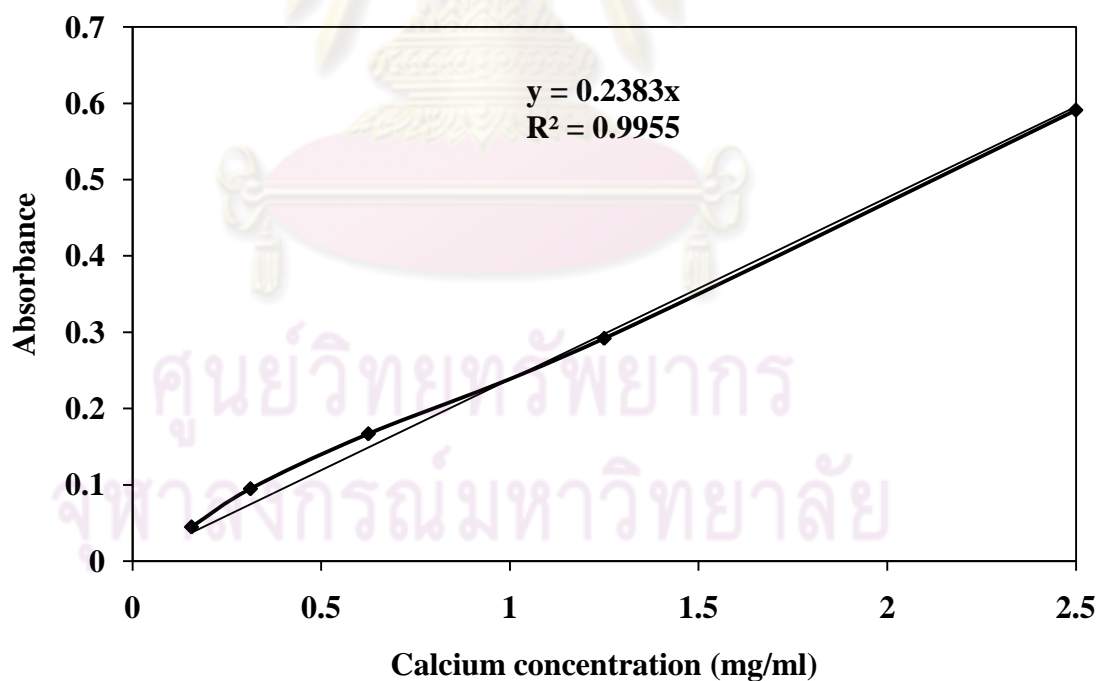


Figure D-3 Standard curve of CaCO_3 standard solution for calcium content.

APPENDIX E

Raw data of elemental analysis on cell surface after 28 days culture in osteogenic medium using dispersive X-ray spectroscopy (EDX)



ศูนย์วิทยทรัพยากร
จุฬาลงกรณ์มหาวิทยาลัย

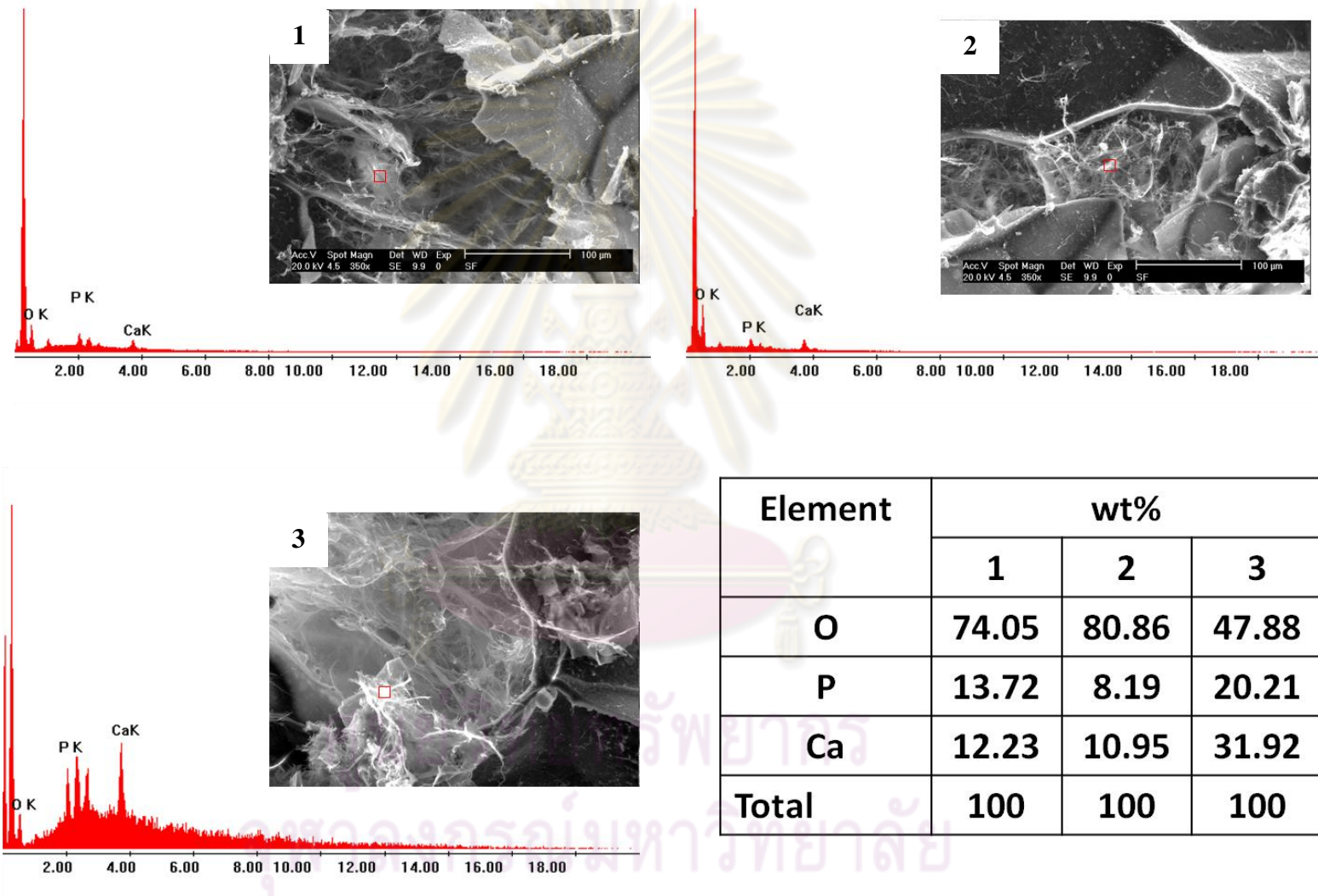


Figure E-1 Elemental analysis using EDX of periosteum derived cell after 28 day culture in osteogenic media; 0/100

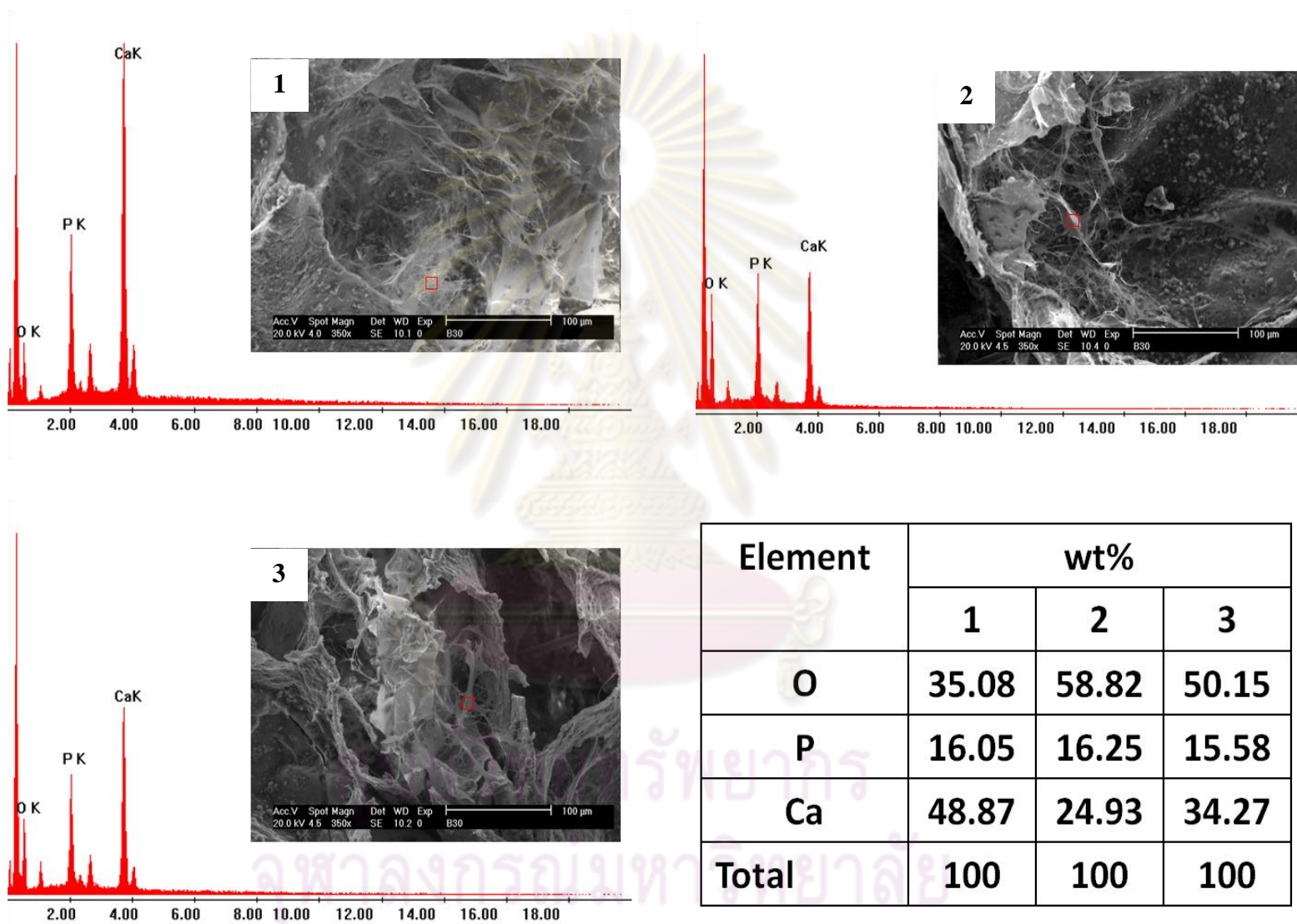


Figure E-2 Elemental analysis using EDX of periosteum derived cell after 28 day culture in osteogenic media; 30 β -TCP/70

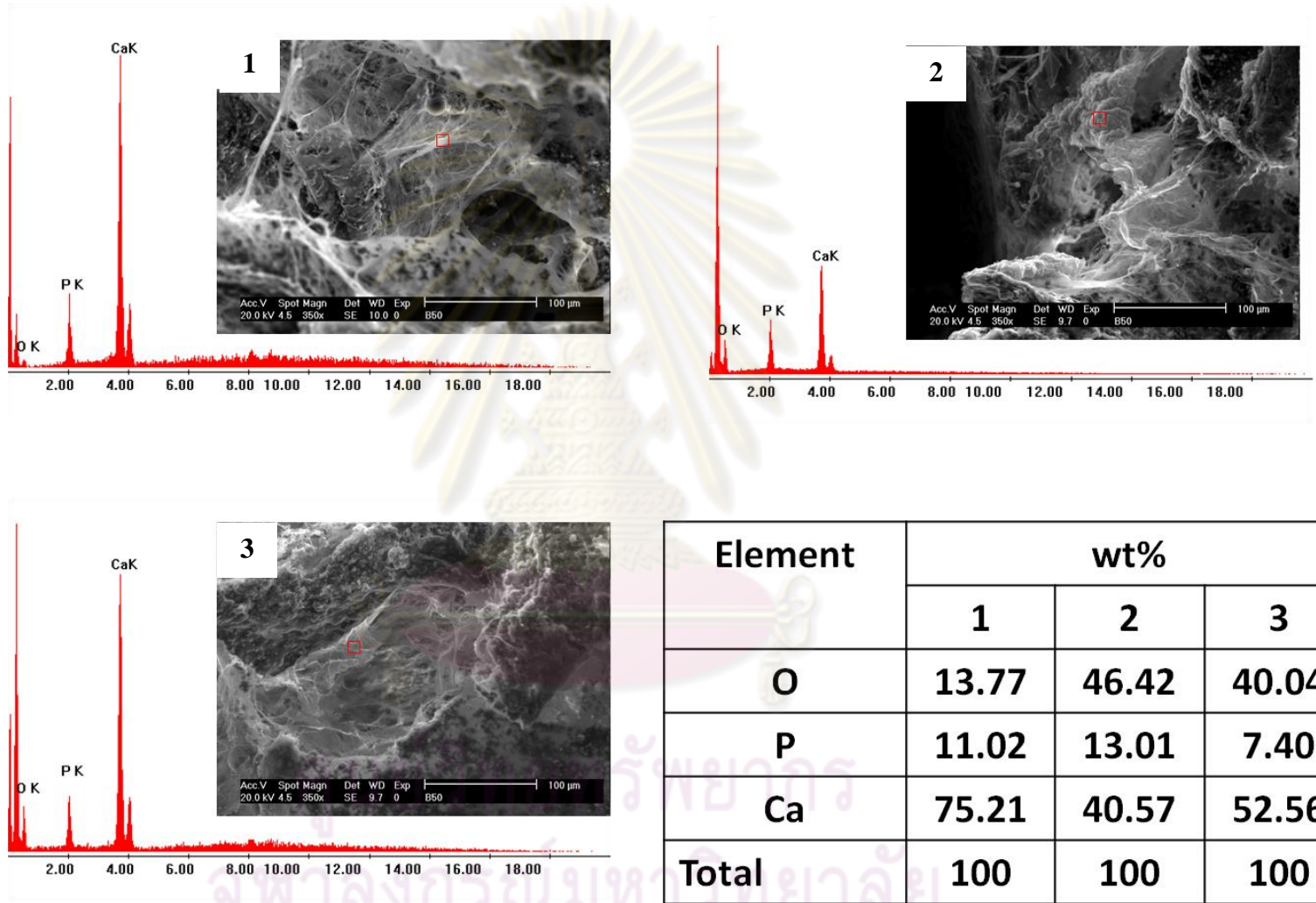


Figure E-3 Elemental analysis using EDX of periosteum derived cell after 28 day culture in osteogenic media; 50 β -TCP/50

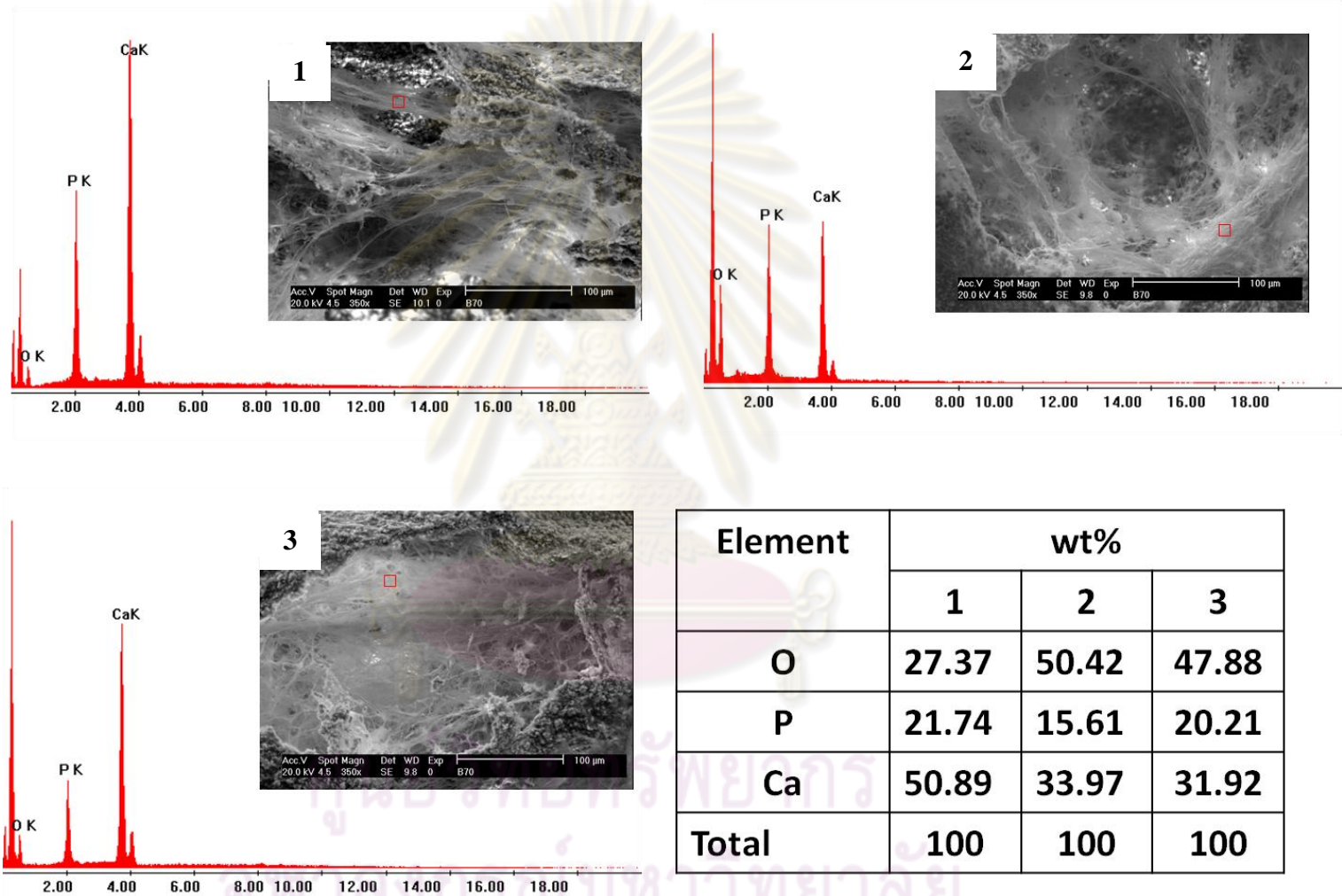


Figure E-4 Elemental analysis using EDX of periosteum derived cell after 28 day culture in osteogenic media; 70 β -TCP/30

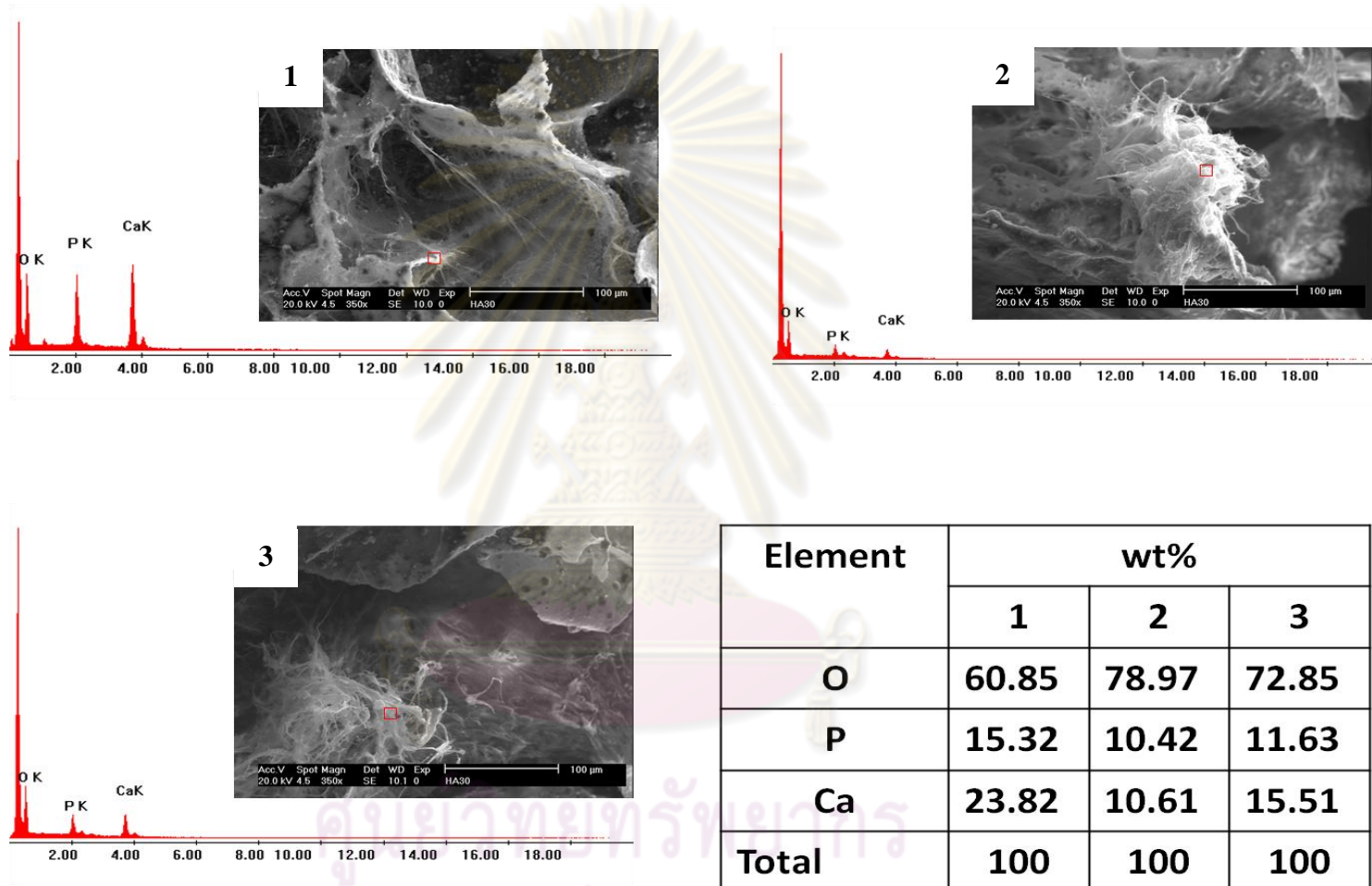


Figure E-5 Elemental analysis using EDX of periosteum derived cell after 28 day culture in osteogenic media; 30HA/70

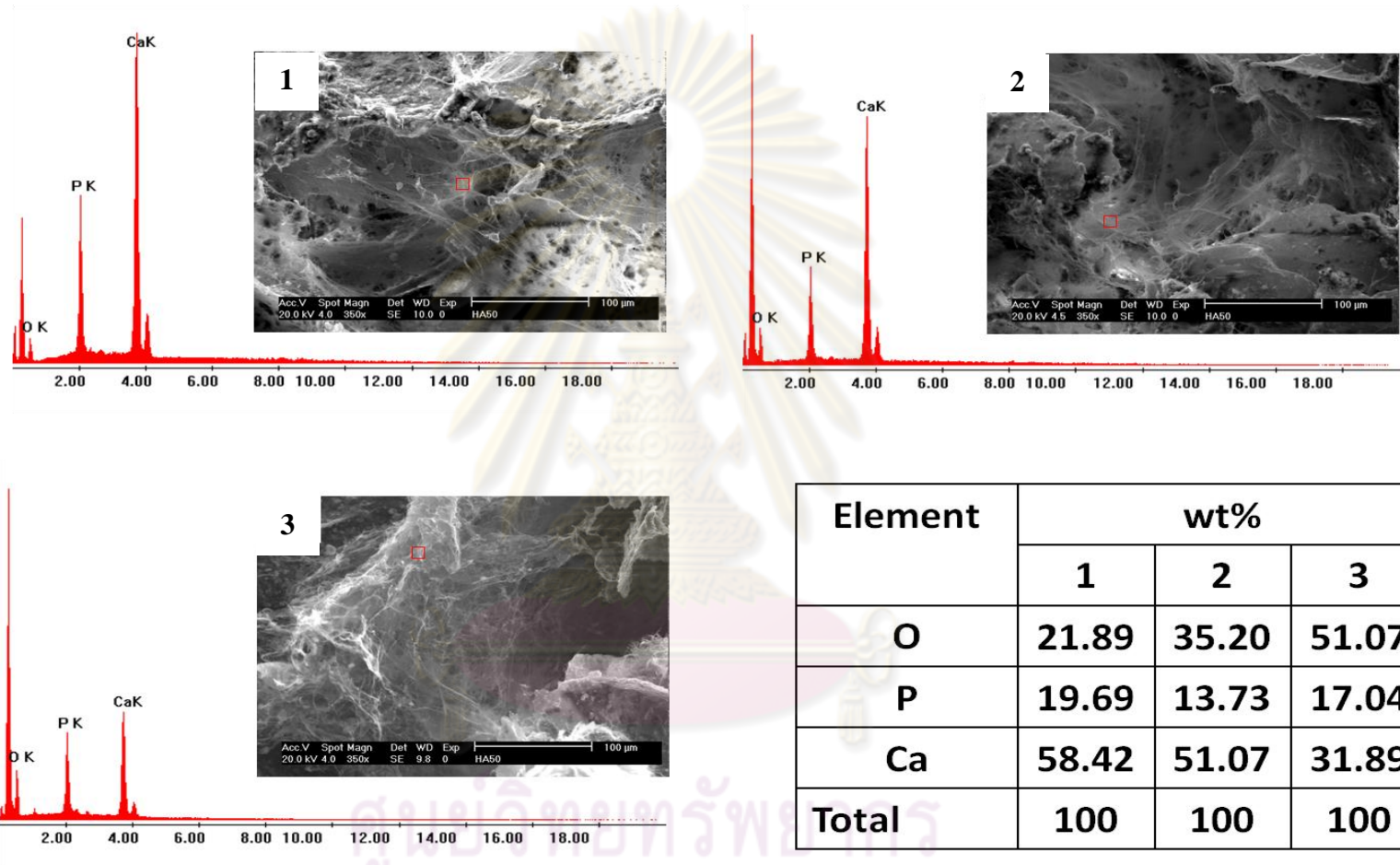


Figure E-6 Elemental analysis using EDX of periosteum derived cell after 28 day culture in osteogenic media; 50HA/50

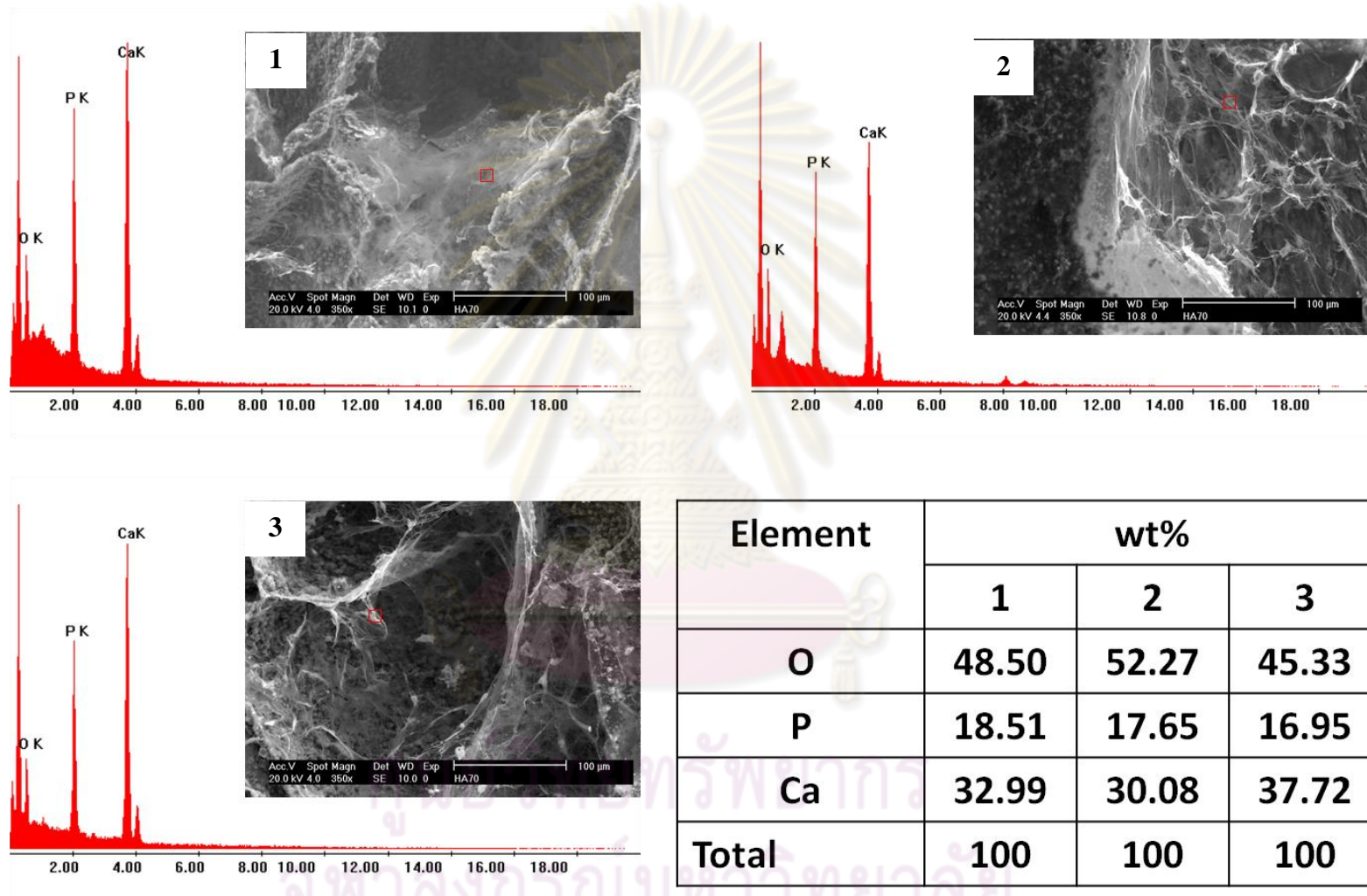


Figure E-7 Elemental analysis using EDX of periosteum derived cell after 28 day culture in osteogenic media; 70HA/30

Biography

Miss Chotika Dararutana was born in Chonburi, Thailand on March 28, 1986. She finished the high school education in 2003 from Chonratsadornumrung School. In 2007, she received her Bachelor Degree of Engineering with a major of Chemical Engineering from Faculty of Engineering, Burapha University. After the graduation, she pursued her graduate study in Master of Engineering (Chemical Engineering), the Faculty of Engineering, Chulalongkorn University.

Some parts of this work were presented at two international conferences as follows;

- 1.) C. Dararutana, S. Honsawek, S. Damrongsakkul, Effects of hydroxyapatite and β -tricalcium phosphate on the physical properties of Thai silk fibroin/gelatin scaffolds, Pure And Applied Chemistry International Conference (PACCON 2010), Sunee grand hotel and convention center, Ubonratchathani, Thailand, 21 – 23 January, 2010 (Oral presentation)
- 2.) C. Dararutana, S. Honsawek, S. Damrongsakkul, Characterization of Thai silk fibroin/gelatin based scaffolds incorporated with hydroxyapatite and β -tricalcium phosphate Biomedical Engineering International Conference (BMEiCON 2010), Kyoto University, Kyoto, Japan, 27-28, August, 2010 (Oral presentation)

ศูนย์วิจัยทรัพยากร
จุฬาลงกรณ์มหาวิทยาลัย